WRDC-TR-90-4091

X-RAY TOMOGRAPHIC INSPECTION OF PRINTED WIRING ASSEMBLIES AND ELECTRICAL COMPONENTS

Richard H. Bossi
Robert J. Kruse

Boeing Aerospace & Electronics
P.O. Box 3999
Seattle, WA 98124

October 1990

Interim Report for Period July 1989 to June 1990

MATERIALS LABORATORY
WRIGHT RESEARCH AND DEVELOPMENT CENTER
AIR FORCE SYSTEMS COMMAND
WRIGHT-PATTERSON AIR FORCE BASE, OHIO 45433-6533

NOTICE

WHEN GOVERNMENT DRAWINGS, SPECIFICATIONS, OR OTHER DATA ARE USED FOR ANY PURPOSE OTHER THAN IN CONNECTION WITH A DEFINITELY GOVERNMENT-RELATED PROCUREMENT, THE UNITED STATES GOVERNMENT INCURS NO RESPONSIBILITY OR ANY OBLIGATION WHATSOEVER. THE FACT THAT THE GOVERNMENT MAY HAVE FORMULATED OR IN ANY WAY SUPPLIED THE SAID DRAWINGS, SPECIFICATIONS, OR OTHER DATA, IS NOT TO BE REGARDED BY IMPLICATION, OR OTHERWISE IN ANY MANNER CONSTRUED, AS LICENSING THE HOLDER, OR ANY OTHER PERSON OR CORPORATION; OR AS CONVEYING ANY RIGHTS OR PERMISSION TO MANUFACTURE, USE, OR SELL ANY PATENTED INVENTION THAT MAY IN ANY WAY BE RELATED THERETO.

THIS REPORT HAS BEEN REVIEWED BY THE OFFICE OF PUBLIC AFFAIRS (ASD/PA) AND IS RELEASABLE TO THE NATIONAL TECHNICAL INFORMATION SERVICE (NTIS). AT NTIS IT WILL BE AVAILABLE TO THE GENERAL PUBLIC INCLUDING FOREIGN NATIONS.

THIS TECHNICAL REPORT HAS BEEN REVIEWED AND IS APPROVED FOR PUBLICATION.

Charles F. Buynak

CHARLES F. BUYNAK
Nondestructive Evaluation Branch
Metals and Ceramics Division

Thomas J. Moran

THOMAS J. MORAN, Acting Chief
Nondestructive Evaluation Branch
Metals and Ceramics Division

FOR THE COMMANDER

Norman M Tallan

DR. NORMAN M. TALLAN, Director
Metals and Ceramics Division
Materials Laboratory

IF YOUR ADDRESS HAS CHANGED, IF YOU WISH TO BE REMOVED FROM OUR MAILING LIST, OR IF THE ADDRESSEE IS NO LONGER EMPLOYED BY YOUR ORGANIZATION PLEASE NOTIFY WRDC/MLLP, WRIGHT-PATTERSON AFB, OH 45433-6533 TO HELP MAINTAIN A CURRENT MAILING LIST.

COPIES OF THIS REPORT SHOULD NOT BE RETURNED UNLESS RETURN IS REQUIRED BY SECURITY CONSIDERATIONS, CONTRACTUAL OBLIGATIONS, OR NOTICE ON A SPECIFIC DOCUMENT.

UNCLASSIFIED
SECURITY CLASSIFICATION OF THIS PAGE

REPORT DOCUMENTATION PAGE

Form Approved
OMB No. 0704-0188

1a. REPORT SECURITY CLASSIFICATION UNCLASSIFIED	1b. RESTRICTIVE MARKINGS APPROVED FOR PUBLIC RELEASE DISTRIBUTION IS UNLIMITED
2a. SECURITY CLASSIFICATION	3. DISTRIBUTION/AVAILABILITY OR REPORT
2b. DECLASSIFICATION/DOWNGRADING SCHEDULE	
4. PERFORMING ORGANIZATION REPORT NUMBER(S)	5. MONITORING ORGANIZATION REPORT NUMBER(S) WRDC-TR-90-4091
6a. NAME OF PERFORMING ORGANIZATION BOEING AEROSPACE & ELECTRONICS 6b. OFFICE SYMBOL (if applicable)	7a. NAME OF MONITORING ORGANIZATION MATERIALS LABORATORY (WRDC/MLLP) WRIGHT RESEARCH AND DEVELOPMENT CENTER
6C. ADDRESS (City, State, and ZIP Code) P. O. BOX 3999 SEATTLE, WA 98124	7b. ADDRESS (City, State, and ZIP Code) WRIGHT-PATTERSON
8a. NAME OF FUNDING/SPONSORING ORGANIZATION 8b. OFFICE SYMBOL (if applicable)	9. PROCUREMENT INSTRUMENT IDENTIFICATION NUMBER F33615-88-C-5404
8c. ADDRESS City, State, and ZIP Code)	10. SOURCE OF FUNDING NUMBERS

PROGRAM ELEMENT NO.	PROJECT NO.	TASK NO.	WORK UNIT ACCESSION NO.
63112F	3153	00	06

11. TITLE (Include Security Classification)
X-RAY TOMOGRAPHIC INSPECTION OF PRINTED WIRING ASSEMBLIES AND ELECTRICAL COMPONENTS

12. PERSONAL AUTHOR(S)
RICHARD H. BOSSI AND ROBERT J. KRUSE

13a. TYPE OF REPORT	13b. TIME COVERED	14.. DATE OF REQUEST (Year, Month, Day)	15. PAGE COUNT
INTERIM	FROM JULY 89 TO JULY 90	90 OCTOBER 31	88

16. SUPPLEMENTARY NOTATION

17. FIELD	GROUP	SUB-GROUP
11	06	
01	03	

18. SUBJECT TERMS (Continue on reverse if necessary and identify by block number)
automated insepction, computed tomography, connectors, electronics, inspection, laminography, leadless chip carrier, nondestructive inspection, optical transducer

19. ABSTRACT (Continue on reverse if necessary and identify by block number)

The viability of X-ray tomography techniques for printed wiring assembly (PWA) solder bond evaluation and several categories of electronic components has been studied. The effort was performed as a final testing task assignment in the Advanced Development of X-Ray Computed Tomography Application program. The primary area for testing was surface mount technology solder bonds. During the course of the task assignment several other categories of electronic devices were examined including transformers, connectors, and an optical transducer. Five different X-ray systems for computed tomography (CT), laminography and radioscopy were used.

The results of this final task assignment indicate that X-ray tomographic techniques can be useful for solder bond evaluation, and innerlayer trace analysis for PWA's and as a failure analysis tool for a broad range of electrical and electronic components. Investment in PWA solder bond evaluation systems using X-rays commonly show a short term (<1 year) payback. The particular system to be used and the economic payback rate depends on the assembly design and manufacturing throughput. Radioscopy (real-time radiography) and scanned beam laminography are the primary techniques recommended for solder bond evaluation. Printed wiring board innerlayer copper traces were imaged with laminographic inspection using industrial CT systems. This "reverse trace analysis" technique can be applied to individual layers in multilayer boards. Failure analysis/destructive sectioning of electronic components, such as connectors and transformers, is an area where CT offers an alternative nondestructive approach that has been demonstrated to be cost effective in a variety of cases.

20. DISTRIBUTION/AVAILABILITY OF ABSTRACT [X] UNCLASSIFIED/UNLIMITED [ ] SAME AS RPT [ ] DTIC USERS	21. ABSTRACT SECURITY CLASSIFICATION UNCLASSIFIED
22a. NAME OF RESPONSIBLE INDIVIDUAL CHARLES F. BUYNAK	22b. TELEPHONE (Include Area Code) (513) 255-9802 22c. OFFICE SYMBOL WRDC/MLLP

DD Form 1473, JUN 86 *Previous editions are obsolete.* SECURITY CLASSIFICATION OF THIS PAGE
UNCLASSIFIED

BLOCK 18 (CONTINUED)

printed wiring assemblies
radiography
radioscopy
scanned beam lamniography
solder bonds
surface mount technology
transformers
x-ray

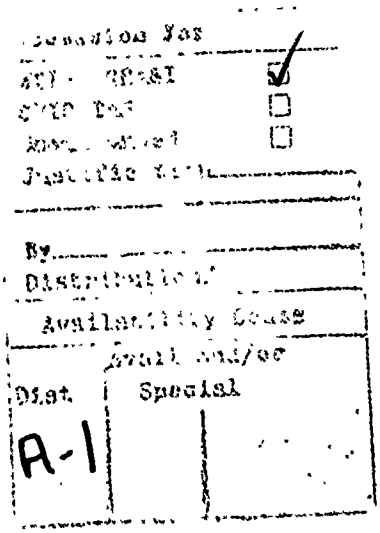

TABLE OF CONTENTS

TABLE OF CONTENTS - concluded

APPENDICES

LIST OF FIGURES

LIST OF FIGURES - Concluded

ACKNOWLEDGEMENT

The authors acknowledge the contribution of test components, scanning assistance, data analysis support and technical input to this report provided by a variety of individuals from firms in the aerospace and electronics industry, and manufacturers of inspection systems including: ARACOR, BIR, Delco Electronics, Fein Focus USA, Four Pi Systems, General Electric, Hughes Electro-Optical & Data Systems Group, Nicolet, SMS, Skaimetrics, Sun Microsystems and TRW Electronic Systems Group. Special Thanks are extended to John Knopp and Gretchen Kunze of Boeing Aerospace & Electronics.

DISCLAIMER

The information contained in this document is neither an endorsement nor criticism for any X-ray imaging instrumentation or equipment used in this study.

1.0 INTRODUCTION

The goal of the Advanced Development of X-ray Computed Tomography Applications demonstration (CTAD) program is to evaluate applications for which computed tomography (CT) can provide a cost-effective means of inspecting aircraft/aerospace components. The program is task assigned so that specific CT applications or application areas can be addressed in separate task assigned projects. Three categories of task assignments are employed in this program including preliminary testing, final testing and demonstrations with economic analysis. This report is the result of a final testing task assignment which followed from a preliminary testing study previously reported [1]. References 2 - 4 are additional preliminary testing reports from this program in other application areas.

X-ray tomographic imaging techniques have existed since early in the twentieth century. The most common being body section tomography (laminography). Since the 1960's, with the advent of computer technology, computerized tomography has developed very rapidly for medical and more recently industrial applications. The CTAD program uses a variety of X-ray inspection techniques to evaluate where X-ray CT and associated tomographic methods may be economically applied.

1.1 Scope

This task assignment, designated "Task 5 - Final Electronics," is a final testing task directed at the inspection of electrical devices with an emphasis on printed wiring assemblies (PWA's, circuit boards with mounted electronic components). This report discusses the items selected for testing, the testing, the results, and conclusions. This study includes the inspection of solder bonds for surface mounted electronic devices on multilayer circuit boards, transformers, connectors, and other components. Items were selected for testing based on industry interest in improved inspection capability. The examples selected for discussion in this report are some of the more informative images of the numerous scans taken in this task effort.

A number of different radiographic systems were used during the course of this task assignment. Resolution and contrast sensitivity phantoms (Appendix B) were used on each CT system employed to provide a quantitative measure to assess the image quality of scans obtained. For non-CT systems, resolution values were estimated or obtained from system manufacturers and are listed in the system characteristics table (Figure 2.2-1).

The use of laminographic techniques for inspection was included in the scope of this task assignment because PWA's have a planar geometry that is not necessarily well suited to the CT data acquisition technique. Laminography (body section tomography - Appendix A) uses X-ray imaging with several source/object/detector orientations to focus on specific depth planes in the object, while defocussing undesired planes. Computed laminography or tomosynthesis using an industrial CT system for data acquisition was performed to obtain results on circuit board innerlayer traces. Scanned beam laminography was performed on PWA solder bonds. A comparative analysis with radioscopic (real-time radiography) techniques for inspection was included to provide a means of comparison to widely accepted existing technology.

1.2 Objectives

The overall program goal is to demonstrate the economic benefits of using CT and laminography in the aircraft/aerospace industry. The objective for this task assignment was to identify the applicability of CT and laminography to the inspection of electronic PWA's and other electrical components and form a comparison with existing radiographic techniques. Currently the electronics industry uses radioscopy in routine circuit board inspections and nonroutine component inspections. CT and laminography offer another means by which these components can be evaluated nondestructively.

2.0 TEST PLAN

The test plan for the Task 5 assignment included: test sample acquisition; radiographic, radioscopic, CT and laminographic examination; metallurgical analysis; image analysis; and evaluation. The primary focus of the testing was to image features of solder bonds and innerlayer traces of PWA's.

2.1 Test Samples

Printed wiring assembly solder bond evaluation was identified in the Task 1 report, "Computed Tomography of Electronics," [1] as a key area for the use of CT related inspection technology. The inspection of PWA's encompasses a broad range of board types including conventional through-hole technology (Dual In-line Packages or DIPs), surface mounted technology (SMT), fine pitch technology (FPT), discrete components, chip on board (COB), tape automated bonding (TAB), flip chip and hybrid technologies, combinations of the above, and others.

The SMT technology is particularly pertinent because in this technology the solder connection is not only an electrical connection but also a mechanical bond. SMT allows for close packaging of components on both sides of a PWA. This combination is very difficult to inspect with traditional inspection techniques.

The primary SMT test board for this study was custom manufactured at Boeing from a design supplied by TRW of San Diego. Additional boards were obtained from various sources throughout Boeing and industry. All boards were manufactured with a range of defects suited to test the capability of inspection systems for solder bond evaluation. The test boards were prescreened by Boeing Quality Assurance to characterize defects using film radiography to select the boards of greatest interest for X-ray inspection technology evaluation.

Miscellaneous electrical components were also obtained for CT scanning. The Task 1 report showed that failure analysis of certain types of electronic components would be cost effective using CT. Figure 2.1-1 lists several of the test samples scanned, their typical costs and their application. All components tested under the program are referenced by a part identification number (PID).

Component	Replacement Cost	Aircraft/Equip. Used On
Computer PC Board, PID #010105 (Figure 3.3-24a)	$10,000	Aircraft Avionics
Small Trans. Assy., PID #010304 (Figure 4.2-1)	$1400	Power Supplies
Firewall Connector, PID #010513 (Figure 4.1-1)	$100	All Aircraft
Fiber Optic Sensor, PID #010803 (Figure 4.3-1)	$20,000*	Future Aircraft

* Prototype development cost, flight unit should be less.

Figure 2.1-1 Typical component costs

2.2 System Technologies and Performance

The inspection of PWA's and electrical components utilized five different X-ray inspection technologies including radiography, radioscopy (Fein Focus, model FXS-160.50 and Nicolet, model NXR-1200), computed tomography (BIR ACTIS, SMS CITA Model 101B+, GE Bench XIM, and ARACOR Tomoscope), computed laminography (SMS CITA Model 101B+, and BIR ACTIS), and scanned beam laminography (Four Pi Systems model 3DX-2000). Conventional film radiography was used to prescreen the PWA's and test components. Radioscopy was performed using two different microfocus systems. These systems employed similar sources but used different detector types. Computed tomography (CT) was used on electronic components for volumetric feature detection. Imaging was performed at discrete locations within the devices. Computed laminography (CTLAM) and scanned-beam laminography (SBLAM) were performed on PWA's for solder bond evaluation and also for innerlayer trace detection. Appendix A discusses the fundamental principles of radioscopy, CT, and laminography.

The actual systems used in this study to test the technologies varied significantly: from small research systems allowing very small components to systems equipped to handle large PWA's on an automated basis. While some of these systems were newly released and operator experience was minimal, others were operated by more experienced staff. Overall, the operator's knowledge of the system mostly affected setup and scan time and only to a lesser degree the overall image quality of the systems.

No universally accepted and certified phantoms translatable between radiography, radioscopy, CT, CTLAM and SBLAM exist. For CT, the CTAD program has been utilizing a set of phantoms to measure spatial resolution and contrast sensitivity. These phantoms are discussed in Appendix B. Figure 2.2-1 shows a sample of the system characteristics of each system. The IRT model CXI-5500 system is included for reference but was not used in the study.

System	Estimated Cost (a)	Inspection Modes	System Weight	Floor Space	X-Ray Source (b)	Estimated Inspection Time	MBL Field of View	Spatial Resolution	Signal/ Noise	Max. Part Size
Fein Focus FXS-160.50	$260,000	Manual & Auto position RTR (c) 5-Axis	3100 kg	3.3 sq m (e) 1.5 sq m (f)	160kV 20 W 3-200 µm fs	5-10 minutes (d) manual positioning	150 mm	50 lp/mm @ high mag.	NA	370 mm x 750 mm 11 kg
IRT CXI-5500	$365,000	Manual & Auto RTR (c) 2-Axis	2700 kg	1.8 sq m (e) 0.5 sq m (f)	160 kV 35 W 10 µm fs	45 60 seconds (d) Auto algorithm inspection	25 mm x 25 mm	14 lp/mm @ 25 mm FOV	NA	
Nicolet NXR-1200	$90,000	Manual RTR (c) 2 Axis	590 kg	2 sq m	100kV 40 W 40 µm fs	10 minutes (d) manual positioning	13 mm x 10 mm	17 lp/mm @ 25x mag (a)	NA	475mm x 600 mm circuit board
Four Pi Sys. 3DX 2000	$425,000	Manual & Auto RTR (c) SBLAM	2700 kg	5 sq m	160kV 20 W 10 µm fs scanning	1-1.5 minutes (d) Auto algorithm inspection	10 mm x 9.5 mm	10 lp/mm (a)	NA	425 mm x 475 mm circuit board
ARACOR Tomoscope	$1,000,000	DR, CT, CTLAM	1800 kg	3.4 sq m (e) 4.6 sq m (f)	120kV 100 µm fs	CT: 2hr/slice	100 mm	10 lp/mm (g)	NA	100 mm x 254 mm 22 kg
GE XIM	$1,500,000	DR, CT	10,000 kg	2.83 sq m	420 kV 1.5 mm fs	CT. 30s	150 mm	2 lp/mm (g)	30 (g)	150 mm 30 kg
SMS Model 101B+	$750,000	DR, CT CTLAM	570 kg (e)	3.4 sq m (e) 2 sq m (f)	420 kV 1.5 mm fs	CT. 5 min/slice CTLAM 60 min (h) 5 min/laminogram	400 mm 400 mm	4 lp/mm (g) NA	6 (g) NA	570 mm 22 kg
BIR ACTIS	$1,700,000	DR, CT CTLAM	9200 kg (e)	26 sq m (e) 14 sq m (f)	420 kV 1.2 mm fs	CT.5 min/slice	1800 mm	1 lp/mm (g)	100 (g)	1800 mm 1000 kg

(a) Estimate from best available data
(b) Vendor focal spot specifications
(c) Radioscopy (Real-Time Radiography, RTR)
(d) Single sided SMT circuit board containing 500 joints (see Section 6 for confidence level)
(e) Scanner only
(f) Console plus equipment racks etc.
(g) Measured with Appendix B phantoms
(h) Data acquisition time

Figure 2.2-1 System characteristics

2.2.1 Radioscopy

Radioscopic inspection systems using a microfocal source and an image intensifier offer fast data acquisition with suitably high resolution for PWA solder bond inspection. For simple board constructions, radioscopic imaging offers an advantage of increased speed over film radiography techniques and lower system expense over certain advanced imaging techniques such as laminography and CT. A disadvantage to radioscopy imaging is the superpositioning of overlaying component features making interpretation often ambiguous and quantitative measurement difficult. This is particularly apparent with double-sided PWA's where it may be difficult to interpret which side of the assembly contains a potential defect. Also, the contrast sensitivity in the image is reduced due to the superpositioning of actuators on the two sides. As higher density component packaging is used, the difficulty in interpreting the image is increased.

Radioscopic system manufacturers offer multi-axis component manipulators to enable the assembly to be viewed at oblique angles. This assists in resolving superimposed features, but can still leave some uncertainty when interpreting complicated features.

2.2.2 CT Systems

CT provides more quantitative information about the density and dimensions of the component's internal features than radiography or radioscopy, though at an additional expense of time and money. CT is best suited for electrical components such as transformers and connectors where the features of interest are volumetric and the part geometry is such that the ray paths are consistent. CT is less applicable to planar objects having a high aspect ratio such as PWA's. High aspect ratios cause significant variations in X-ray paths which will limit the system sensitivity due to the dynamic range and partial voluming effects. Artifacts due to the large path length variations in the resulting reconstruction process can disguise desired features of interest.

CT was not extensively investigated for PWA applications. It was, however, used on a variety of other more applicable components.

2.2.3 Laminography

Laminography can be performed on systems that allow source, object and detector manipulation such that a plane of interest in the object can be focussed while other planes are defocussed. Laminography is particularly effective for solder bonds because they are high density features which are spaced about on a surface. As they are moved in an unfocussed plane, their high attenuation effect is averaged with neighboring low attenuation features or air so that their overall influence on the image is rapidly decreased. At the focussed plane, the high density features are imaged with excellent contrast. Thus, laminography is applicable to components that have distributed features such as PWA solder bonds.

Laminography can be performed on an industrial CT system (CTLAM) by taking a series of digital radiographs (DR's) with the part rotated by prescribed angles between each DR. The DR data set can then be analyzed to focus on any desired depth plane in the part. CTLAM scans require relatively longer data acquisition times because they are performed on CT systems that are designed to be less efficient in order to allow greater flexibility of operation for CT reconstructions. On the other hand, the SBLAM systems are efficient with relatively quick scan times (2 - 4 seconds) because of their specific design for high speed PWA solder bond inspection. These systems are limited in flexibility primarily due to the energy and flux available from the source.

2.3 Image Reproduction

All of the X-ray imaging systems display their data on a video terminal, though resolutions (array sizes) vary. Hard copy from these systems employ various techniques such as photographic recorders, high-resolution thermal-type printers, laser printers and film. The best reproductions were obtained by a film recorder or by manual photographs taken of the terminal; however, these options were not always available. Images were stored magnetically when possible and were later retrieved at Boeing for further analysis and photographing. This report uses the best reproductions available, but they are naturally degraded in reproduction from the original images as seen on the video terminals of the actual system.

3.0 PRINTED WIRING ASSEMBLY STUDIES

The rapid advancement of higher packing density for electronics on circuit boards and the continued acceptance of these assemblies into the production of military electronics is placing greater emphasis on understanding solder joint integrity, particularly for surface mount technology (SMT). Recent estimates show that SMT will go from 18 percent of total integrated circuit production in 1989 to 40.2 percent by 1993 [5]. The world growth rate of SMT production has steadily doubled every 6 years since 1980 [6]. The trend towards SMT was also identified in a study on printed wiring board (PWB) production in Japan [7]. Projected sales of PWB's for SMT devices used in industrial applications showed an expected increase of 15.3 percent between 1988 and 1989 [7]. A breakdown by board type of industrial PWB growth is shown in Figure 3.0-1.

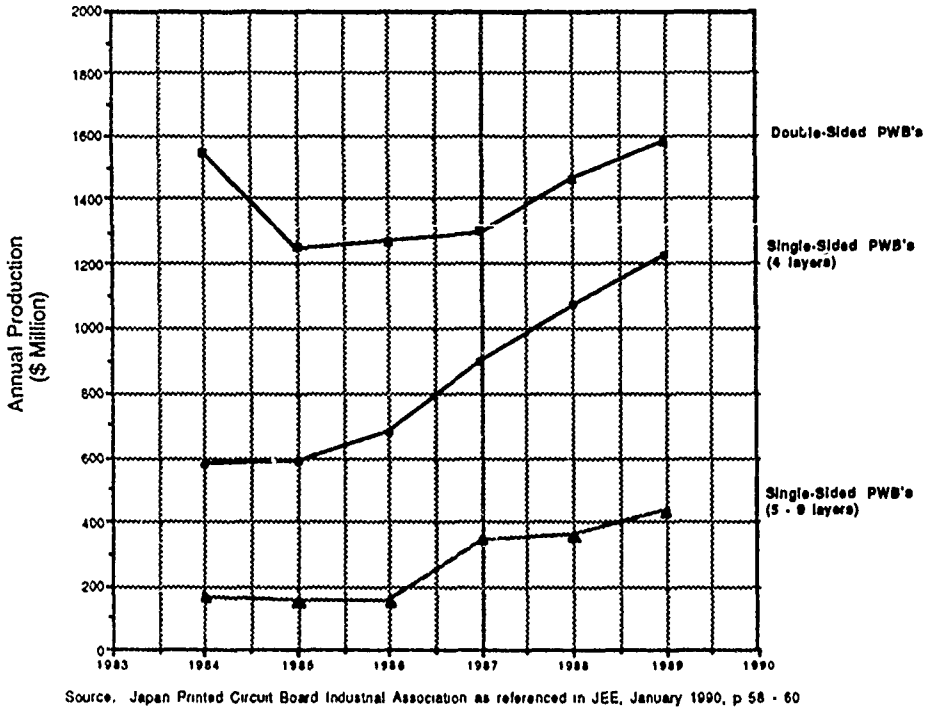

Figure 3.0-1 Annual Japanese production of industrial purpose PWB's by board type

Analysts estimate that much of the demand for SMT components will be through contract manufacturing firms which account for 55 percent - 65 percent of the current market. Large manufacturers will continue to utilize the benefits of contract manufacturing to avoid the risks of excessive in-house capacity. The worldwide SMT market for contract manufacturers is expected to grow at an average rate of 21 percent, while the United States market is expected to grow annually at 19 percent each year [8]. One recent study indicates that the demand for leadless ceramic chip (LCC) carriers will decline due to problems associated with mismatches of thermal expansion coefficients between the package and PC board [9]. The preferred choice then becomes the leaded ceramic chip (LDCC) carrier available in gull and "J" lead package styles [9]. The demand for quad flat packs has risen due to the large variety of pin counts available, and production is expected

to increase by over 900 percent by 1994. Pin grid arrays are also increasing in usage with both through hole and surface mount applications expected to double in production by 1994 [9]. Fine pitch technology will also increase at an average annual growth rate of 57 percent through 1993. During the same period through hole components are expected to drop from the 1989 estimate of 80 percent market share to 52.4 percent [5]. The high growth rate of fine pitch technology devices is indicative of the movement towards higher packing density components.

One of the major challenges to achieving "excellent" automated SMT solder production quality is suitable process control/inspection capability. To remain competitive, manufacturers have or are planning to comply to MIL-STD-2000 (released January 1989), a lengthy compilation of existing specifications and standards. (At the time of this study, MIL-STD-2000 is undergoing continual revisions and is addressing the inclusion of SMT devices. MIL-STD-2000 does not completely address all the package types such as LCC's, "J" leaded packages, pin grid and pad arrays, as well as the upcoming FPT technologies.) The intent of MIL-STD-2000 is to provide a single set of soldering requirements for all armed service branches and reduce conflict and confusion in the production of electronic systems [10]. This is thought to help decrease initial procurement costs and lead times for manufacturer compliance, though it still requires form fitting to the contract. From the manufacturers' standpoint, it forces them to critically examine their soldering process and should yield many benefits through improved process control [11].

The direction of PWA quality control is toward automation and process control. A number of inspection technologies that could be applied to the problem are radically different from one other. Each offers unique abilities relevant to the evaluation of solder joint quality. Adequate inspection, though, may require much more information than any one current system can deliver. Many proponents of the electronics industry recommend that a total inspection capability should consist of a combination of several technologies linked together to form an overall process-control automated-inspection system [10].

For example, it is well known that less technical methods, such as visual inspection, are available for assessing external bond quality. Yet fundamentally the solder joint integrity problem lies in understanding the physics of the solder joint uniformity on a microscopic level. This holds especially true for SMT where the solder bond must serve not only as an electrical and thermal connection but equally important as a mechanical fastener. With the desire to compact electronics into smaller and more electronically dense regions, the inspection issue increases in difficulty with each new development in SMT (Fine Pitch Technology, Tape Automated Bonding, Chip On Board, Flip Chip, etc.) where bonds have a critical dual purpose - electrical and mechanical.

With the trend toward increased applications of SMT, manufacturers are seeking high reliability inspection systems that will cost effectively characterize hidden as well as visible solder joints. Manufacturing quality managers are seeking to achieve a 6 sigma (99.9999998 percent) level of quality in their products [12]. This quality level is a formidable challenge. The development of high reliability inspection systems to meet this challenge may be difficult, but the market demands it [13] and manufacturers are competing to achieve it.

This study has concentrated on X-ray based technologies and their economic payback for inspecting PWA's. The choice of automated versus semiautomated inspection technologies fit into three main categories: single-sided assemblies, double-sided assemblies, and special applications (prototype development, research and failure analysis). A comprehensive analysis of bond defect phenomena, including environmental and electrical testing together with destructive and nondestructive techniques is beyond the intended scope of this study.

3.1 Radiation Effects on Electronics

The use of ionizing radiation on semiconductor electronics for inspection risks permanent damage to the devices. Fast neutrons, alpha, beta and gamma rays all can adversely affect the performance of semiconductor devices by upsetting the charge carrying characteristics. Studies have been conducted in an effort to determine the amount of radiation that is harmful to semiconductor components [14,15]. The chart in Figure 3.1-1 shows the results of tests conducted by ICS Radiation (similiar results were obtained by Sandia National Laboratories). The tests concluded that while permanent damage can occur in devices exposed to large dose rates of ionizing radiation ($> 10^4$ Rads), some sensitive devices (PMOS, NMOS) can be affected by as little as 100 Rads.

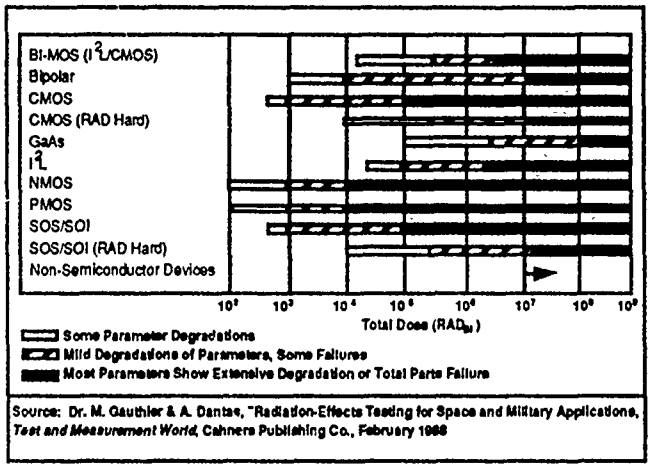

Figure 3.1-1 Total dose radiation analysis of semiconductor technologies

Radiation total dosage measurements were performed during X-ray inspections in this study to attempt to monitor the total absorbed dose received by components. Lithium flouride thermo-luminescent dosimeters (TLD's) were calibrated and used to measure the total incident radiation during radioscopic, CT and laminography scans. The results are summarized below in Figure 3.1-2. CT systems delivered the most dose to the components during CTLAM scanning while radioscopy and SBLAM delivered the least amount of dose. Total dosage depends most strongly upon the inspection time. Optimized inspection routines can be developed to minimize the dose to susceptible components and should be a consideration in X-ray inspection system selection.

System Type	Mode	Energy, Current	Approximate Scan Time	Average Measured Dose*
Radioscopy	RT	120 kV, 0.10 mA	5 min.	275 Rads
Industrial CT	DR	420 kV, 3.5 mA	12 min.	93 Rads
Industrial CT	CT	420 kV, 3.5 mA	60 min.	440 Rads
Industrial CT	CT	420 kV, 3.5 mA	12 min.	40 Rads
SBLAM	LAM	150 kV, 0.1 mA	5 min.	215 Rads
SBLAM	LAM	150 kV, 0.1 mA	0 5 min.	20 Rads

* As measured using calibrated Thermo Luminescent Dosimeters

Figure 3.1-2 Radiation dose measurements

3.2 Solder Defect Criteria

Imaging of subtle solder bond features requires the maximum performance of any inspection system. Typical features of interest such as cracks and disbonds are in the range of 0.013 mm (0.0005 inch) and greater, and pose a challenge. Visual inspection techniques could suffice in most instances to evaluate important solder quality criteria such as solder volume and shape of the solder joint. The primary issues surrounding solder bond quality are:

- Solder volume/shape
- Insufficient solder
- Excess solder
- Bridging
- Solder balls, spikes and unwanted solder
- Fillet height along the solder castellation.

X-ray techniques can also inspect for these characteristics with greater ease and automation than visual, making their development of keen interest to the electronics industry. The X-ray methods can detect bonds hidden behind most packages that visual cannot. The significant advantage of X-ray methods is the potential of automating the solder inspection through image analysis algorithms.

Voiding in the bond is also detectable with X-rays, though there is no significant evidence that voids are really a problem for solder integrity.

3.3 Test Results

Circuit boards were initially screened using radiography and radioscopy prior to CTLAM and SBLAM inspections. CT inspections were not conducted for solder bond analysis due to the unavailability of sufficiently high resolution CT systems during the period of this study. Defect correlation was conducted on a small sample of inspected bonds. Destructive tests were reserved for further study when data from very high resolution (greater than 10 lp/mm) CT systems becomes available.

Voids, however, remain a concern for manufacturers because excessive voiding obviously reduces the quantity of bonding material present in the joint. There is also the potential for voids to act as initiation points for cracks, particularly when they are near component edges. Conversely, it has been suggested that solder voids may serve as fatigue crack growth stoppers; no definitive research has confirmed this. Cracks are generally not a problem with production inspection because they result primarily from operational and environmental cycling.

3.3.1 Single-Sided Test Boards

3.3.1.1 Phantom Circuit Board (PID #010104)

The printed circuit board in Figure 3.3-1 is the test phantom board used in quantifying solder ball sensitivity, void detectability and measurement characteristics of the systems used. The board consists of an LCC and "J" leaded package vapor phase soldered to a standard epoxy (FR-4 type) board. The board contains solder balls ranging from 0.1 to 1.0 mm (0.004 - 0.040 inch) in diameter. The phantom board was examined by radioscopy, CT laminography and scanned beam laminography. The phantom board was examined using CT during the Task 1 "CT of Electronics" [1] study and the results are documented in that report.

The phantom board was initially radiographed; an enlargement of the LCC from the radiograph is shown in Figure 3.3-2. The radioscopic images in Figures 3.3-3 and 3.3-4 show a portion of the

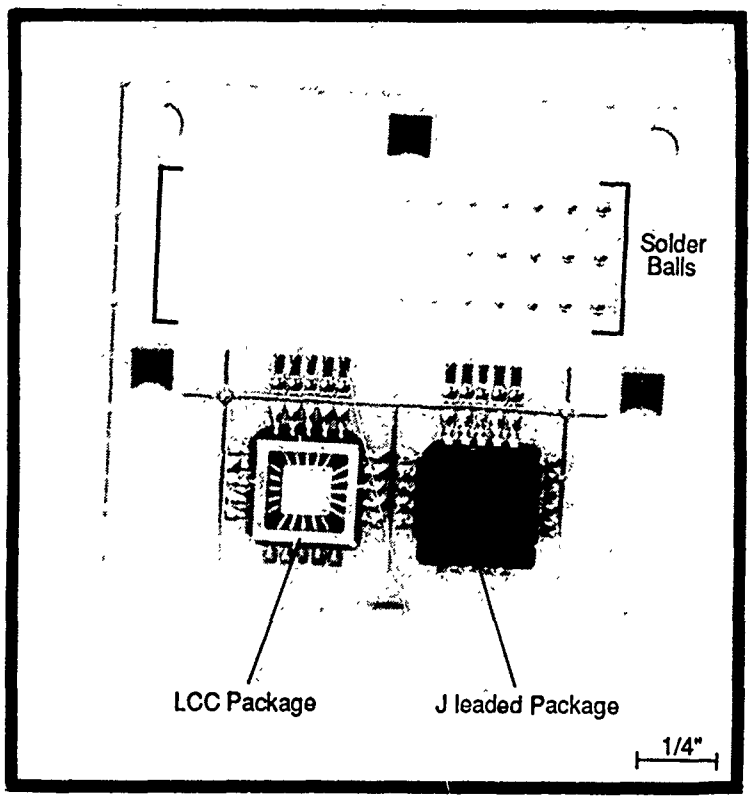

Figure 3.3-1 Photograph of phantom circuit board

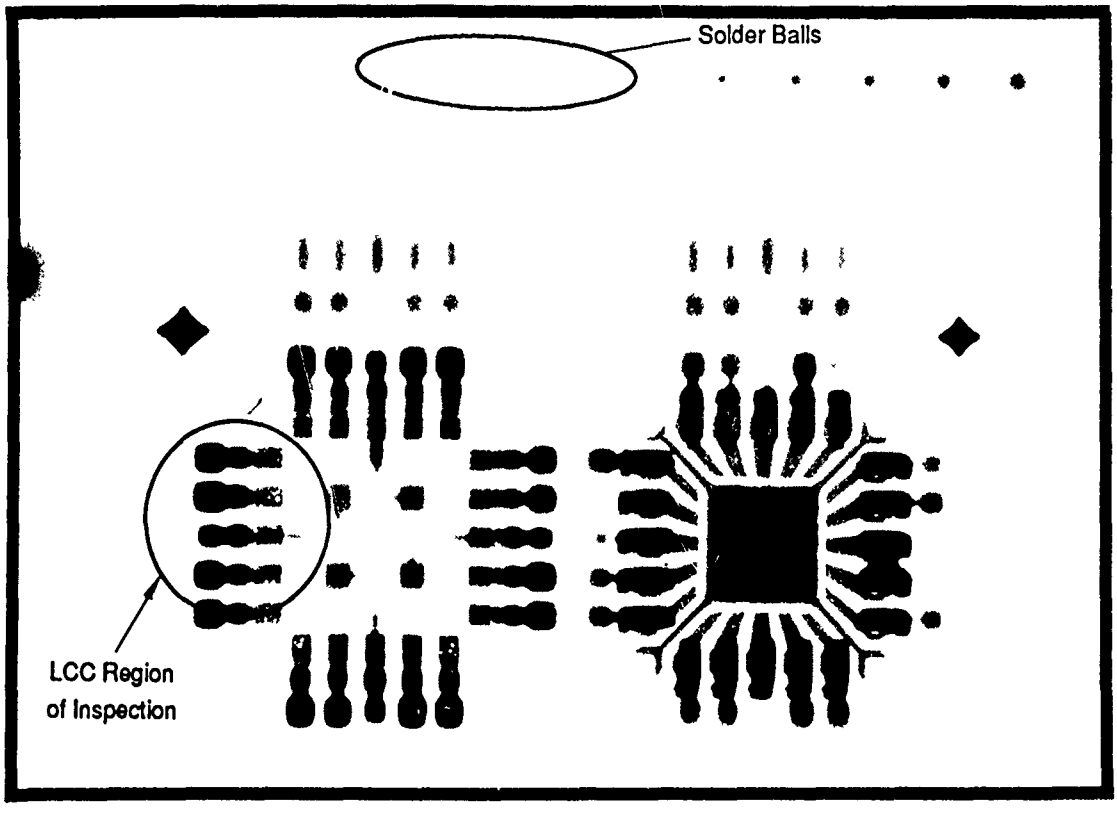

Figure 3.3-2 Film radiograph of phantom board

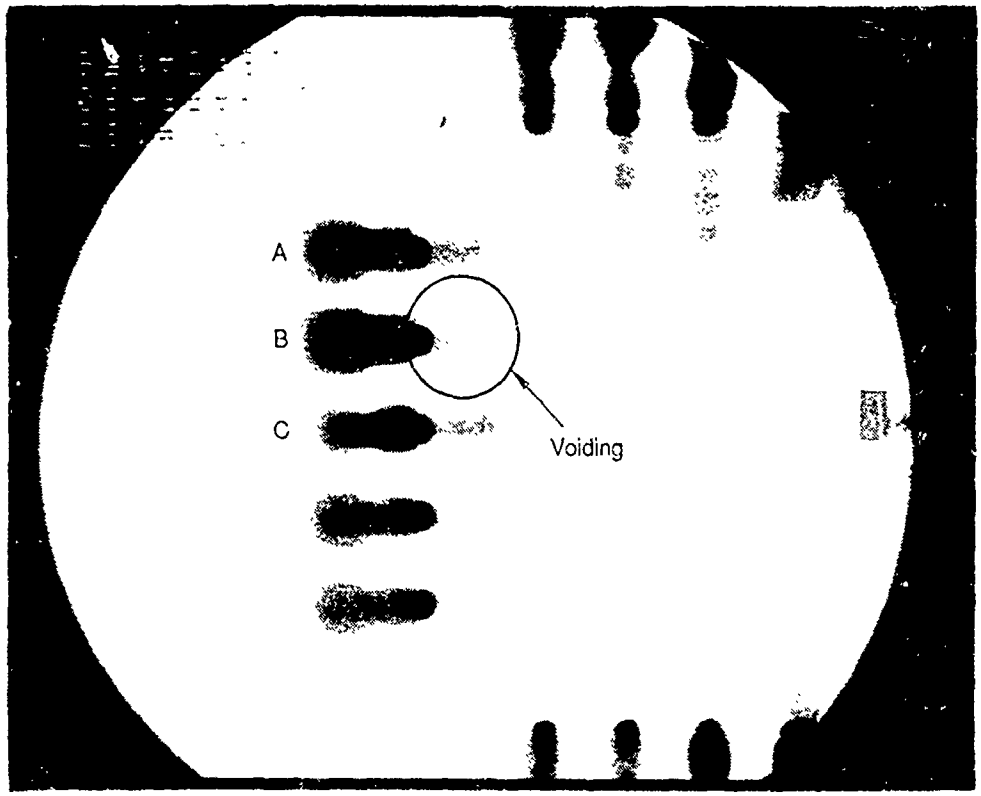

Figure 3.3-3 Radioscopic image of LCC showing solder voids

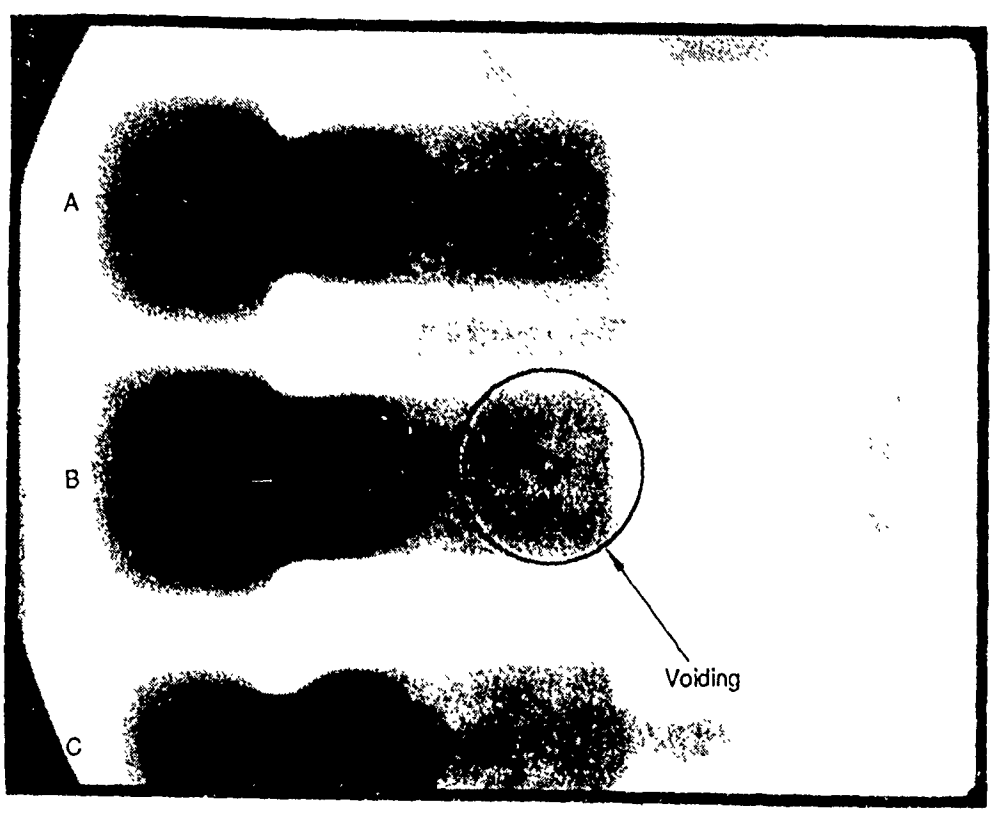

Figure 3.3-4 Zoom of radioscopic image of LCC showing solder voids

LCC solder pads taken on two different radioscopy systems. The two radioscopy systems used in this study show basically equivalent image quality for the details in the phantom board. The radioscopic images are nearly as sensitive as the Figure 3.3-2 radiograph. Both radioscopy systems resolved the solder balls down to 0.1 mm (0.004 inch). Solder voids under the LCC packages were resolved down to an estimated 0.05 to 0.25 mm (0.002 to 0.010 inch). Simulated bridging, approximately 0.05 mm (0.002 inch) wide, was identified by both systems with about the same image clarity. The radioscopic image of simulated bridging is shown in Figure 3.3-5a. Figure 3.3-5b is an edge enhanced image of Figure 3.3-5a.

Using CTLAM the phantom board was imaged on a high-resolution (4 lp/mm) CT system with laminographic reconstruction capability. A sequence of 24 digital radiograms (DR) were taken, with the object rotating several degrees between each. The data was then backprojected to form the image shown in Figure 3.3-6. Gross features can be identified in the CT laminographic image set; however, there is insufficient resolution to identify the features such as the simulated bridging and internal voids.

Laminograms, taken on the scanned beam laminography system, clearly reveal all of the solder balls, simulated bridging and internal solder voiding under the LCC package of the phantom board. Figure 3.3-7 is a laminogram which identifies internal solder voids under the LCC on the order of 0.1 mm (0.004 inch).

3.3.1.2 TRW Test Board (PID #010114)

The PWA shown in the Figure 3.3-8 photograph was specially designed by TRW for testing the SMT manufacturing process and features a variety of package styles [16]. Among the SMT styles are LCC's, "J" leaded, gull wing packages and several different discrete components all mounted on a board constructed of standard epoxy (FR-4) fiberglass in six layers. It contains conductive traces as well as reference patterns and is electrically functional for continuity testing. The broad based composition of this board makes it ideally suited for testing the capabilities of various X-ray inspection techniques.

The TRW assembly was built at Boeing into three different board thicknesses. The traces are separated by epoxy and prepreg of equal thicknesses. The board design is shown in the cross-section view in Figure 3.3-9. The boards are numbered by a first digit which refers to the spacing between copper traces in thousandths of an inch and a dash number for the board serial number. By convention, the integrated circuits for the assemblies are designated by "U" numbers.

Using film radiography, 23 boards were initially screened by certified level III radiographers experienced in PWA inspection. Prior to CTLAM and SBLAM testing, additional inspections were performed using a 5-axis radioscopy system to determine the optimum test boards. Test boards were selected on the basis of defect content and variety. Principal boards contained solder bonds with no defects to varying degrees of voiding, solderballs and bridging as well as lead placement. Four principal TRW single-sided test boards were selected, board numbers 8-4, 12-5, 16-4, 16-5.

Figure 3.3-10 is a radiograph of test board 16-5. Inspections on test board 16-5 at LCC package U12 using a radioscopy system are shown in Figure 3.3-11a. An enlargement of four pads on the right of the package is shown in Figure 3.3-11b. The images clearly show the presence of significant solder voiding with detail on the order of 0.025 mm (0.001 inch). The metallurgical analysis of the package (U12) in Figure 3.3-12 for comparison show average void sizes to be roughly 0.06 to 0.2 mm (0.0025 to 0.008 inch) in diameter on 0.6 mm (0.025 inch) pads. The same package (U12) is shown in the SBLAM image in Figure 3.3-13. The SBLAM system distinguishes the major voiding pattern but with less detail sensitivity than the radioscopy.

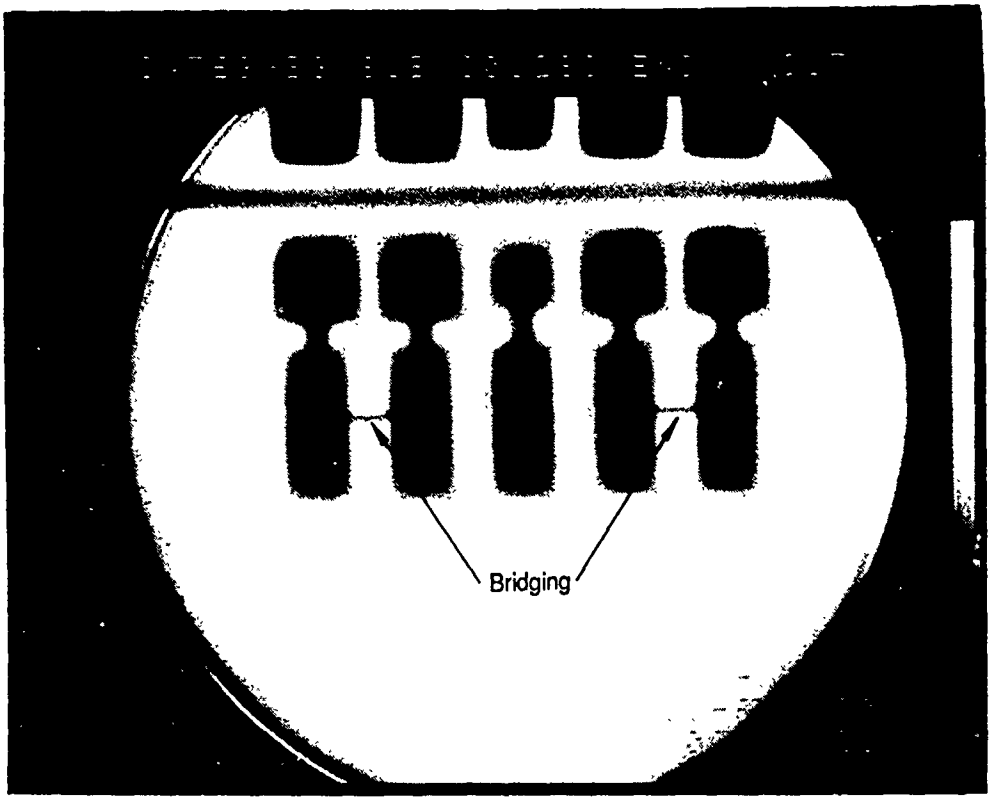

Figure 3.3-5a Radioscopic image of simulated bridging

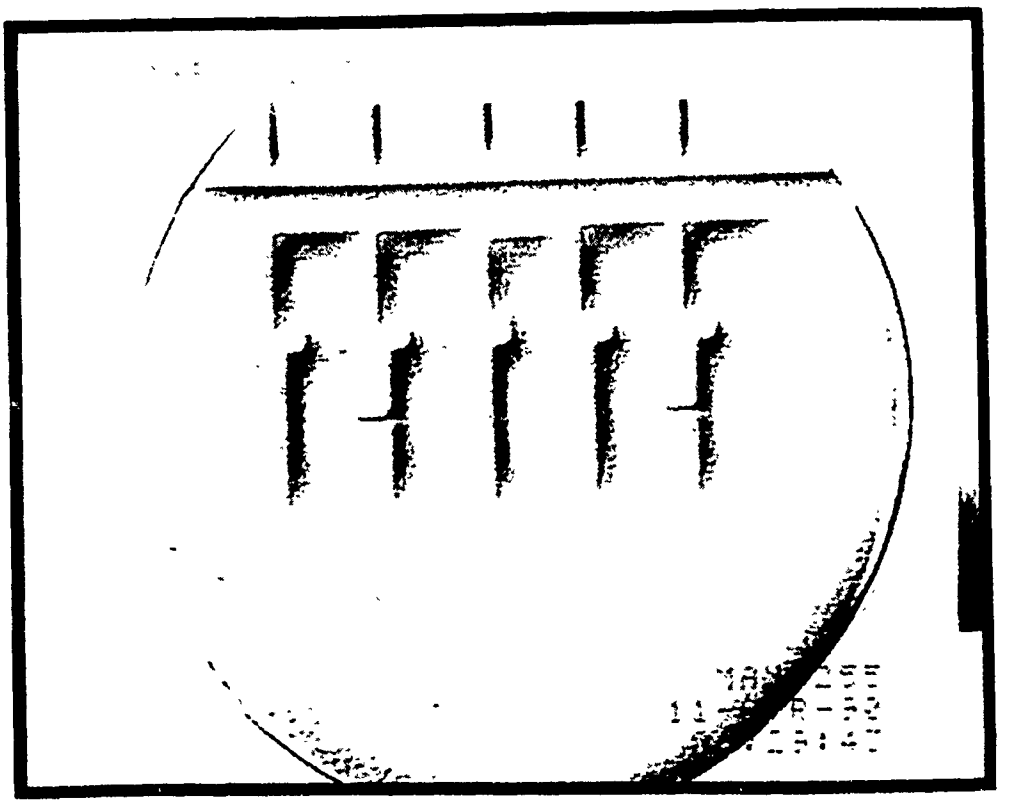

Figure 3.3-5b Edge enhanced radioscopic image of bridging

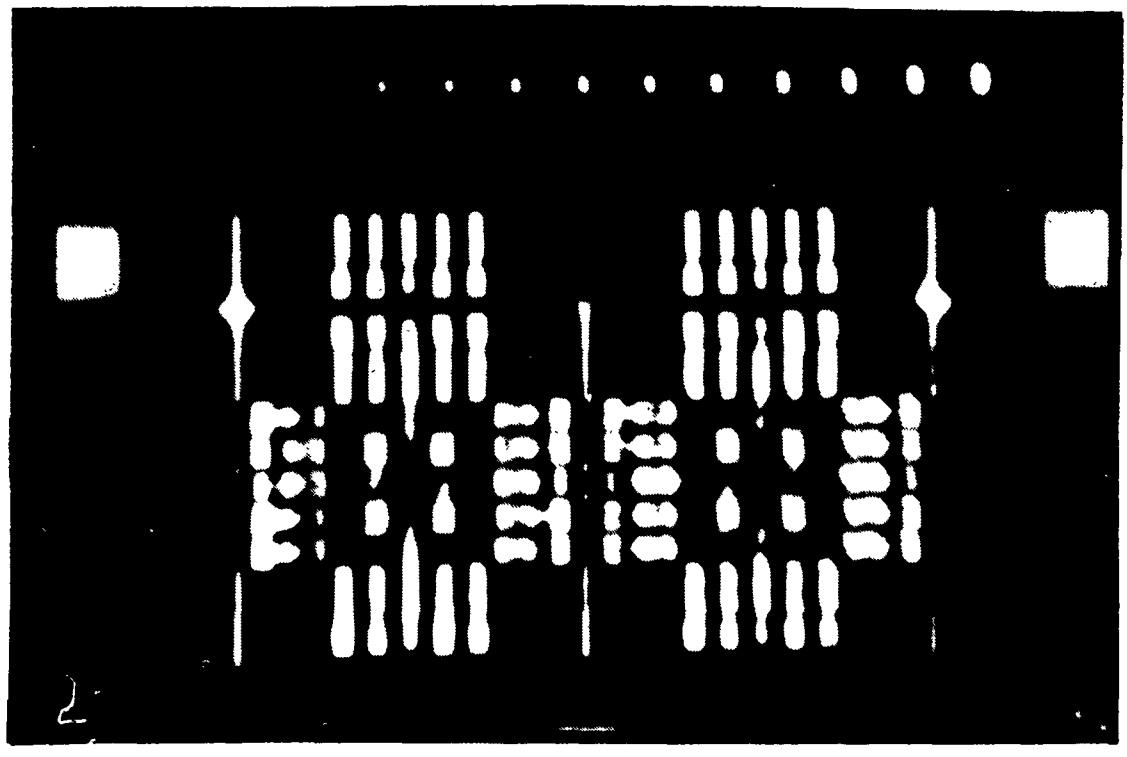

Figure 3.3-6 CTLAM of phantom board

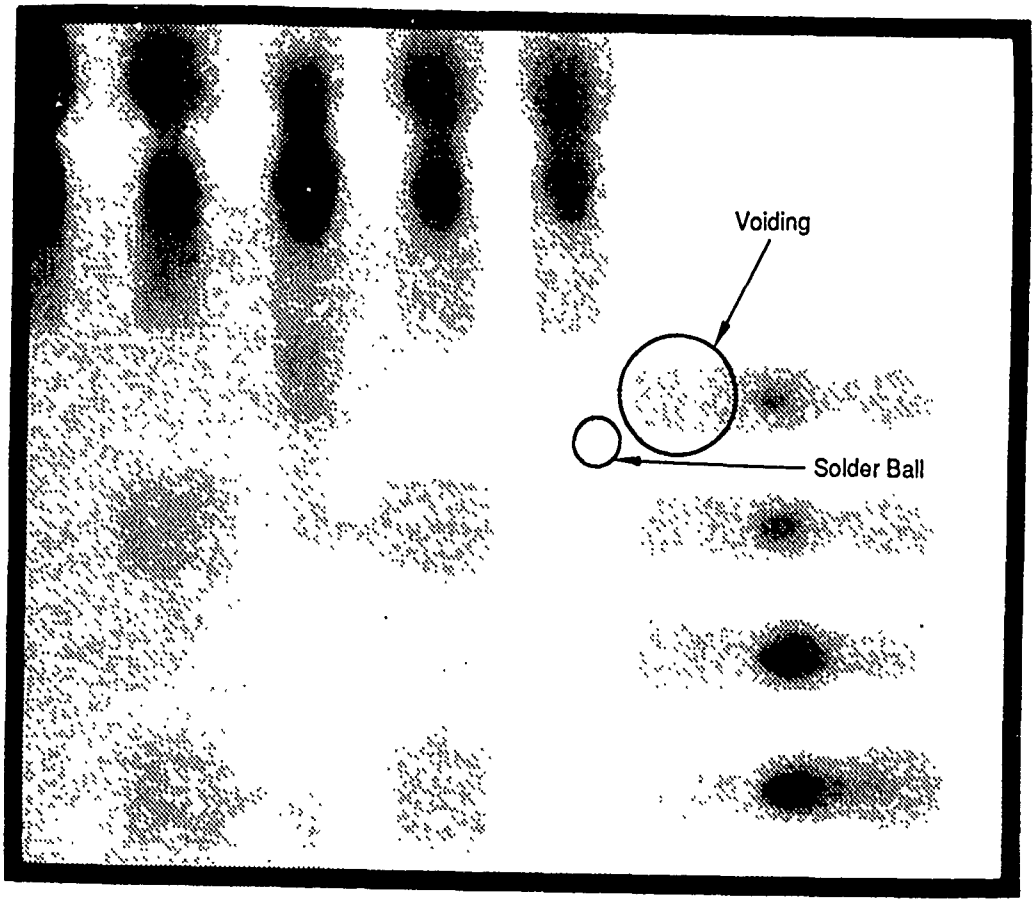

Figure 3.3-7 SBLAM image showing LCC voids on phantom board

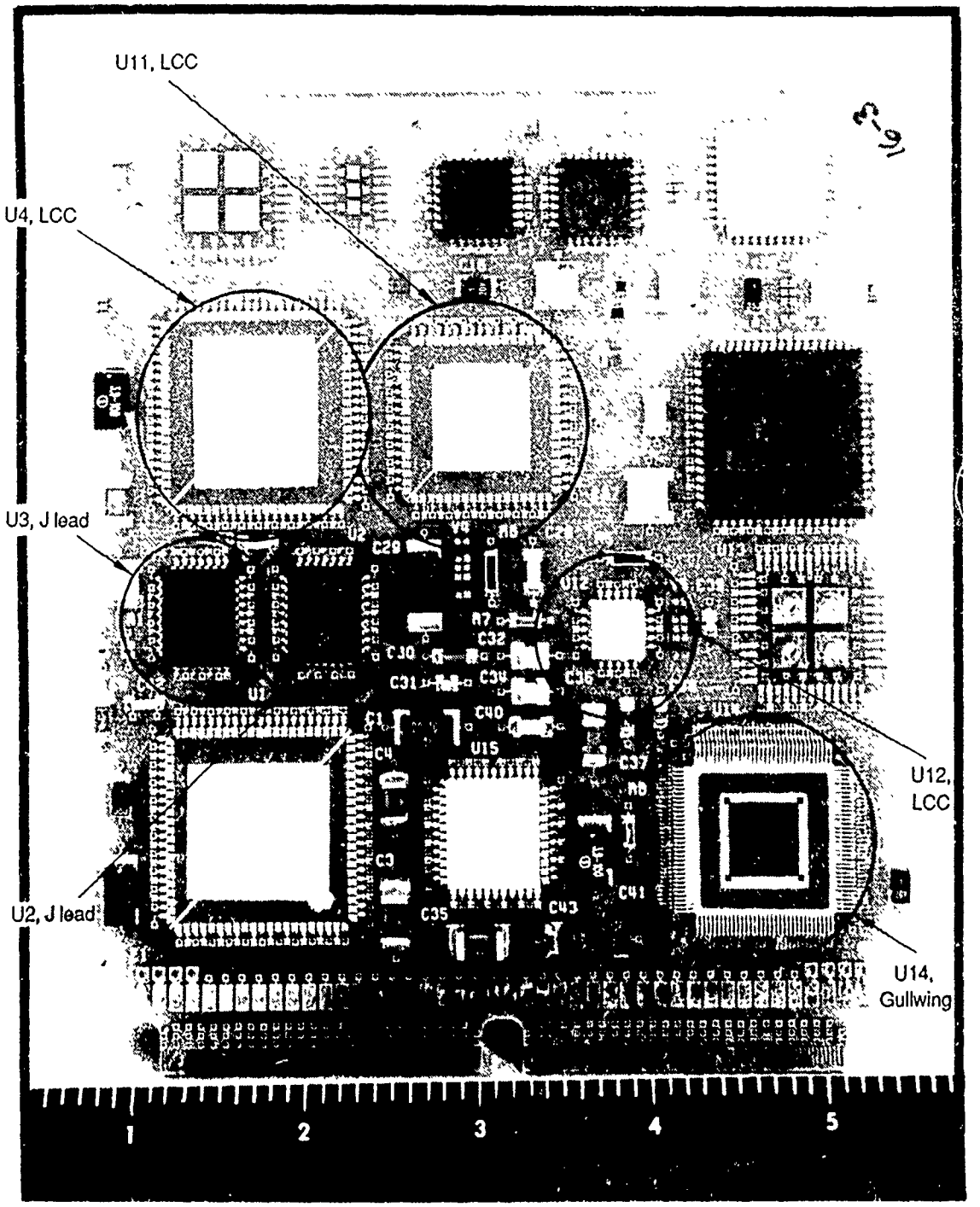

Figure 3.3-8 Photograph of TRW PWA

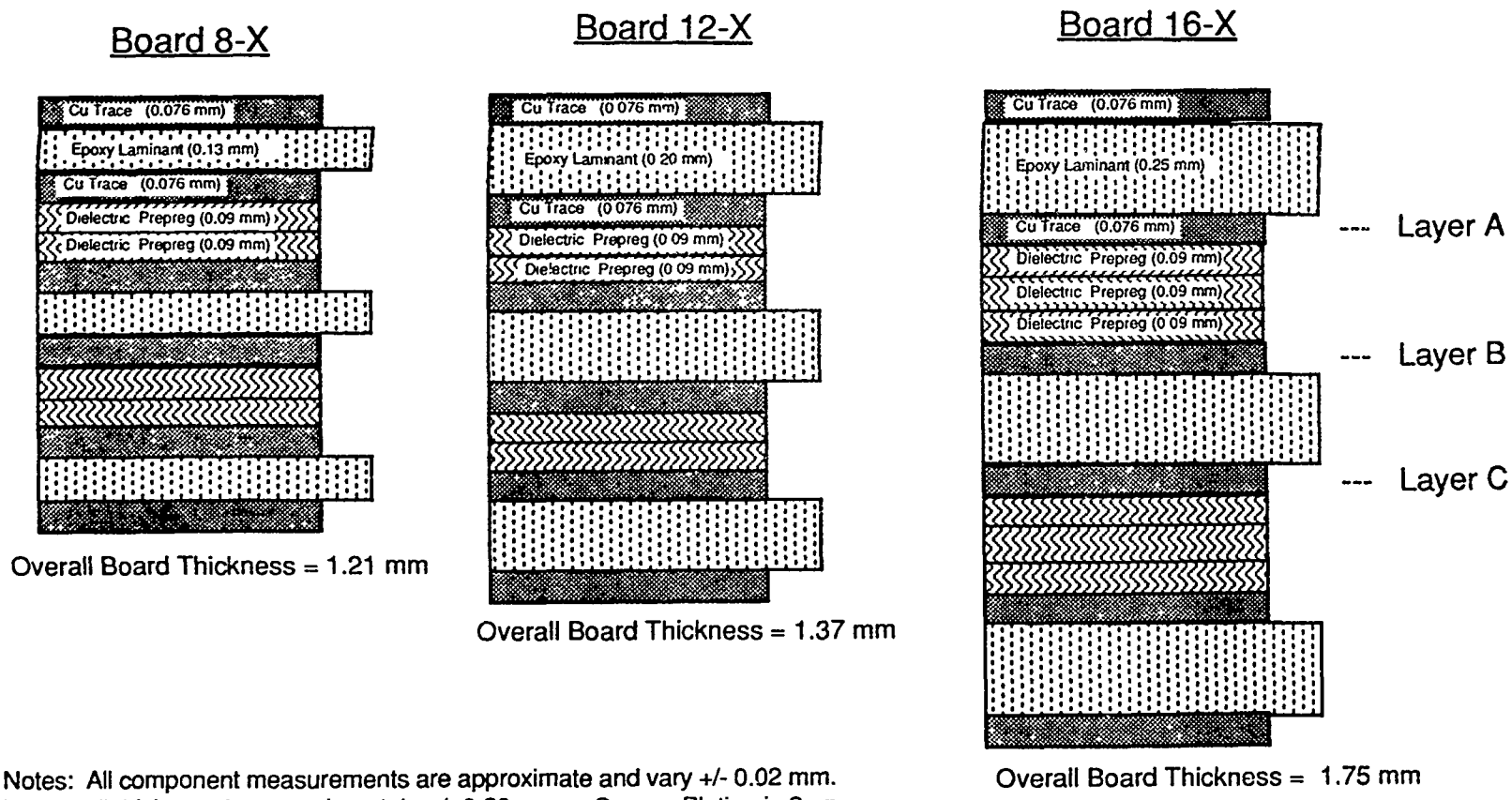

* Notes: All component measurements are approximate and vary +/- 0.02 mm.
The overall thickness is approxiamately +/- 0.20 mm. Copper Plating is 2 oz.

Figure 3.3-9 Cross-Section Layup of TRW Board

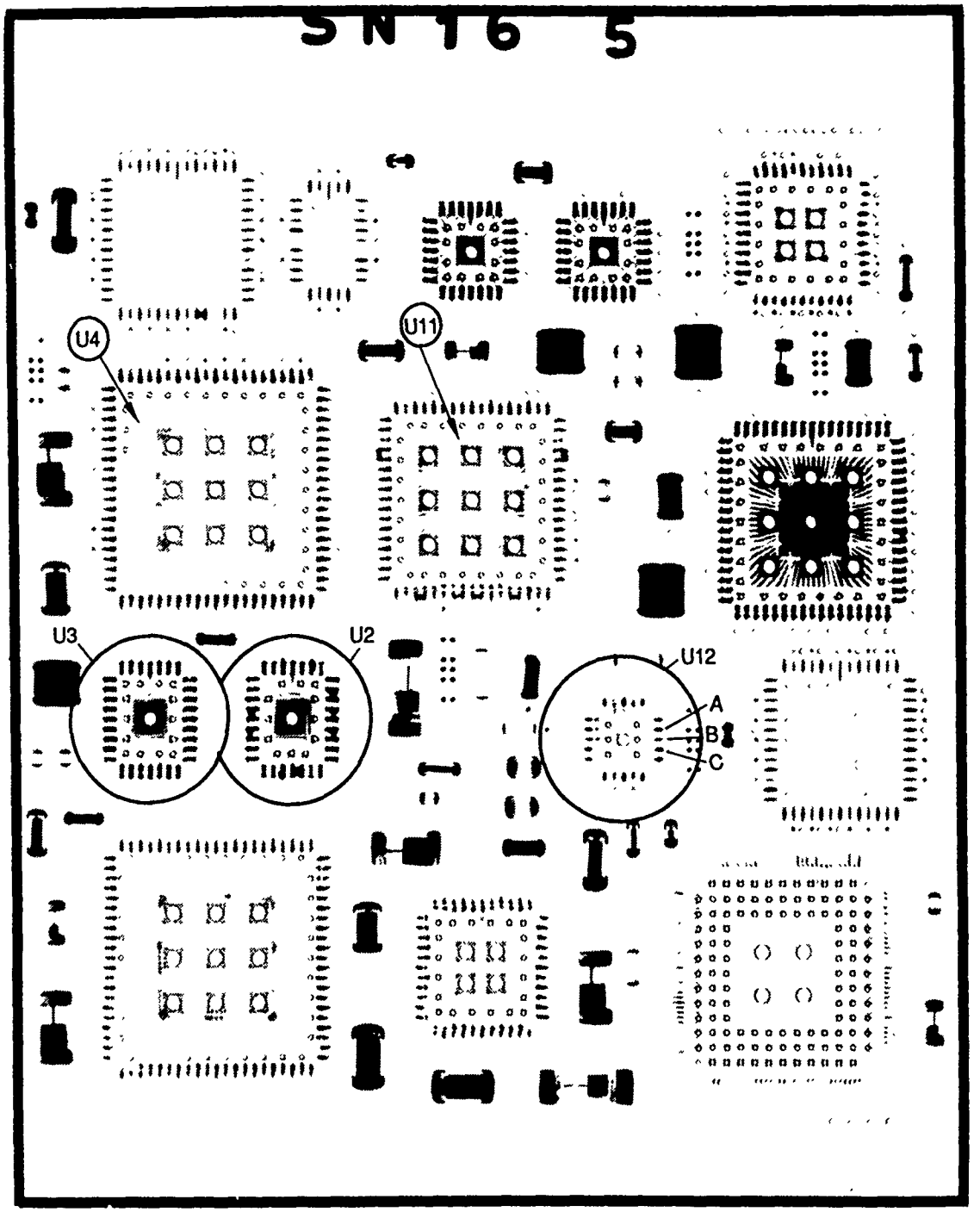

Figure 3.3-10 Film radiograph of test board No. 16-5

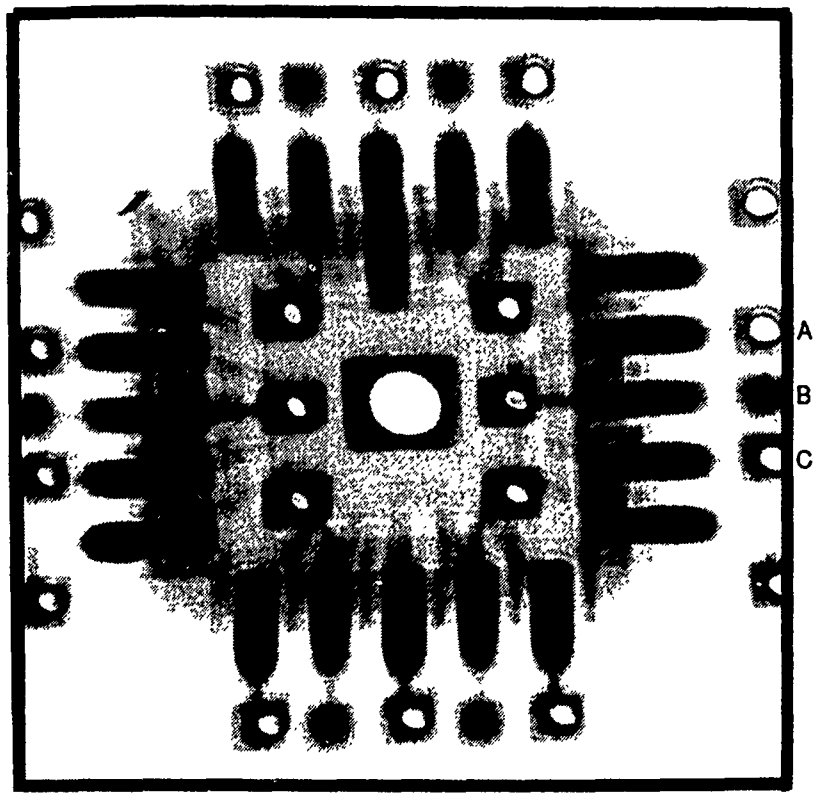

Figure 3.3-11a Radioscopic image of LCC U12 on TRW board no. 16-5

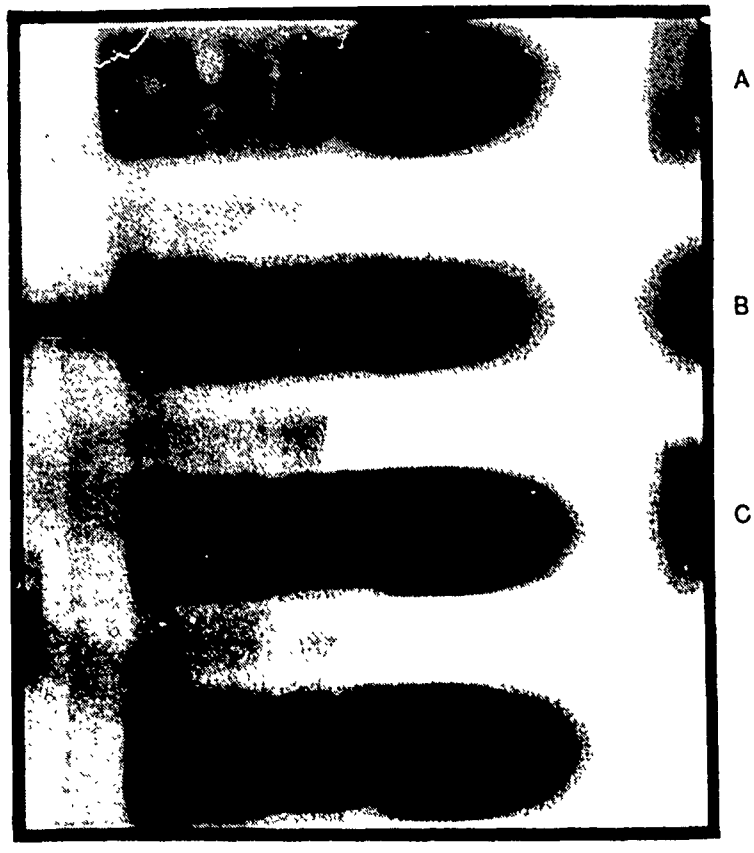

Figure 3.3-11b Enlargement of right side of LCC U12

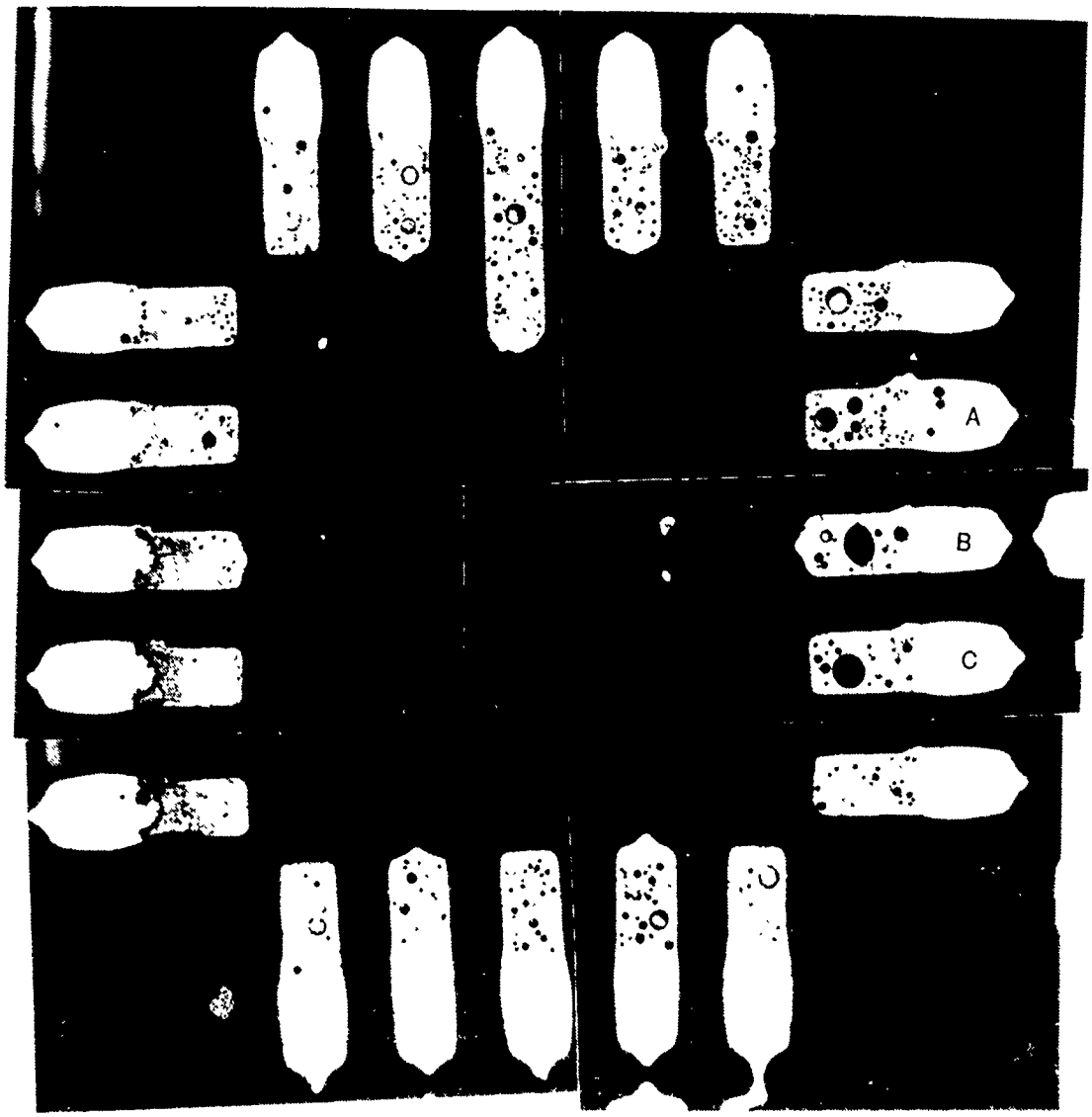

Figure 3.3-12 Metallurgical section of LCC U12

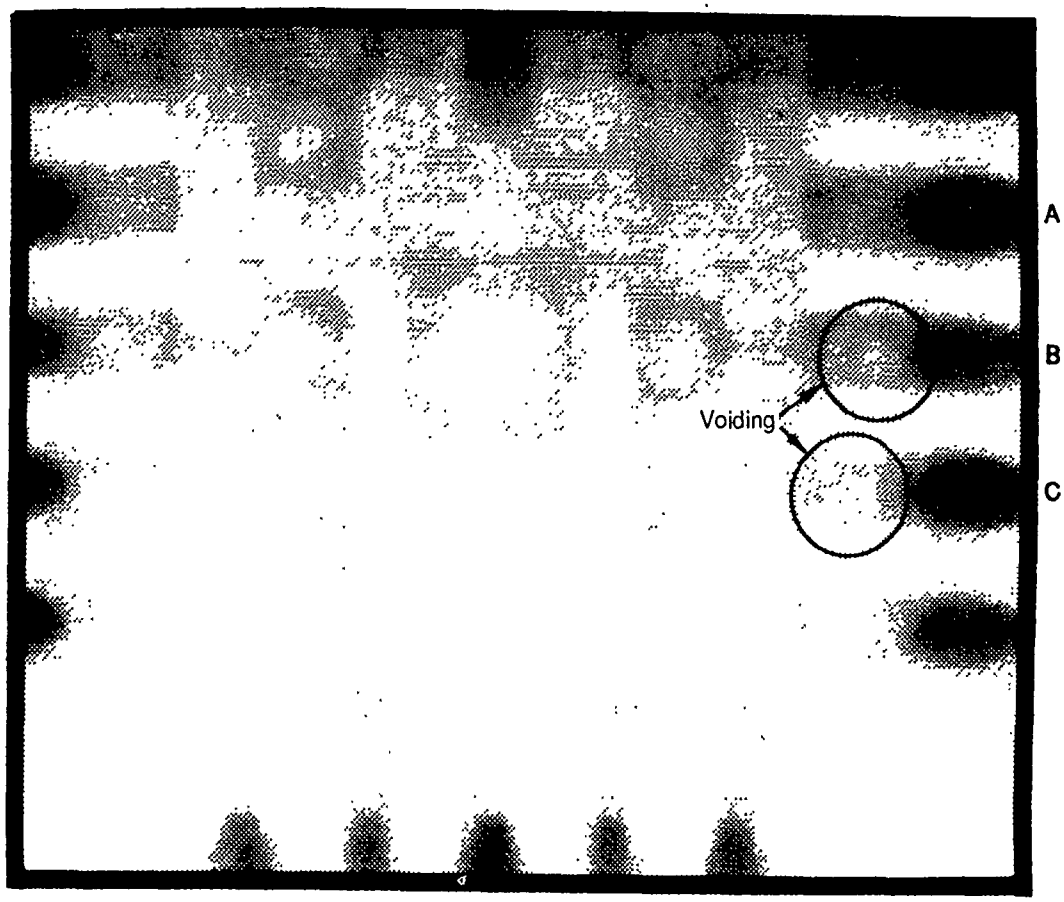

Figure 3.3-13 SBLAM image of LCC U12

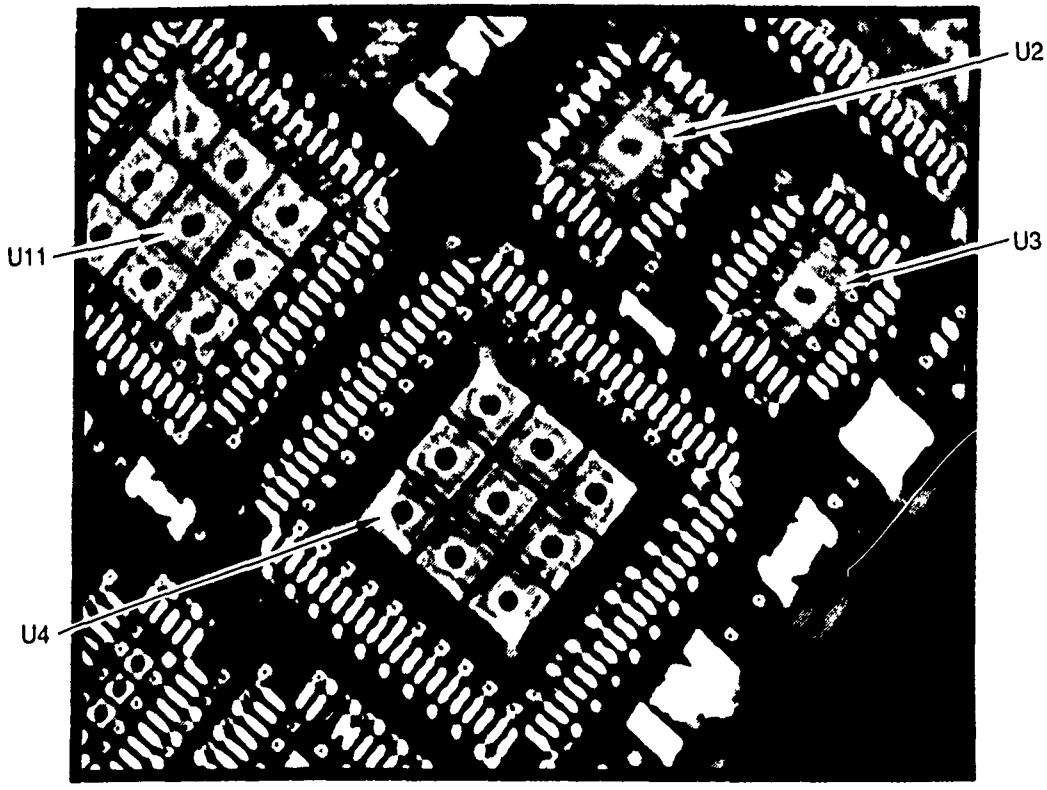

Figure 3.3-14 CTLAM image of TRW board

CTLAM on test board 16-5 at location U2, U3, U4, and U11, shown in Figure 3.3-14, is able to outline the package and solder locations but is unable to identify the internal voiding.

3.3.2 Double-Sided Circuit Board Inspections

Double-sided versions of the TRW boards having the same overall thickness were produced containing a 3.7 mm (0.15 inch) aluminum core. The double-sided boards with an aluminum core increased the level of inspection difficulty from that of the single-sided case previously discussed. The addition of an aluminum core decreased the X-ray through transmission intensity by 20 percent, making imaging more of a challenge. The final board examined in this section contained a copper-invar-copper (CIC) core which decreased the X-ray through-transmission by nearly 80 percent relative to the single-sided case (and a factor of 4 over the aluminum core example) and proved to be an even greater challenge.

3.3.2.1 TRW Test Assembly with Aluminum Core (PID #010116)

The double-sided TRW test assembly with an aluminum core was constructed using two TRW boards, numbers 12-3 and 12-4. The assembly is shown in the Figure 3.3-15 photograph. The radiograph is shown in Figure 3.3-16 with LCC U7 on board 12-3 in the upper right corner. The overlapping features in the radiograph make interpretation difficult. A radioscopic image, Figure 3.3-17, shows LCC U7 from board 12-3 and U5 (package not mounted) from board 12-4, one on each side of the double-sided board assembly. The units are superimposed over each other making the identification of defects on the solder pads a challenge. Note how the separation of the solder pads on one side are difficult to distinguish from LCC pads on the opposite side. When the same view is tilted the packages become more separated alleviating some of the superpositioning between solder joints of interest (Figure 3.3-18). Figures 3.3-19 and 3.3-20 show the effect of tilting a "J" leaded package U3 with LCC package U12 on the opposite side. The imaging of solder voiding is improved by tilting but the overall inspection process becomes more time consuming as the system is manipulated to achieve the best possible viewing angle.

Figure 3.3-21 is a radiograph of LCC U12 and "J" leaded package U3 superimposed over each other, one on each side of the assembly. Scanned beam laminography was performed in a region of these packages. Figure 3.3-22 shows a portion of the LCC package containing solder voiding. The "J" leaded package is imaged by "focusing" the laminographic plane to the opposite side of the board as seen in Figure 3.3-23. The system acquired these images in about 10 seconds apiece in the manual mode. It identifies solder voids in the order of 0.15 mm (0.006 inch) as measured on digitally stored images during post-analysis. For this double-sided case, the laminography shows the features of interest such as solder shape, solder volume and voiding under LCC packages with adequate sensitivity and without the confusion of superposition or parallax found in the radioscopic images.

3.3.2.2 Double-Sided Military Assembly with CIC Core (PID #010105)

The most difficult PWA inspected was a test assembly simulating a 12-layer board containing a copper-invar-copper (CIC) clad core 1.6 mm (0.063 inch) in thickness. The test assembly was sectioned for testing purposes. Figures 3.3-24a, b and c are photographs of the sectioned assembly. The double-sided assembly with CIC core was inspected with film radiography and shown in Figure 3.3-25 with orientation keyed to Figure 3.3-24a. The solder bonds imaged using film radiography are more difficult to interpret on this assembly than the aluminum core assembly. Not only are the components superimposed but the high X-ray energies necessary for penetration diminished the contrast sensitivity. Similar results were produced with the radioscopic systems and image quality was poor. Figure 3.3-26 shows a radioscopic image of a region of interest on

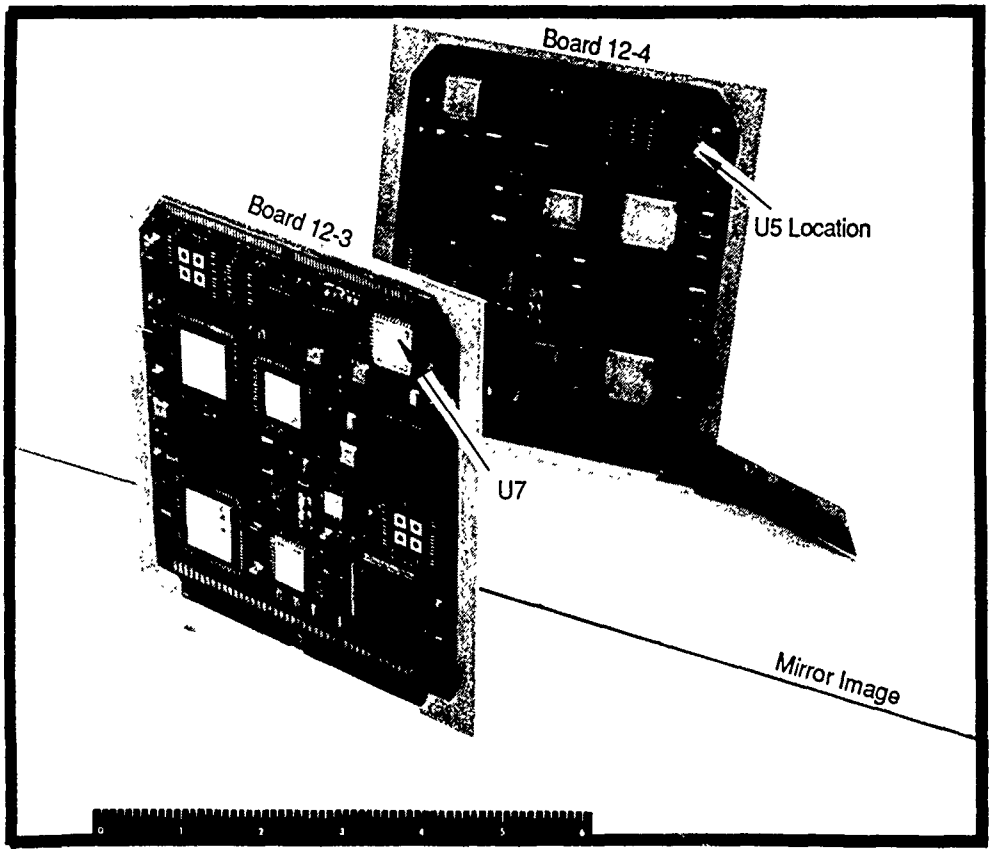

Figure 3.3-15 Photograph of double-sided TRW assembly

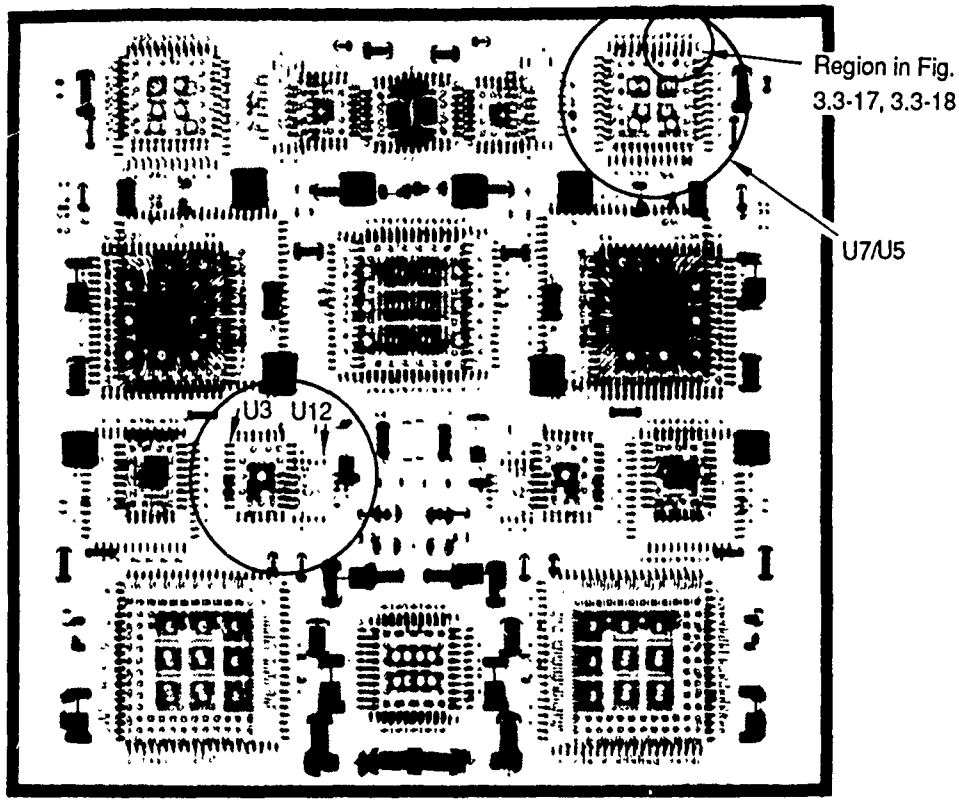

Figure 3.3-16 Radiograph of double-sided TRW assembly of board 12-3 (front), 12-4 (back)

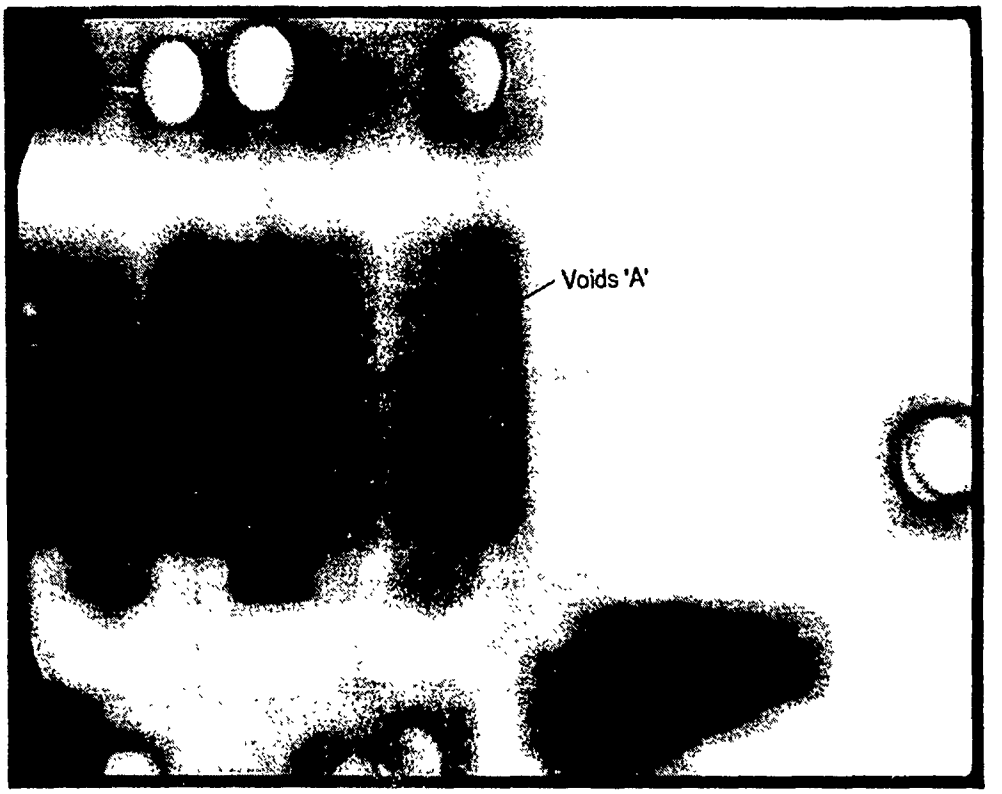

Figure 3.3-17 Radioscopic image of double-sided assembly showing LCC (U5/U7) of board 12-3/4

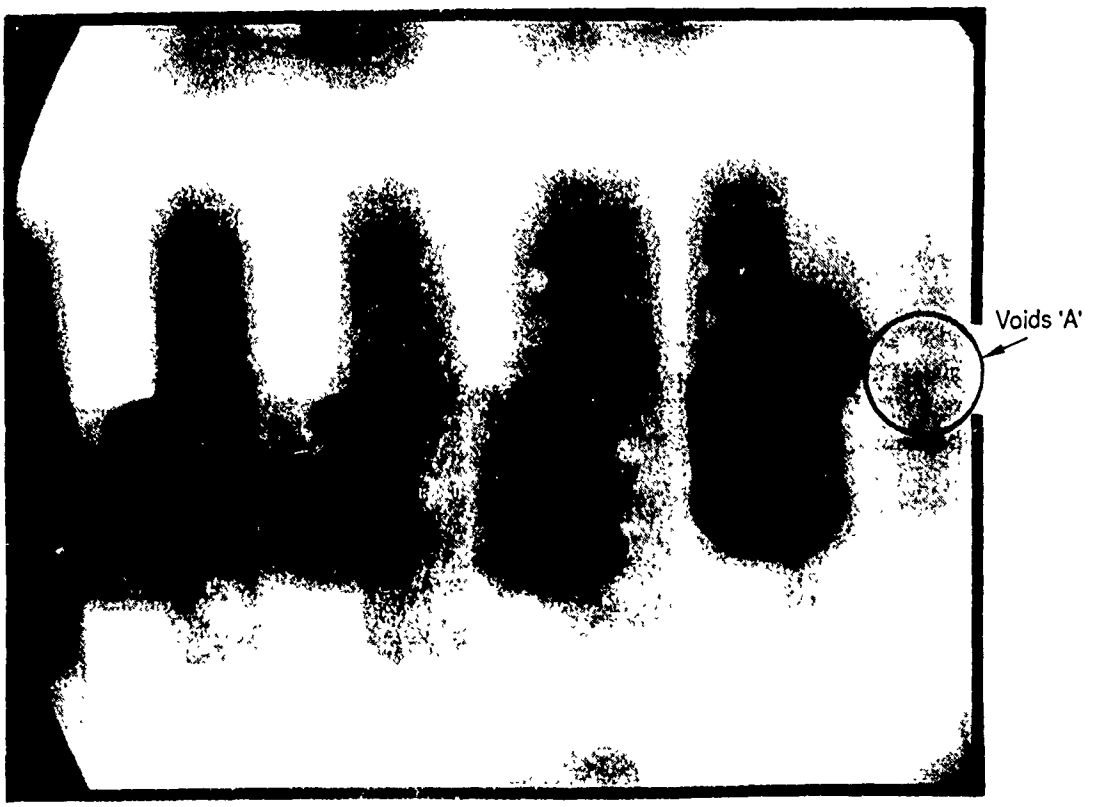

Figure 3.3 18 Radioscopic image of double sided assembly showing tilted view of LCC (U5/U7) of board 12-3/4

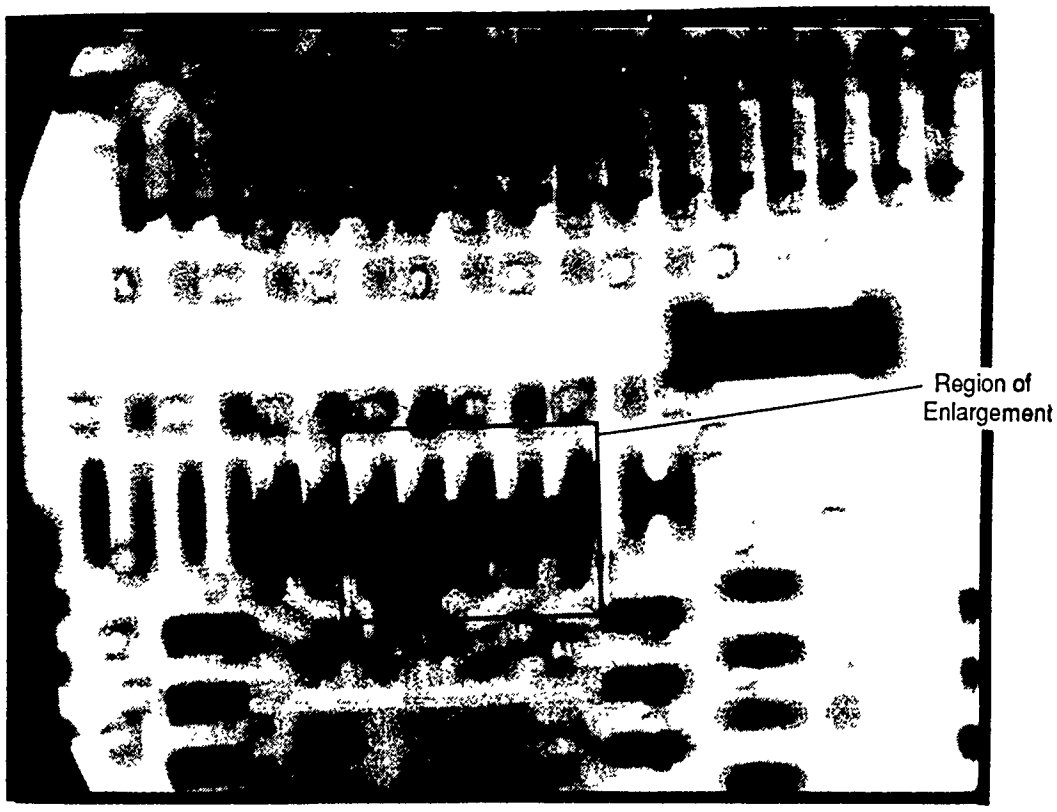

Figure 3.3-19 Radioscopic image of double-sided assembly with J leaded package U3

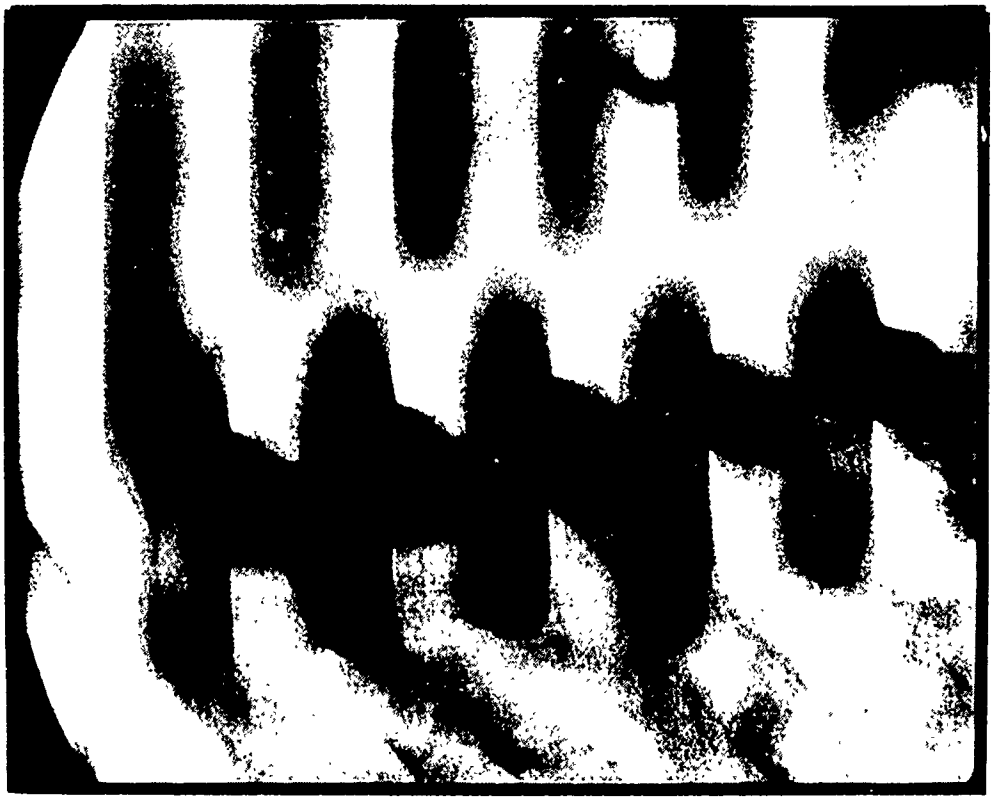

Figure 3.3-20 Radioscopic image showing tilted view of double-sided assembly with J leaded package U3

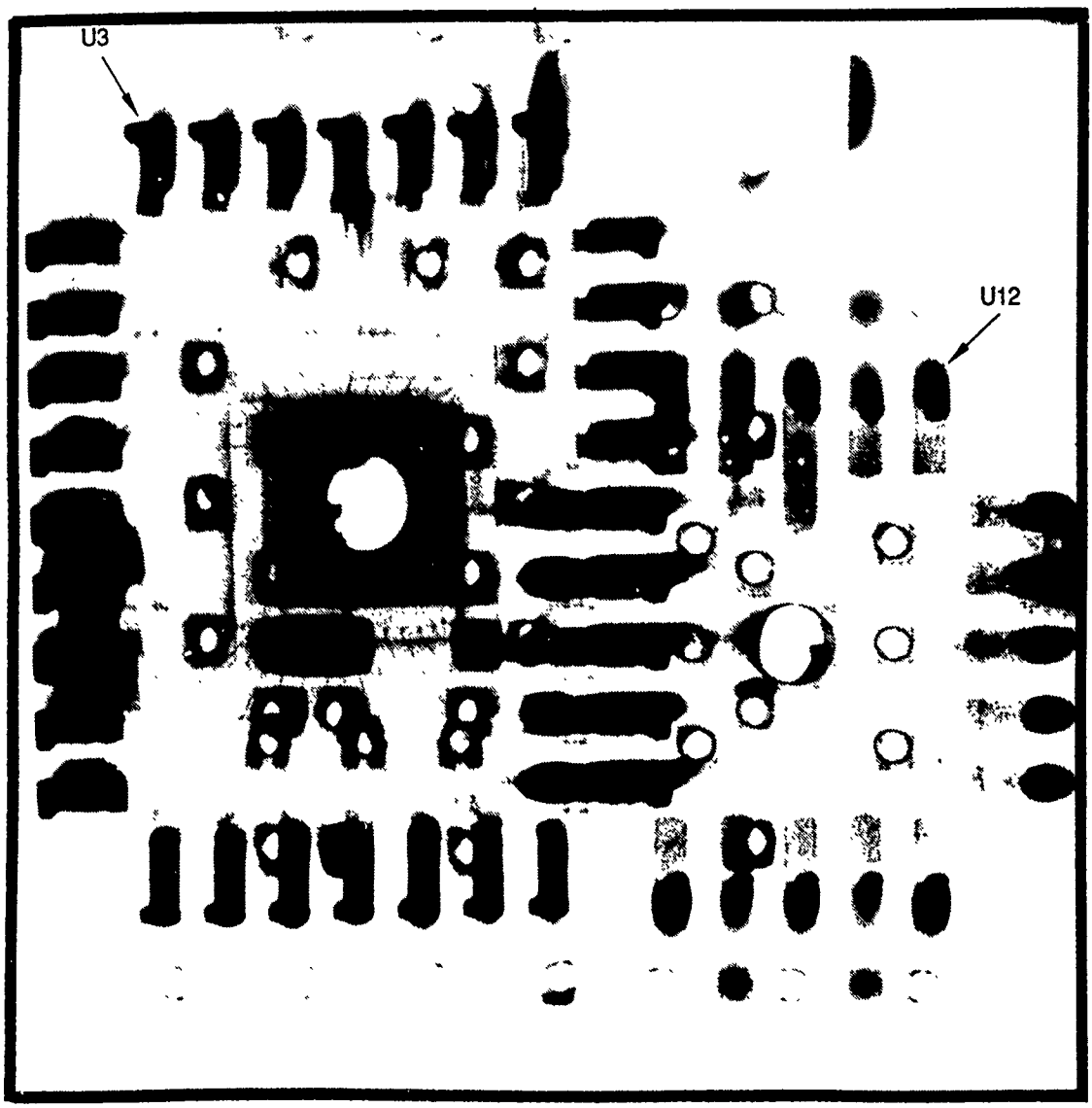

Figure 3.3-21 Radiograph of superimposed LCC U12 and J leaded package U2

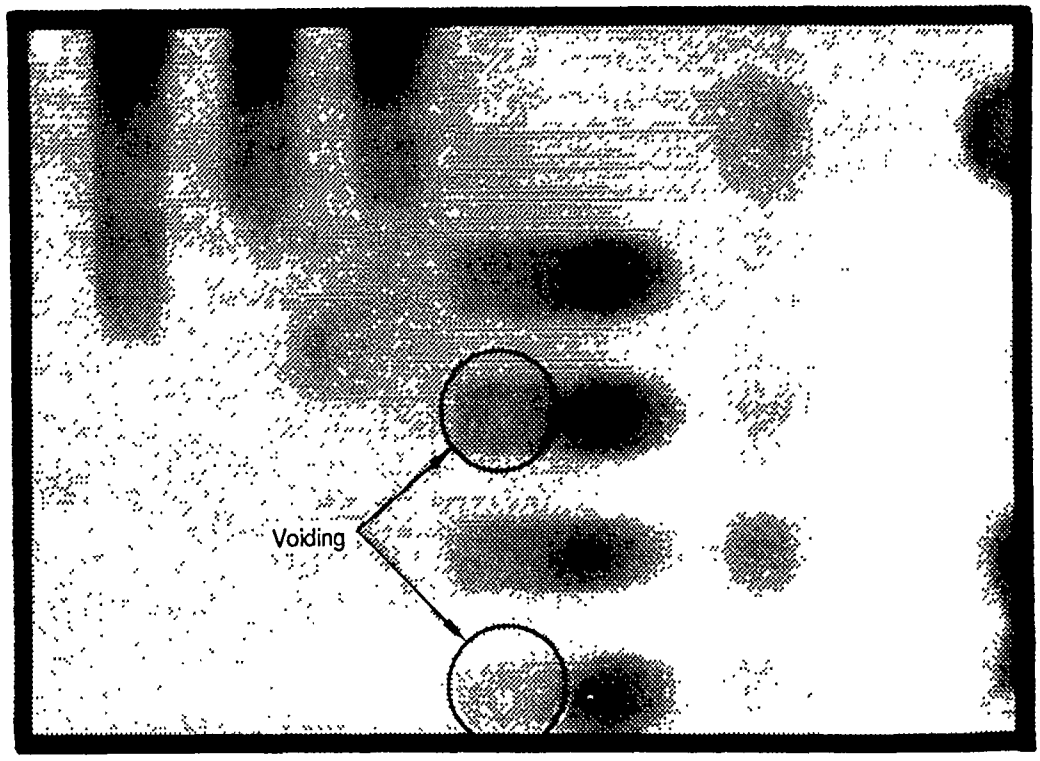

Figure 3.3-22 SBLAM of LCC U12

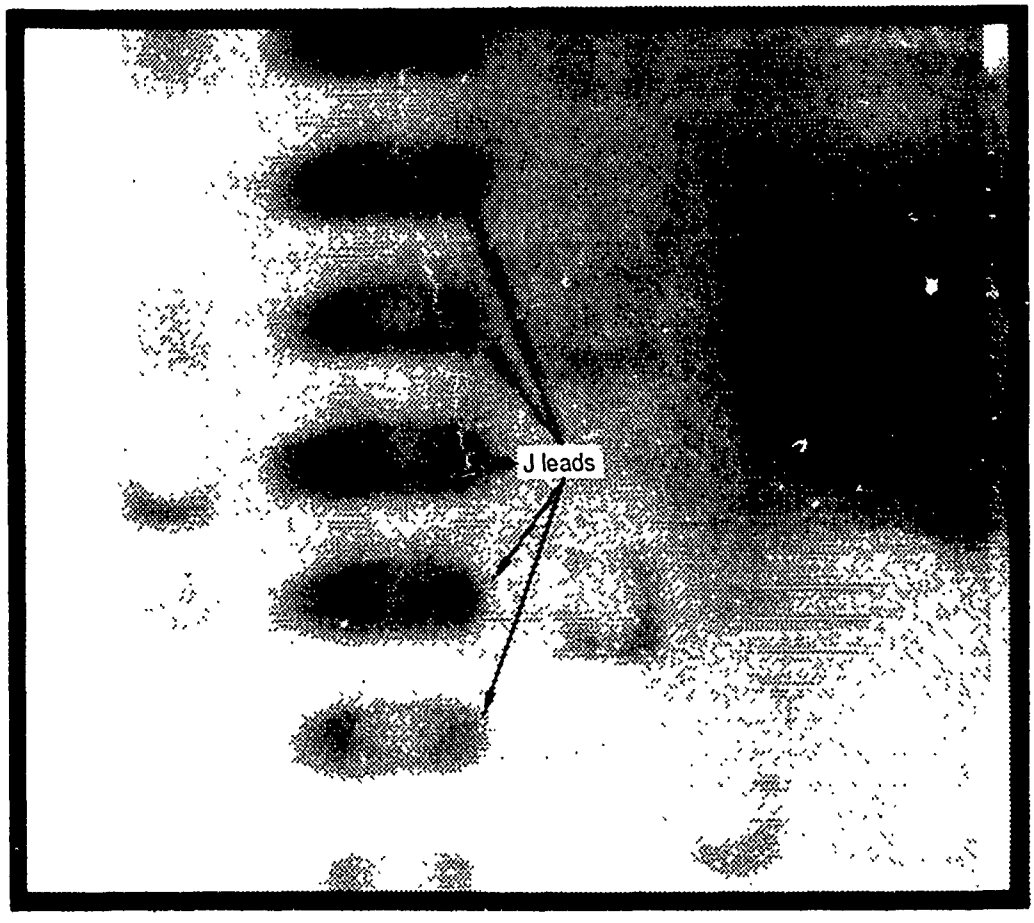

Figure 3.3-23 SBLAM of J leaded package U3

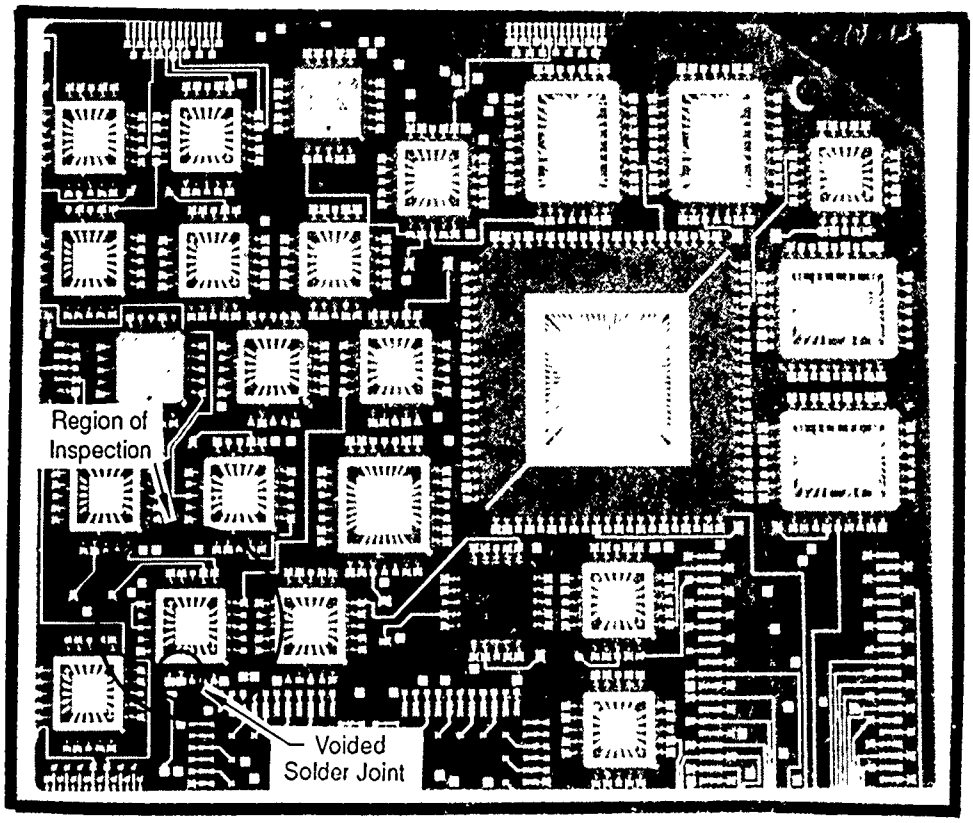

Figure 3.3-24a Photograph of sectioned CIC printed wiring assembly (side 1)

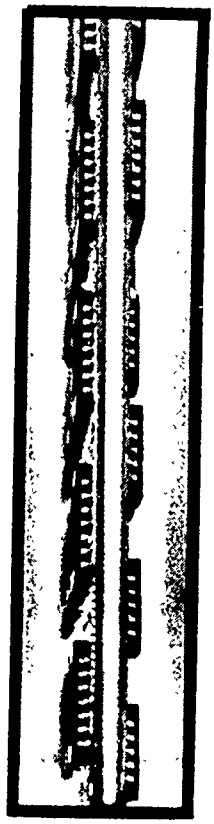

Figure 3.3-24c

Side view of sectioned CIC printed wiring assembly

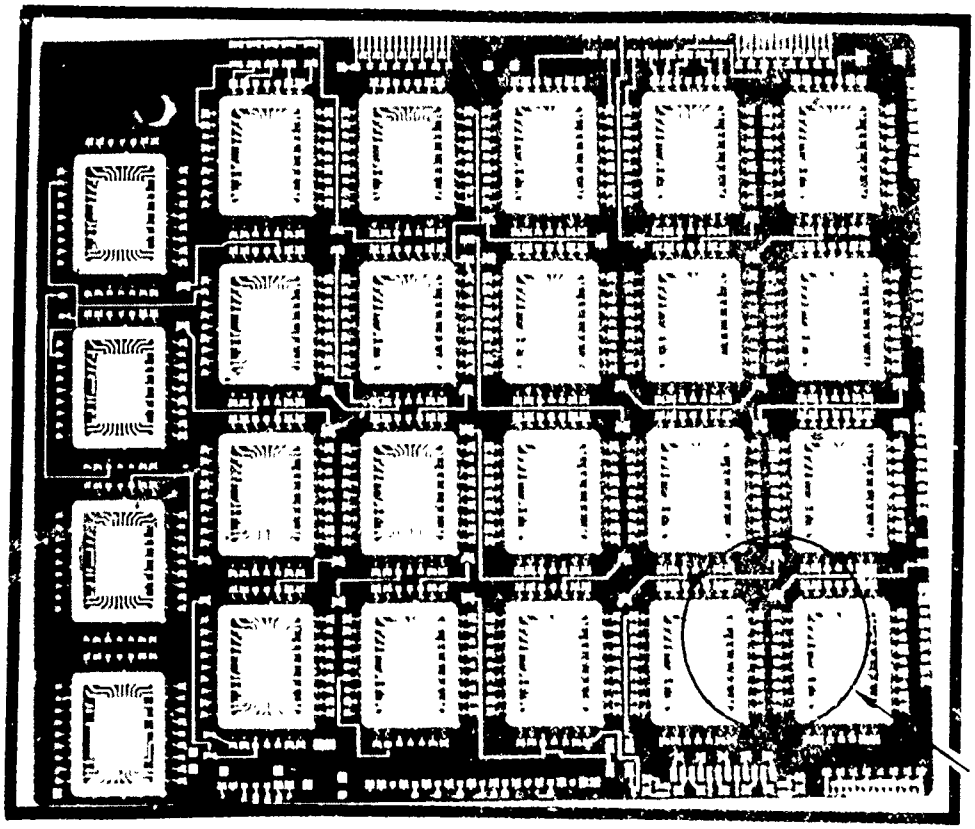

Figure 3.3-24b Photograph of sectioned CIC printed wiring assembly (side 2)

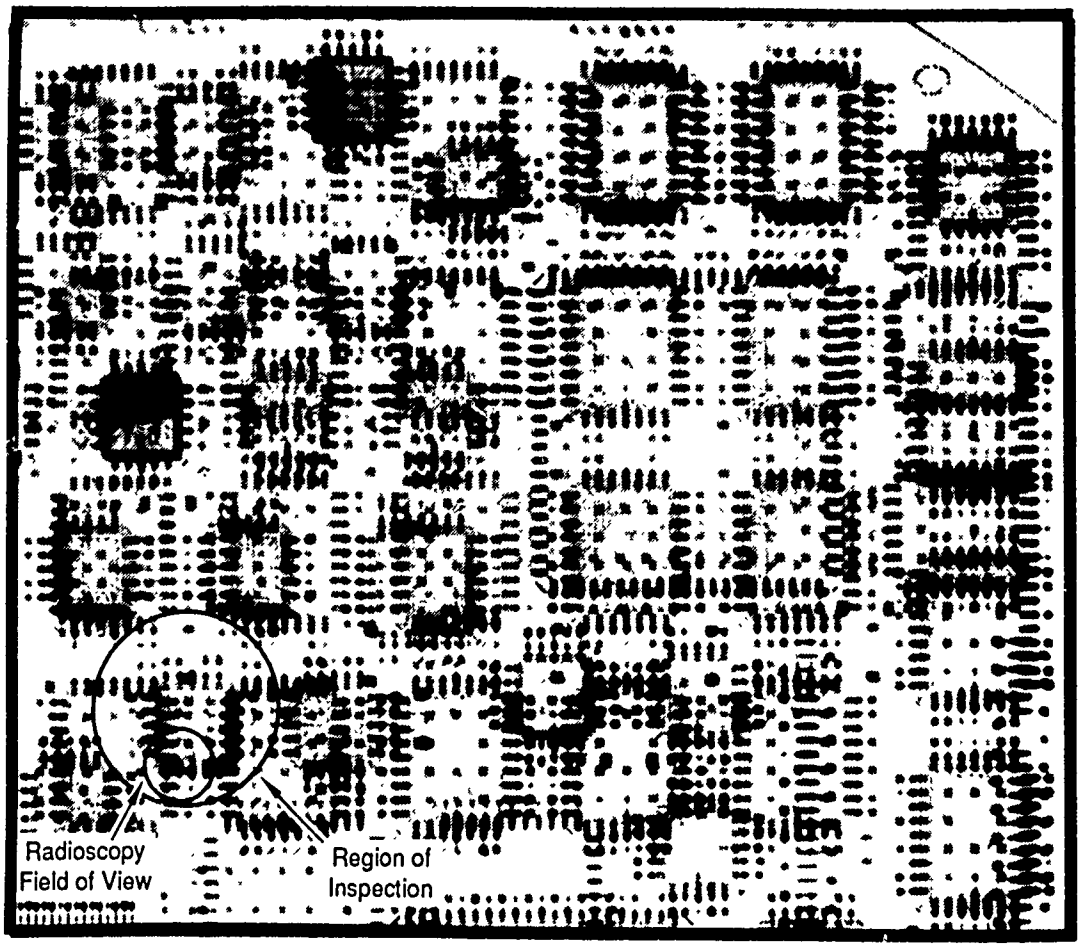

Figure 3.3-25 Radiograph of CIC assembly

the CIC assembly results. Sensitivity to solder features is reduced from the aluminum core assembly. Features can be interpreted; however, the high packing density of this assembly creates considerable confusion in the image.

The CIC assembly was successfully imaged using SBLAM. Laminograms produced using SBLAM image the individual sides of the assembly and identify several solder defects. The front side of the assembly as seen in Figure 3.3-27 identifies solder balls and voiding among the joints. Figure 3.3-28 on the rear side exhibits joints apparently without defects. Solder voids in the range of 0.10 to 0.25mm (0.004 to 0.010 inch) in diameter are readily visible as well as solder balls.

3.4 Innerlayer Trace Analysis Results

Laminography was tested for its ability to image individual copper trace layers within the TRW test board (PID #010114). The thickest boards (type 16 series) with components were used. The traces are 60g (2 ounce) copper which average 0.07 mm (0.0027 inch) thick and are separated by approximately 0.40 mm (0.016 inch).

Laminography reconstruction from the 420 kV CTLAM system data set used to generate the solder bond image in Figure 3.3-14 was performed to reconstruct inner layer traces. Figures 3.4-1a and b show the trace pattern of layer A. Laminograms clearly imaging the inner trace plane A are shown in Figures 3.4-2a and b. Note board warpage is not compensated for and as a result the traces fade out of view and traces of the next layer enter the view. The two images of Figure 3.4-2 show the continuation of the traces in layer A as the warpage changes the focus depth for the laminograms. Additional laminograms were generated using the same data set to separate vertical and horizontal internal test traces from planes B and C shown in Figures 3.4-3 and 3.4-4, respectively. Again, board warpage results in focus depth variation across the board. The results indicate that individual trace planes can be imaged.

Using SBLAM, a laminographic image of the inner traces on this board were generated virtually in real time but the quality level was poor. The SBLAM system used is optimized for imaging solder and is not particularly sensitive to copper inner traces.

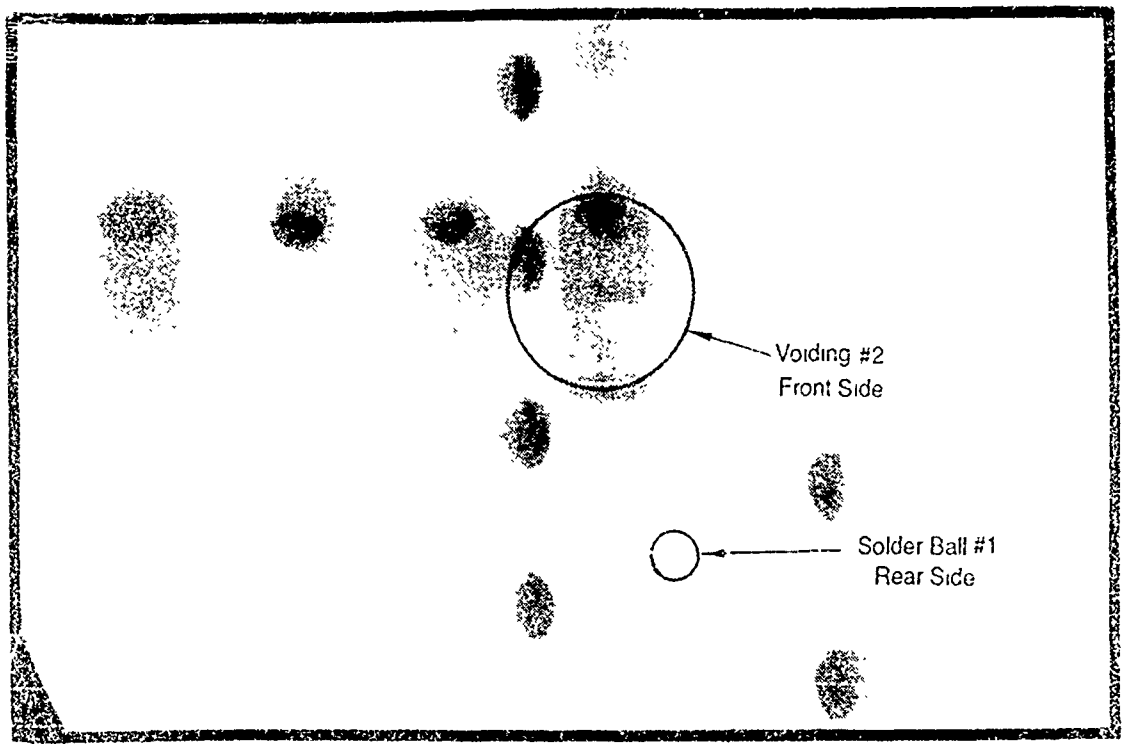

Figure 3.3.26 Radioscopic image of CIC assembly

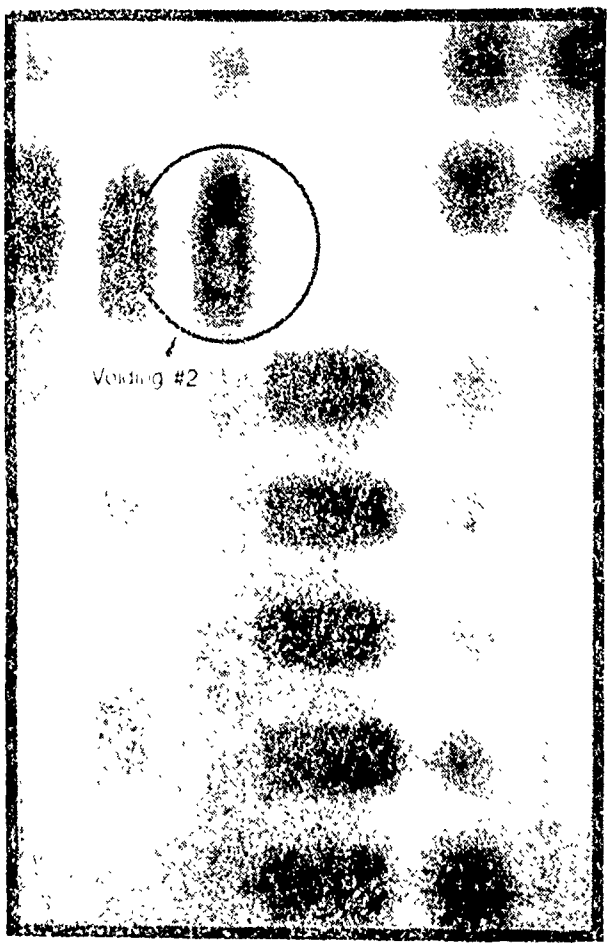

Figure 3.3.27 SBL AM front view of CIC assembly

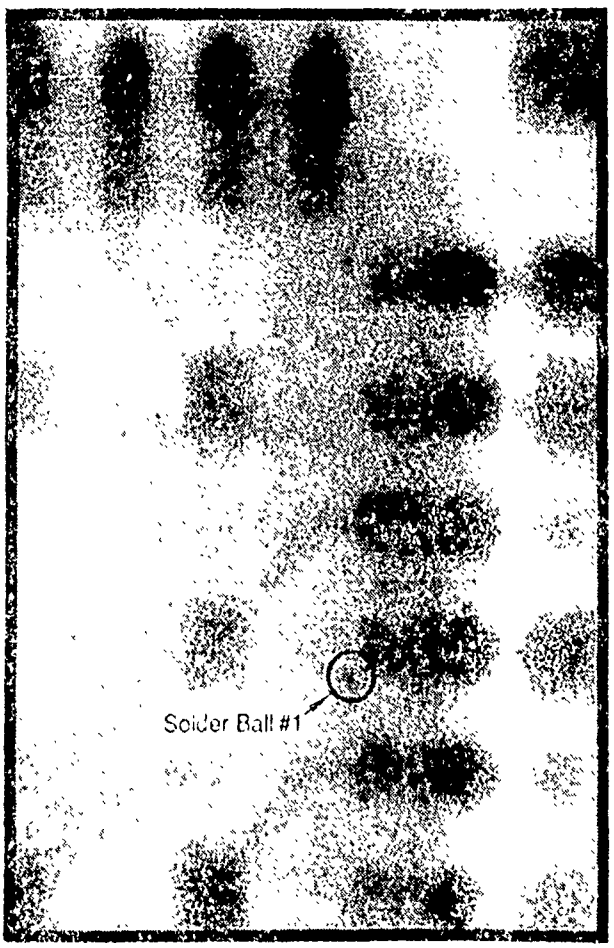

Figure 3.3.28 SBL AM rear view of CIC assembly

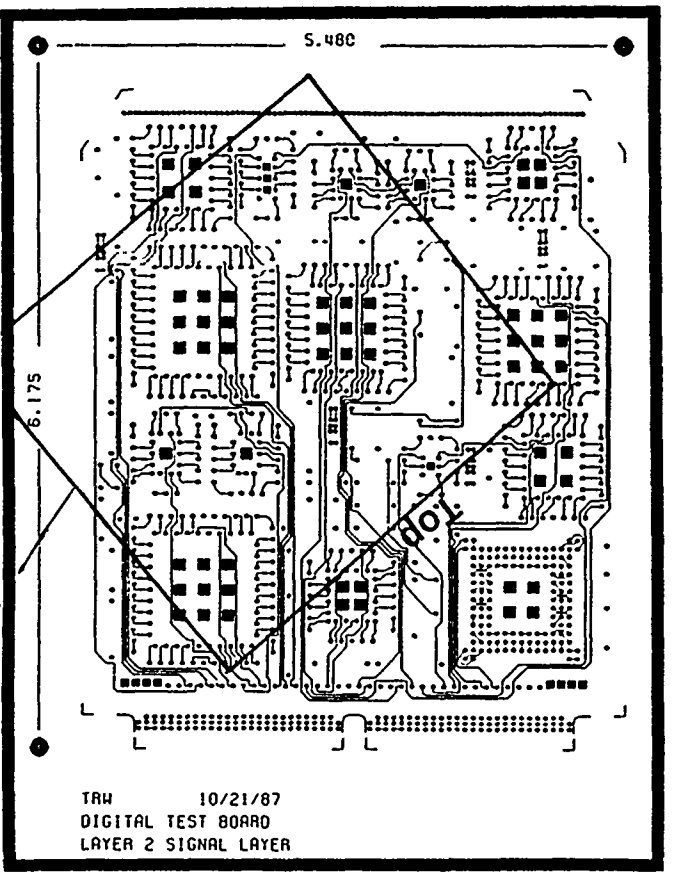

Figure 3.4-1a Pattern of trace plane A (full board)

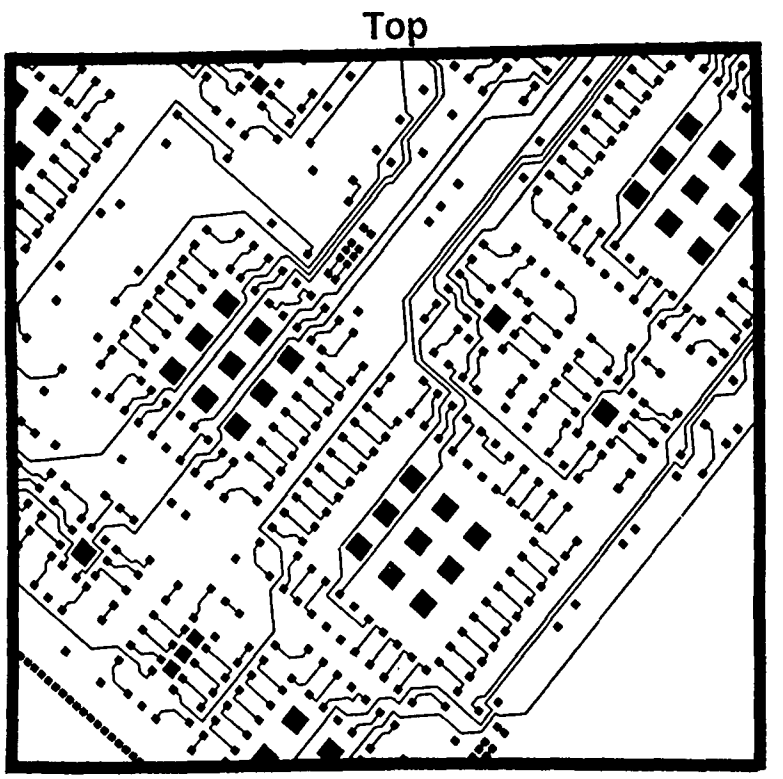

Figure 3.4-1b Enlarged trace pattern of laminographic data set region

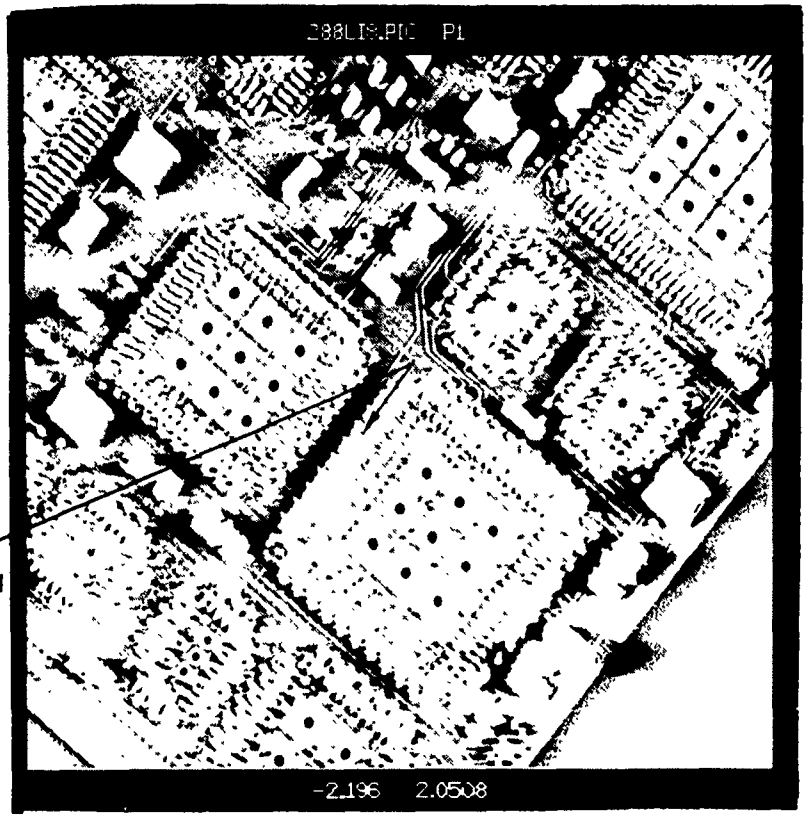

Traces Fade Due to Board Warpage

Figure 3.4-2a CTLAM image of circuit trace, plane A

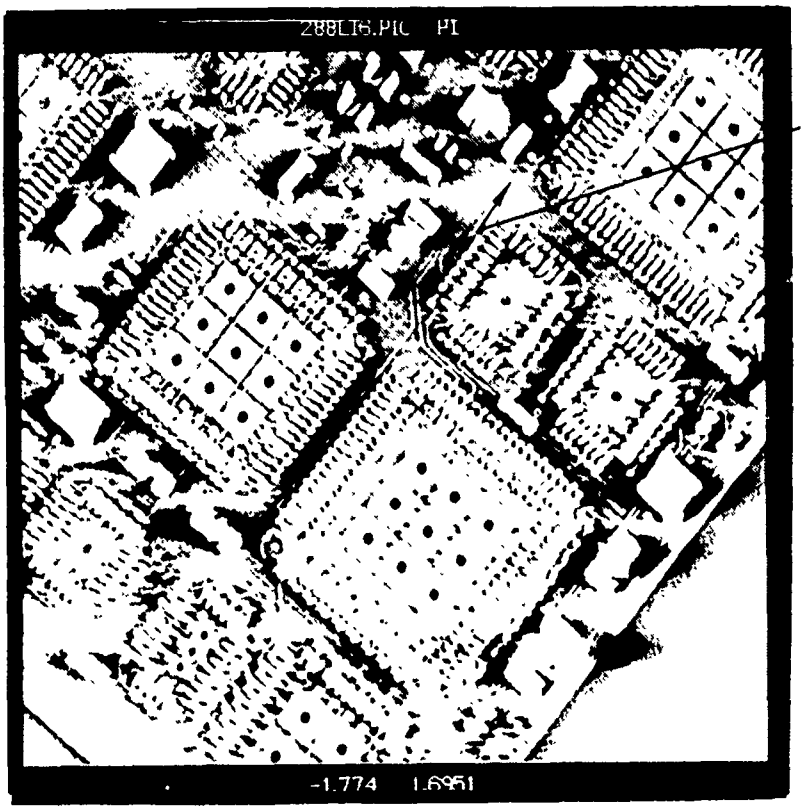

Traces Fade Due to Board Warpage

Figure 3.4-2b CTLAM image of circuit trace, plane A

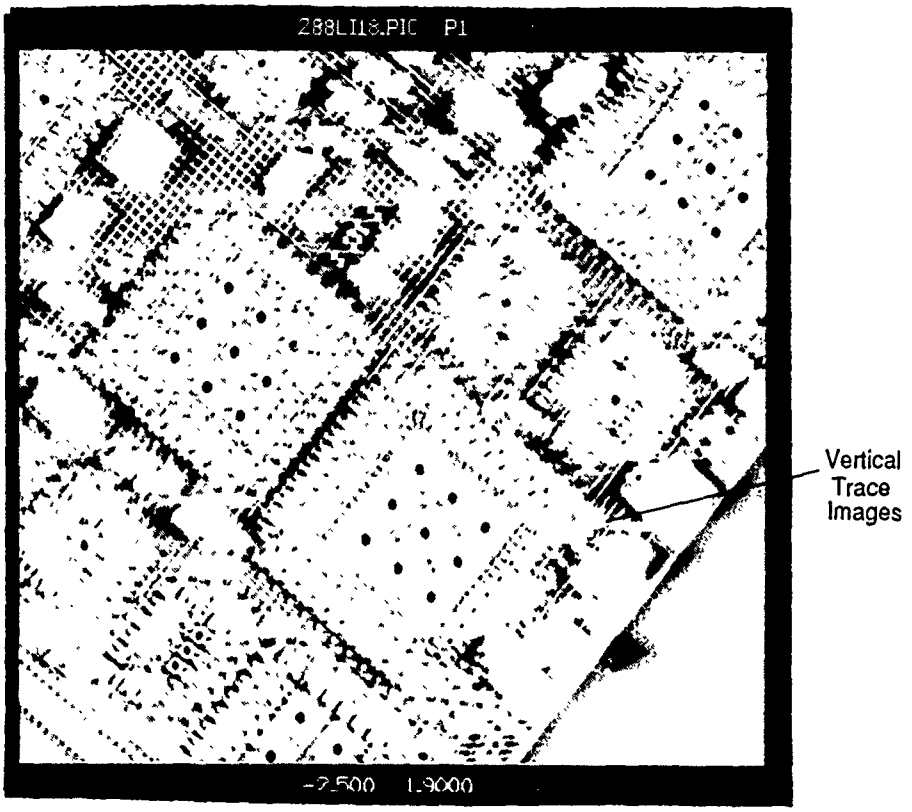

Figure 3.4-3a Vertical trace CT laminogram, plane B

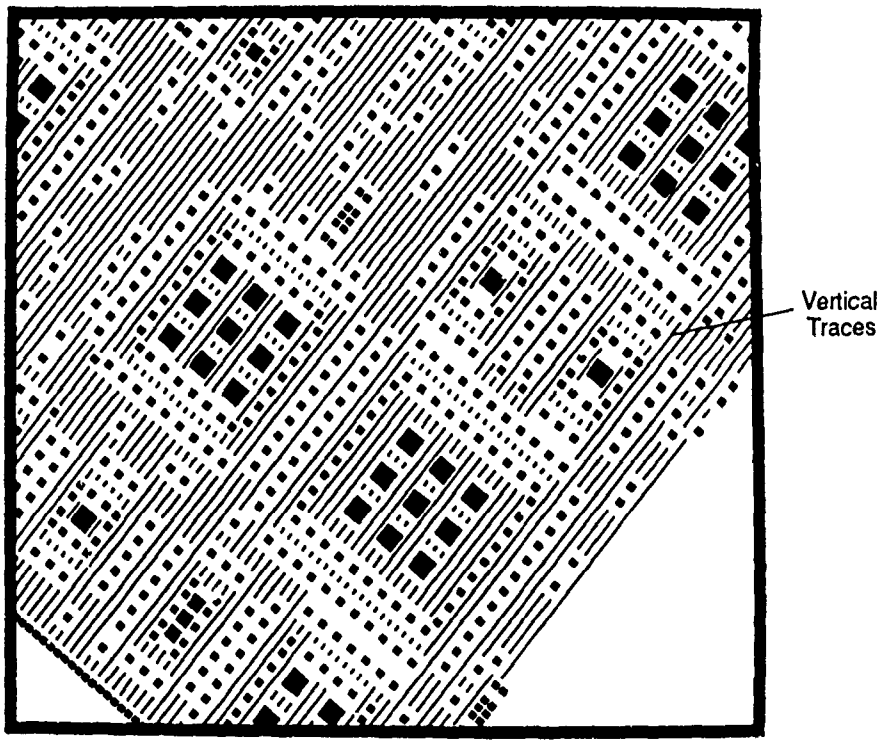

Figure 3.4-3b Vertical trace pattern, plane B

Figure 3.4-4a Horizontal trace CT laminogram, plane C

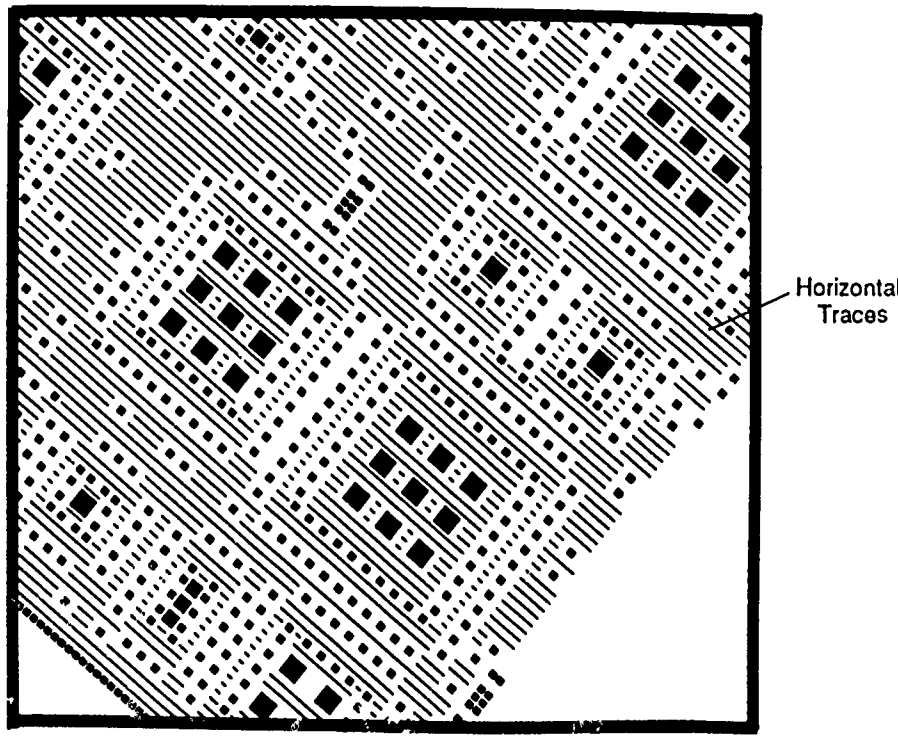

Figure 3.4-4b Horizontal trace pattern, plane C

4.0 OTHER ELECTRICAL COMPONENT STUDIES

The categorizing of all possible electrical components into a few areas oversimplifies the issue of investigating new inspection methodologies in the electronic/electrical component field. The Task 1 report on "CT of Electronics" [1] narrowed the inspection task to the categories with the highest payback potential. It is possible to develop a payback schedule for virtually any type of component, provided the inspection costs can realistically be kept to a reasonable fraction of the total part cost. This section explores electrical components other than printed wiring assemblies which also offer possible economic payback, though not as high or obvious as the solder bond evaluation.

4.1 Connectors

One very important area in electrical applications for CT is on connectors. During assembly connector failures are a key contributor to increased costs in system integration. A defective connector can cause a system test failure resulting in many hours of troubleshooting. With thousands of connectors on military (and commercial) aircraft, it is not surprising that failures continue to occur. Sometimes failures are due to design flaws or manufactured defects. Other times the connector is slightly damaged during assembly and/or installation. It is also possible for connectors to provide sufficient continuity to pass system test but contain defects that may go unnoticed for years until the operational environment causes the defect to manifest itself by means of a mission failure. Highly critical situations involve power supplies, high temperature engine harnesses, avionics, circuit boards, data transmissions, and component sockets.

Common defects of connectors include voiding and high conductivity regions in the pin support structures which allow a short to occur. Other issues involve the soundness of the mechanical support structure (i.e., welds, press fits) rings, seals and contacts (i.e., position, crimp quality). Destructive analysis after a failure is often difficult, costly, time consuming and does not always yield the correct information.

4.1.1 Aircraft Firewall Connector (PID #010513)

The aircraft firewall connector (25 mm (1 inch) diameter) shown in Figure 4.1-1 is used to conduct fire alert signals to the cockpit and is designed to prevent a fire from spreading for at least 5 minutes. The cost is approximately $75 each, with typically about 12 used on a commercial aircraft. Current inspection methods involve destructive testing of a lot sample. The connector, made of a steel shell, was analyzed using CT. The digital radiograph is shown in Figure 4.1-2, and a CT slice is shown in Figure 4.1-3. The image identifies critical features such as the metal to metal contact between connector halves and the pin depth within the socket. Also shown is the clearance between the hard dielectric and the interfacial seal between the connector halves as well as the "O" ring placement and connector threads.

4.1.2 Aircraft Power Connector (PID #010512)

The 50 mm (2 inch) diameter, 4 pin connector in the Figure 4.1-4 photograph is used to conduct primary current from the aircraft power generators. This connector is a prototype and contains a misplaced split metal "O" ring. Metallurgical sectioning performed by Boeing Failure Analysis group revealed that the critical "O" ring had not been properly set at the time of manufacture. The vendor, however, claimed that their manufacturing process was correct and that the defect was generated during sectioning by the failure analysis group. Radiography performed on another connector of the same lot was inconclusive regarding the "O" ring status. CT analysis on a medium-resolution (1 lp/mm) system revealed that the ring had indeed been improperly set by the vendor and the dispute was settled. Figure 4.1-5 shows the axial CT image indicating the locations

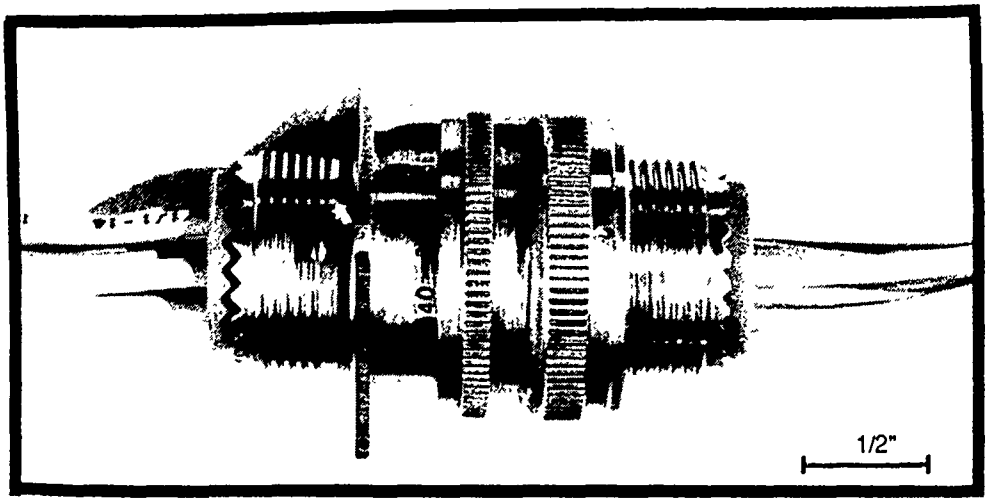

Figure 4.1-1 Photograph of firewall connector

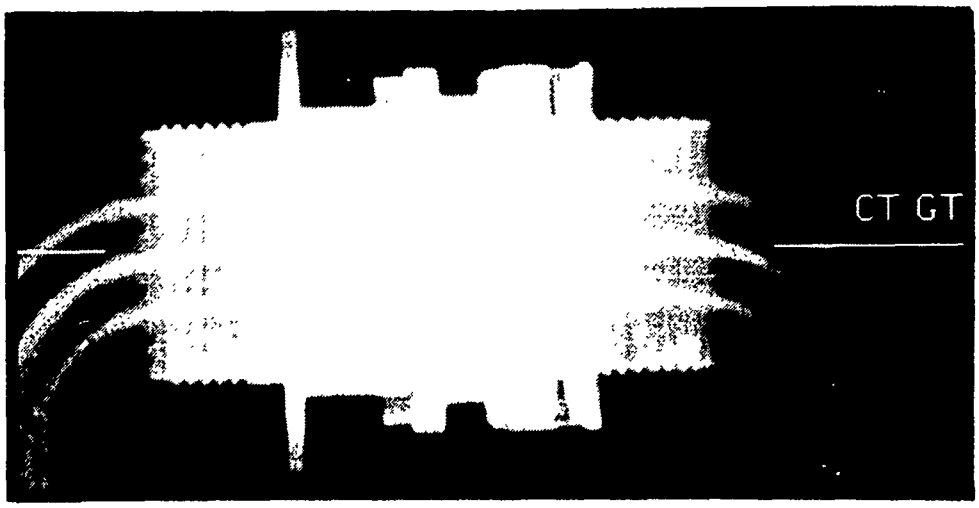

Figure 4.1-2 DR of connector

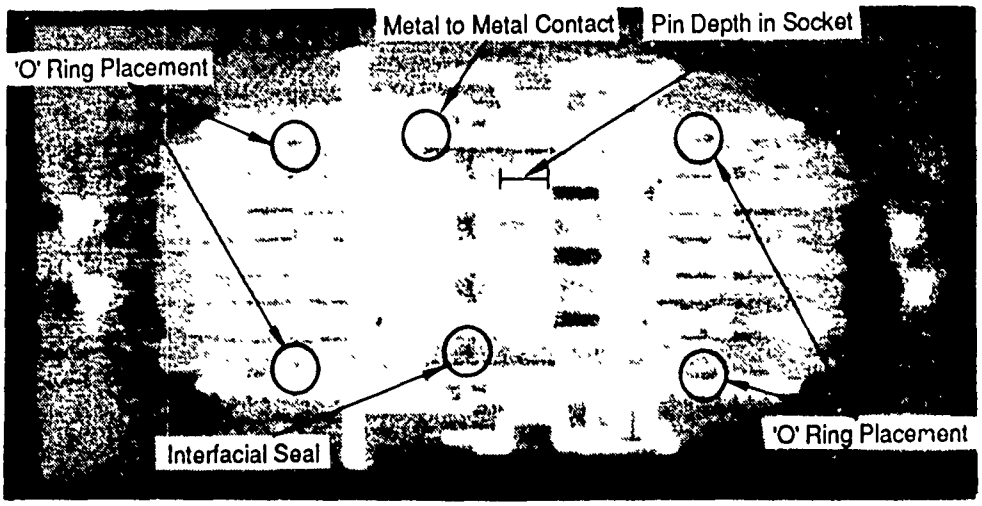

Figure 4.1-3 CT scan of connector

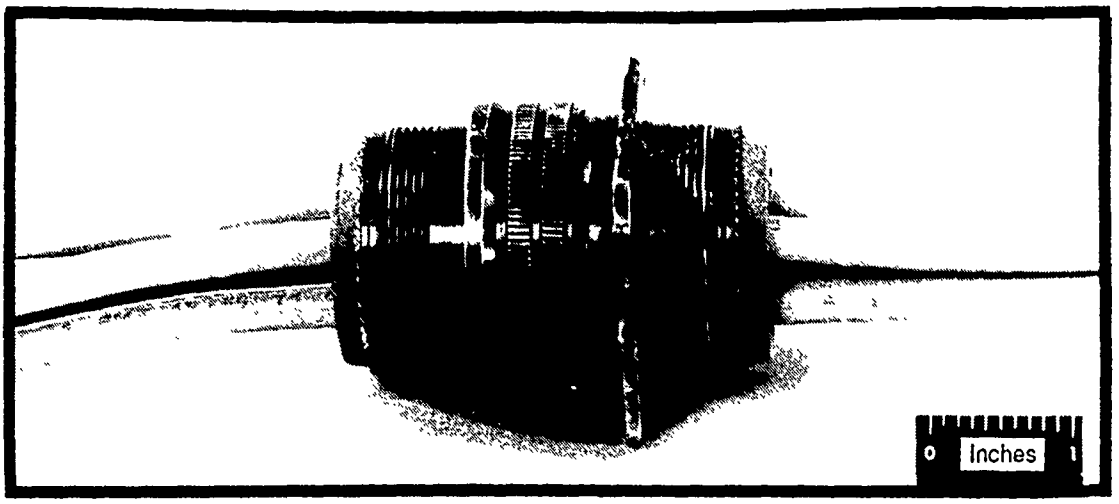

Figure 4.1-4 Photograph of power connector

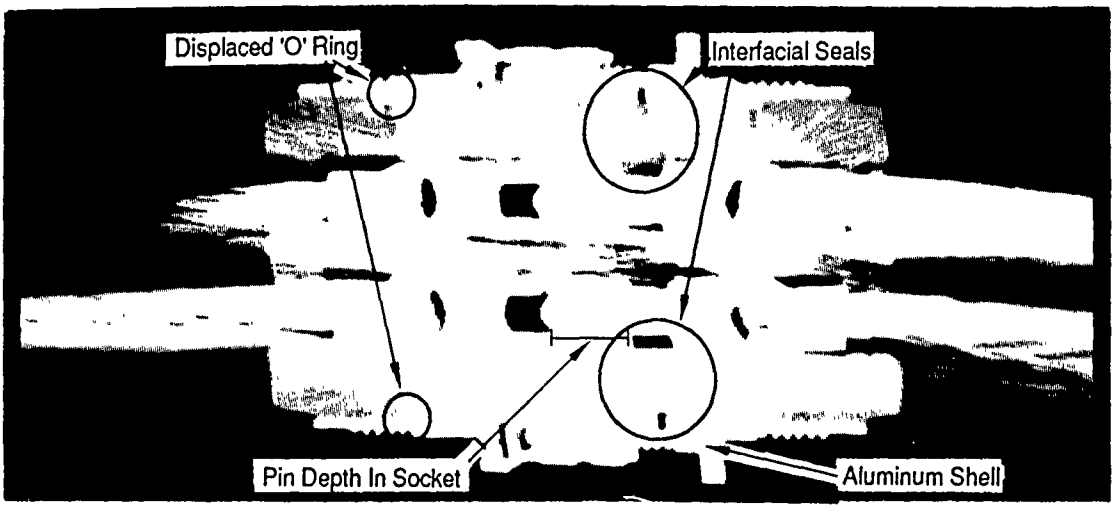

Figure 4.1-5 Axial CT slice showing displaced "O" ring

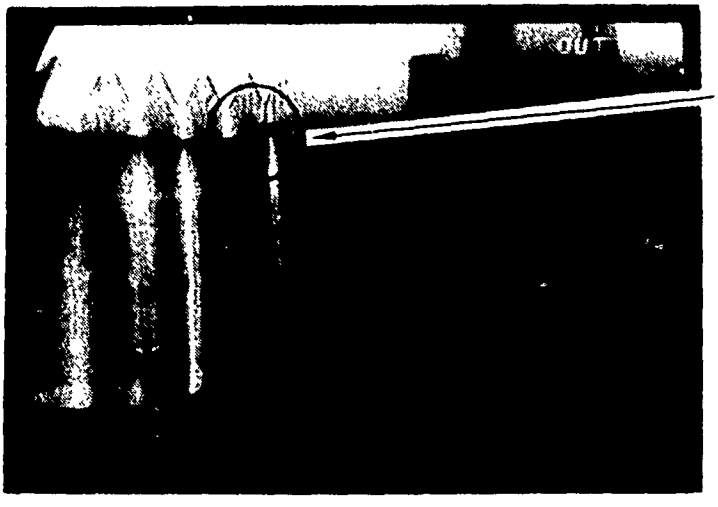

Figure 4.1-6 Radioscopic image showing displaced "O" ring

of the displaced "O" ring, interface seals, pin depth in socket and the aluminum shell indicated. Reproduction does not provide sufficient detail to detect the anomalous condition in the connector image. A line trace analysis at the "O" ring interface on the original image was used to reveal the difference between the seated and unseated condition.

For comparison, the connector was imaged with a microfocus radioscopy system. Figure 4.1-6 shows the displaced "O" ring among the superimposed features. The use of radioscopy in failure analysis can be very effective but requires manipulation of the part and experience in interpretation of details in the projected image.

4.2 Transformers

Transformers, often at the heart of aircraft electrical power systems, are another potentially critical item whose failure could lead to the loss of a mission. Transformer failures are mostly attributed to manufactured defects. Transformers are either designed and built by the aircraft manufacturer or procured from vendors and then subjected to rigorous quality assurance testing. Testing involves 100 percent functional verification of the electrical characteristics and approximately 10 - 20 percent life-cycle testing. Life-cycle testing may consist of vibration testing and 1000 hours of continuous thermal cycling and environmental testing. Other tests include fungicidal or corrosive environments with final verification of quality through destructive sampling.

Destructive sampling requires that selected parts are sectioned, polished and inspected for micro-cracking, shrinkage of the potting material and corrosion of the core. This process is very timely and expensive. It may take several weeks for a newly designed part to pass its certification tests. Sectioning is likely to be accomplished using a diamond or band saw, inducing cracks which are difficult to distinguish from any cracks developed during environmental testing. These induced defects could cause unfolding of steel laminated as well as severe fracturing in compressed ferrite cores virtually destroying any evidence of environmental or manufactured flaws.

4.2.1 Compressed Ferrite Core Transformer Assembly (PID #010304)

The 15-volt compressed ferrite core transformer inverter assembly shown in Figure 4.2-1 is used on a major military program and has a cost of approximately $1400. The transformer consists of 2 compressed ferrite hollow cores each 20 mm (0.8 inch) in diameter by 6.5 mm (0.26 inch) in height for a total height of 13 mm (0.52 inch). The cores contain windings of 34 turns of 24 gauge (0.511 mm (0.02 inch) dia.) and 52 turns of 26 gauge (0.404 mm (0.016 inch) dia.) wire. The cores are adhesively mounted to a plastic terminal plate assembly. The transformer was rejected due to a crack in the core which caused a lower inductance measurement than specified in the design.

The defect in the transformer is a crack in the ferrite located near the interface between the adhesively bonded terminal plate and the bottom core. The crack is slightly visible on the surface which caused the transformer to be rejected. It is thought to have been induced by curing of the adhesive. The testing goal was to determine the depth of the crack without destructive analysis in order to provide information back to the manufacturing group. A radioscopic image was taken, and an edge enhanced image is shown in Figure 4.2-2. The system, which uses a microfocal source, clearly identified the crack as indicated.

The component was CT scanned on a high resolution (4 lp/mm) CT system. The CT image is shown in Figure 4.2-3. The image is also able to resolve the 26 gauge wires. The crack in the core of the connector is also visible in the image. Reproduction of the image has reduced the detail visible in this presentation from that available at the CT system monitor. The inspection time was approximately 30 minutes.

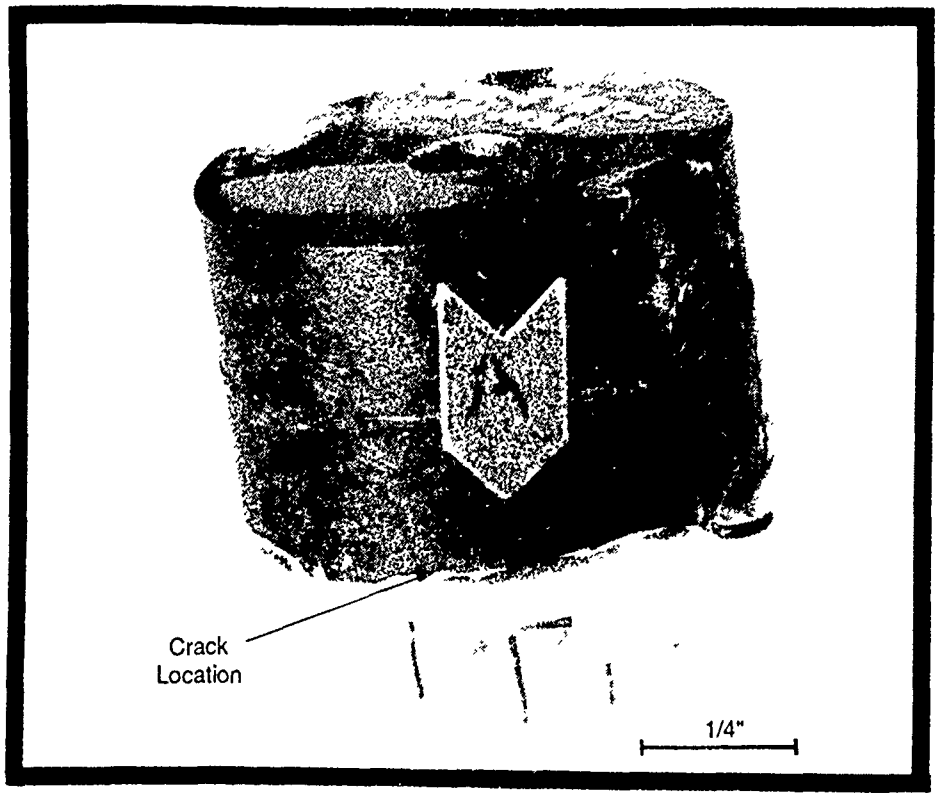

Figure 4.2-1 Photograph of transformer assembly

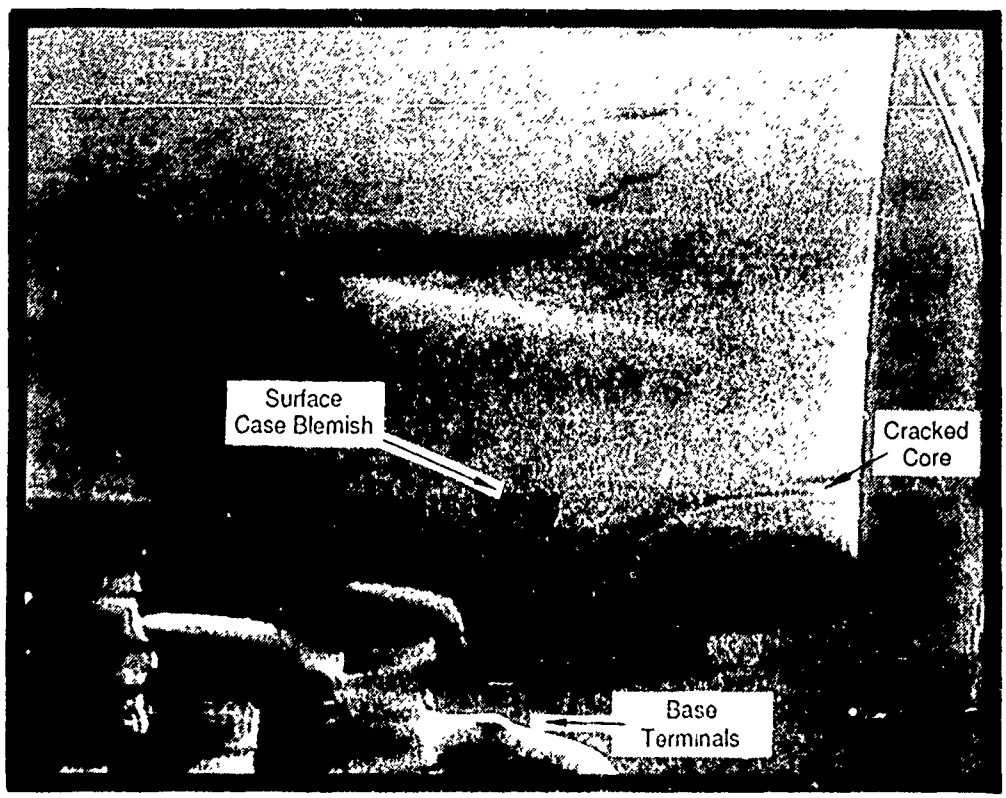

Figure 4.2-2 Radioscopic edge enhanced image of cracked core

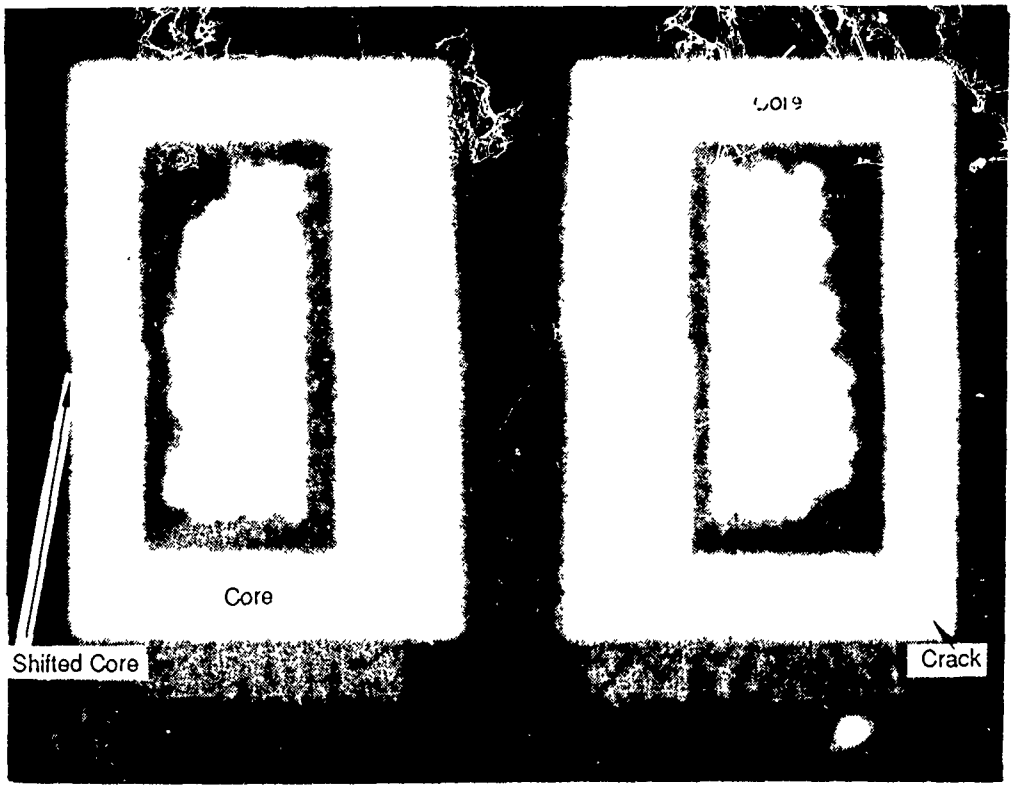

Figure 4.2-3 CT image of cracked core

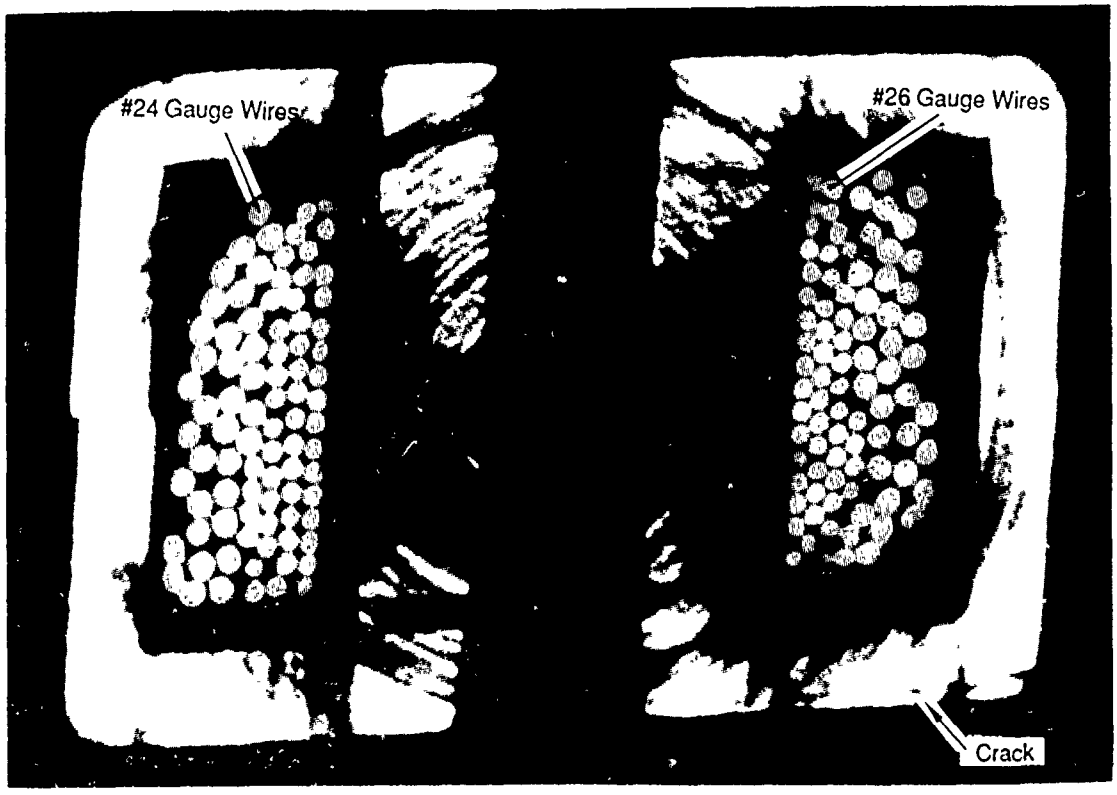

Figure 4.2-4 CT image of cracked core

Using a very high resolution (approximately 10 lp/mm) CT system, a CT scan was taken and successfully imaged the crack as shown in Figure 4.2-4. The Figure shows that the crack moves inward along the bottom of the core and then appears to turn and cut up across the core. In addition, the scan clearly shows the uneven layup of the primary and secondary windings. The 26 gauge wires are clearly resolved. This system uses third generation scanning and therefore some ring artifacts are present. The inspection time for this scan was about 2 hours.

4.2.2 Steel Lamination Core Transformer (PID #010307)

A steel lamination core transformer, suspected of having a faulty secondary winding due to cracks in the potting compound induced during thermal cycling, was examined with a high-resolution (4 lp/mm) CT system. The DR image is shown in Figure 4.2-5 with the CT slice plane indicated. The CT scan is shown in Figure 4.2-6 and identifies the primary winding as a coil around the center leg of the steel lamination core. The secondary windings are identified as a larger coil surrounding the primary coil. The CT imaging system was not able to identify cracks in the potting material or in the secondary winding. Contiguous scans were taken on this transformer and are shown in Section 5.3 on 3-D modeling.

4.3 Fiber Optic Rotary Transducer (PID #010803)

Fiber optic technology for the transmission of critical data in aerospace applications offers many benefits including lighter weight, greater bandwidth, lower cost and insusceptibility to electromagnetic interference to name a few. The ability of engineers to design sensors to fit this emerging technology is crucial to its success. Highly accurate sensors requiring precision machining and optics will need to operate under the most extreme circumstances for extended periods of time. Prototype development is time consuming, costly and few samples are built, thus limiting the opportunities for destructive analysis. Fly-by-light technology will see its applications increasing on aircraft over the next 15 years.

A rotary optical transducer similar to the one shown in Figure 4.3-1 would relate position data to an aircraft avionics computer. The prototype shown has a cost over $20,000 and is built with an aluminum case. A DR from a high-resolution (4 lp/mm) CT system, displayed in Figure 4.3-2, shows the internal features and CT scan planes. Figure 4.3-3 shows a CT scan taken in scan plane DT1 through the complex optics arrangement . The image identifies the critically dimensioned fiber optic region where lenses focus the light data through the prism indicated. Figure 4.3-4 shows a CT scan taken in scan plane DT4 and reveals the bearing arrangement attached to the optical disk and the outer shell dimensions.

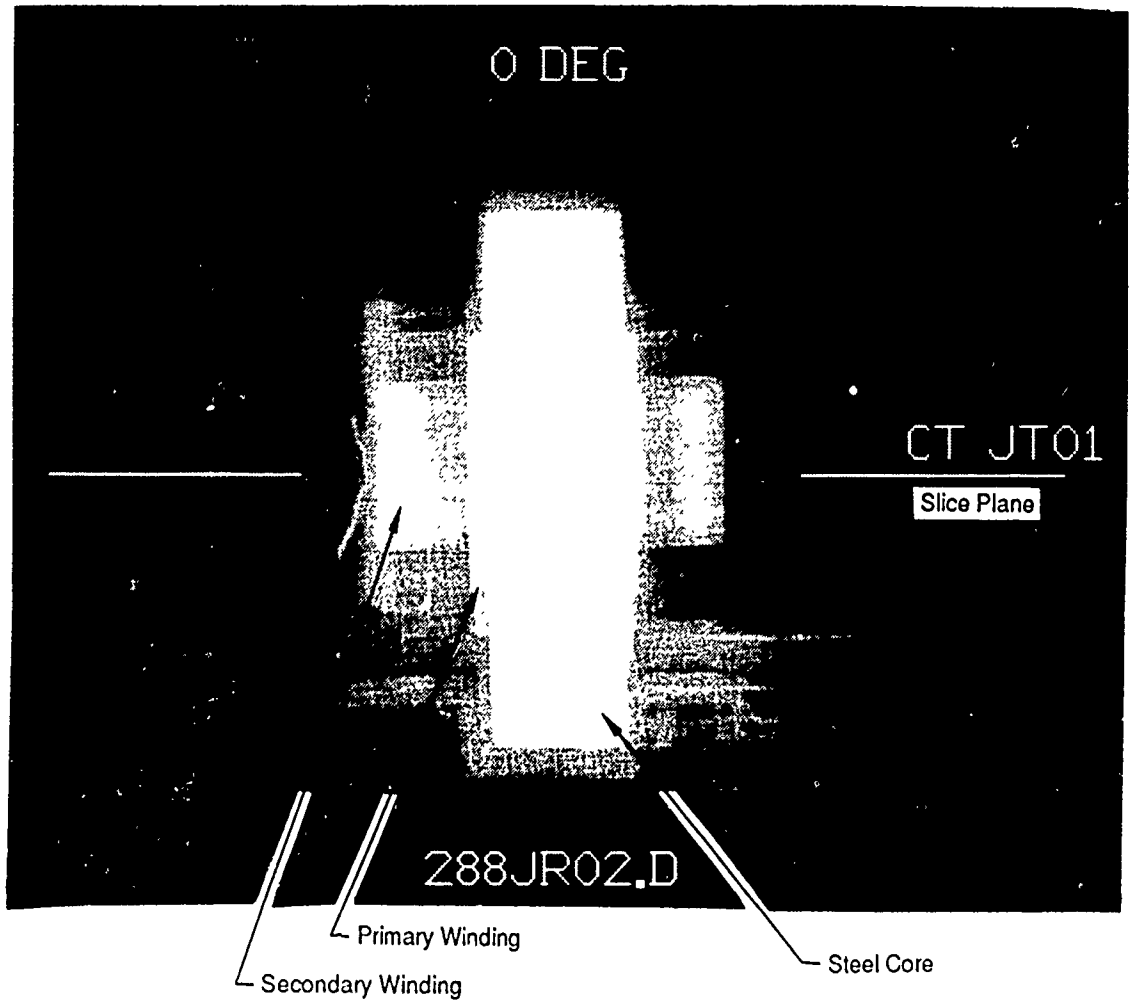

Figure 4.2-5 DR of steel lamination core transformer (CT slice plane noted)

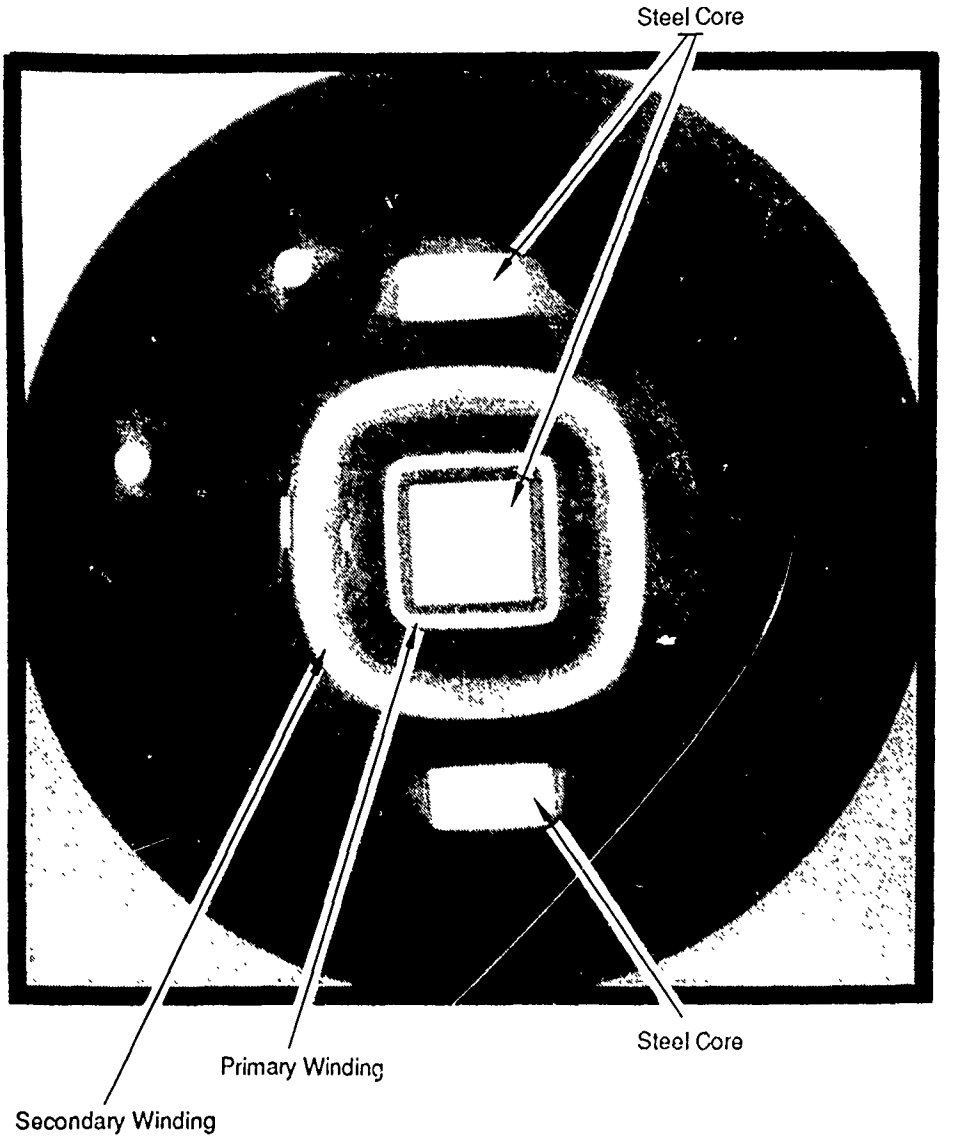

Figure 4.2-6 CT of steel lamination core transformer

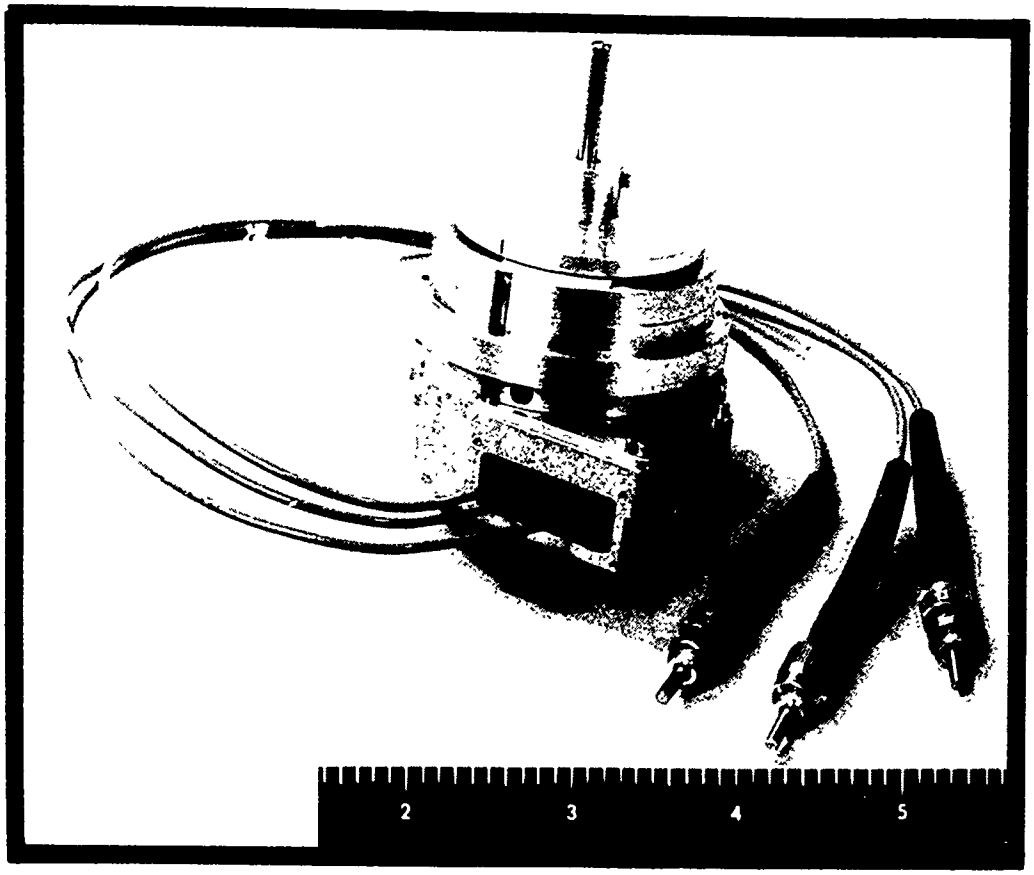

Figure 4.3-1 Photograph of optical sensor

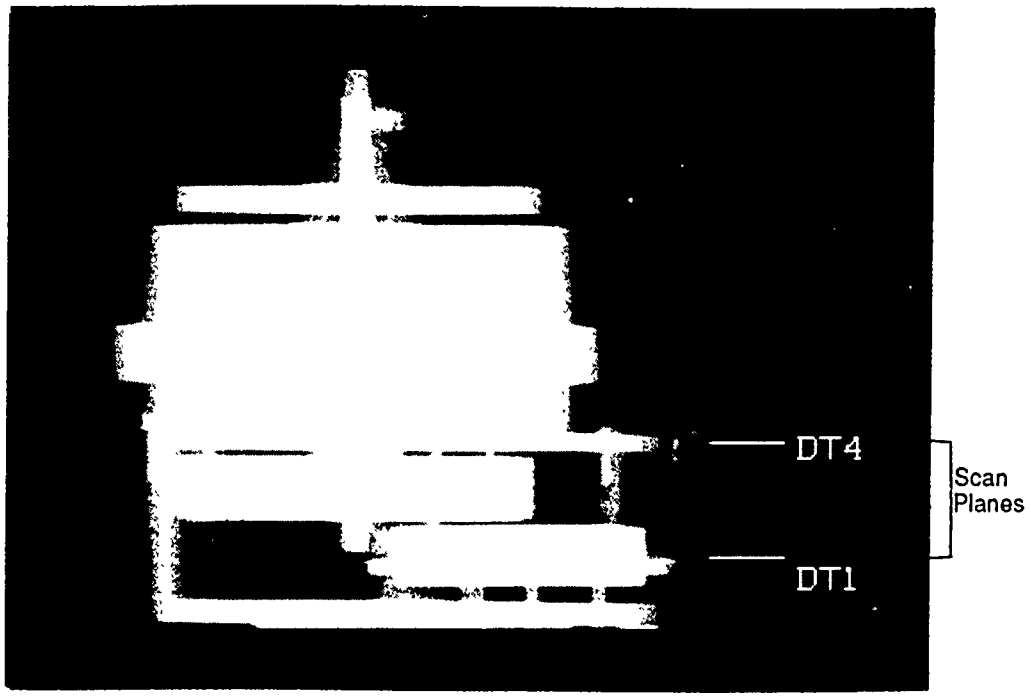

Figure 4.3-2 DR of optical sensor showing scan planes DT1 & DT4

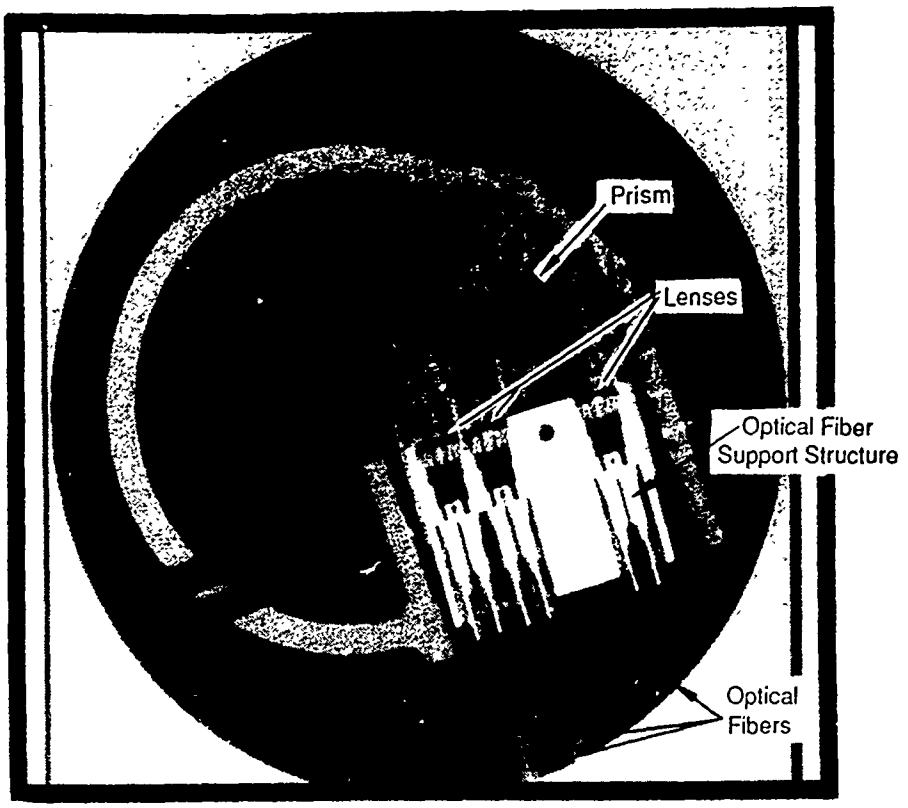

Figure 4.3-3 CT of optics arrangement, scan plane DT1

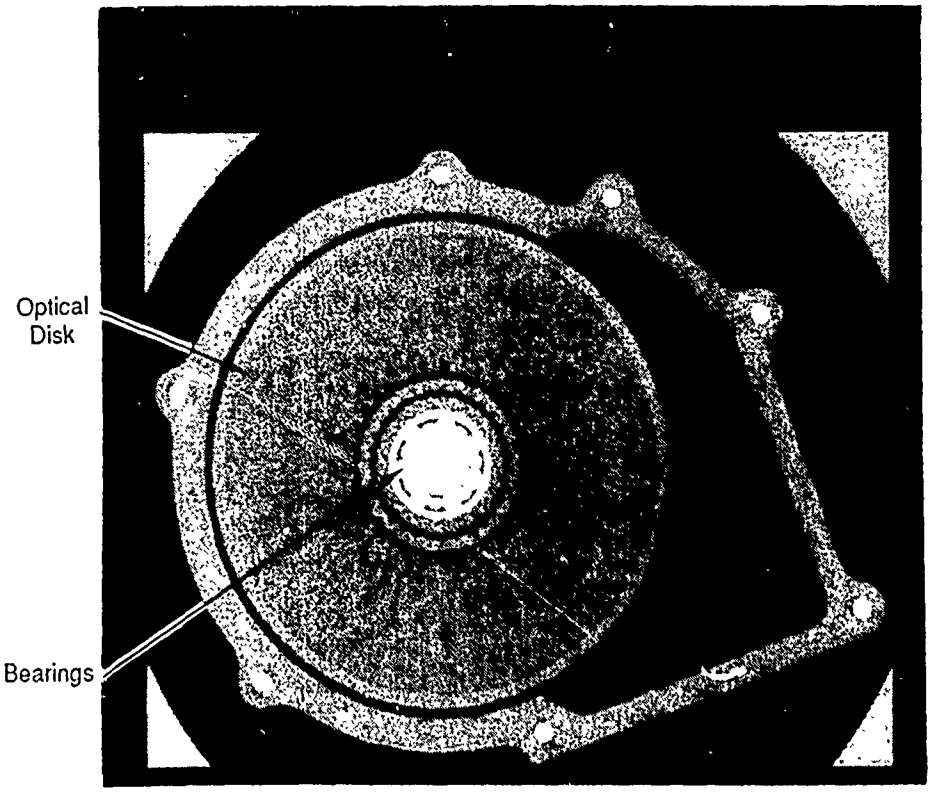

Figure 4.3-4 CT of bearing and optical disk, scan plane DT4

5.0 3-DIMENSIONAL COMPONENT MODELING

CT and laminography produce 2-D cross-sectional images of 3-D objects. It is possible to display "stacks" of 2-D tomographic data and reproduce the entire 3-D volumetric object. There are several volumetric graphic display systems on the market which are capable of high-performance image processing for image analysis and manipulation of 2-D and 3-D images.

5.1 3-D Modeling Test Results Using CT

Three-dimensional modeling has commonly been used in medical diagnosis where some medical CT systems offer 3-D capabilities, as an auxiliary feature for creating a model immediately after acquiring the data. The model can be manipulated to allow for the optimum viewing angle in performing a prognosis. Similarly, industrial CT images can be manipulated to provide a more comprehensive structural analysis of the component. More advanced modeling techniques involve converting the CT data into 3-D surface models for standard format (i.e., IGES-based) CAD/CAM applications.

5.1.1 Steel Lamination Core Transformer

A 3-D model of the transformer from Section 4.2 is shown in Figure 5.1-1. It was generated from 200 CT slices taken on a high-resolution (2 lp/mm) CT system at 420 kV. The total data acquisition time was 100 minutes (about 0.5 minute per slice). The model is a surface rendering of the transformer by SunVision from Sun Microsystems. Figure 5.1-1 shows the transformer with a cut displaying the secondary windings surrounding the central steel core. Figure 5.1-2 shows a vertical cut through the transformer. In this view the core is shown to have an "E" shape with the prongs pointing vertical. The primary and secondary coils are wound around the central core. The primary winding is longer than the secondary. The shading of the image changes for the center core over the length of the secondary windings. This is due to beam hardening effects for the CT slices that cover the secondary windings. The same is true at the bottom where the steel core represents a large beam path for the X-rays in the CT scan and causes a difference in the shading. Figure 5.1-3 shows a 3-D view with a diagonal cut which cuts through a portion of the secondary winding. The ability to visualize cuts at various orientations through the part can be very helpful for as-built engineering analysis of components.

5.2 Laminography Modeling

Similar to the CT images laminographic planes can also be "stacked" to form 3-D models. Surface rendering of solder joints can be performed in this manner. Because the shape of the solder joint is one of the most critical issues in solder bond integrity, this information can be useful. Complete solder modeling of pre-production circuit boards will provide a 3-D set of input parameters for optimizing the solder process. Once the process has achieved the desired quality level the system can be used in standard laminographic mode for maximum throughput.

5.3 Emerging Technologies

Several emerging technologies in CT related areas are worth mentioning in this report. These techniques (cone beam CT and stereolithography) were not available for testing during the course of this task assignment due to scheduling. Overall, high speed CT and laminography systems will open the door to more regular use of modeling; however, more efficient means of acquiring, reconstructing and most importantly interpreting the data will be needed. As high speed image processors and image analysis workstations come down in price, automated image analysis

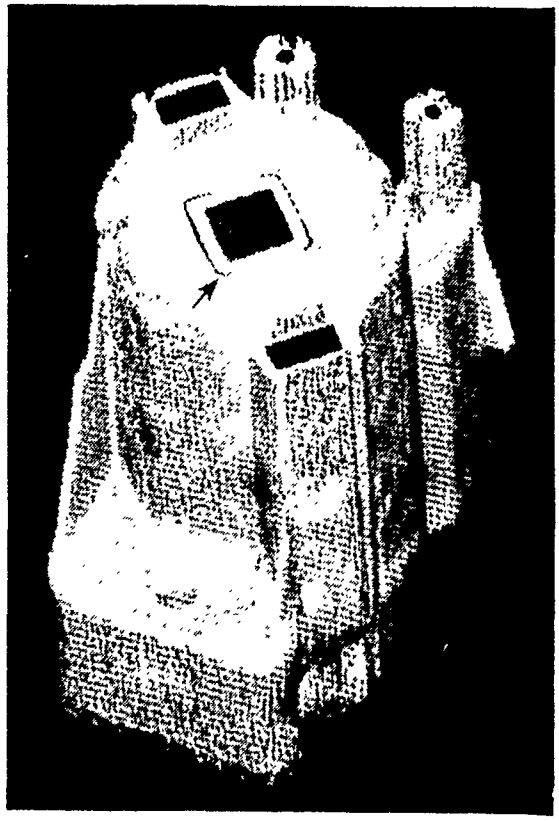

Figure 5.1-1 3-D model of steel lamination core transformer

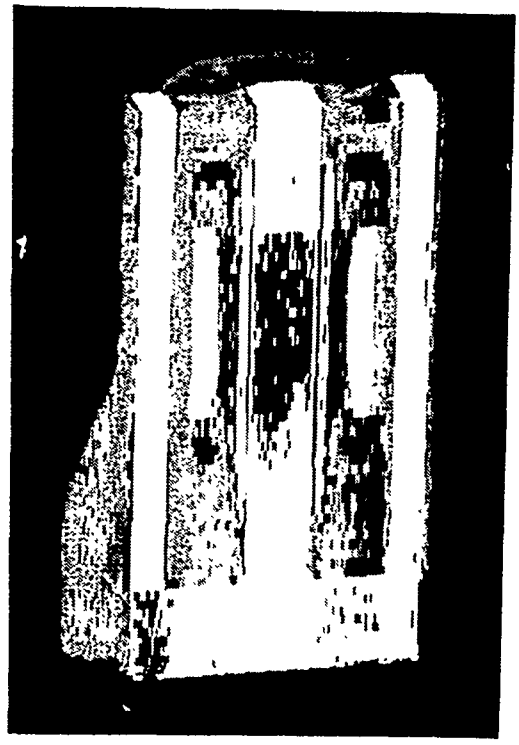

Figure 5.1-2 Vertical cut through 3-D model of steel lamination core transformer

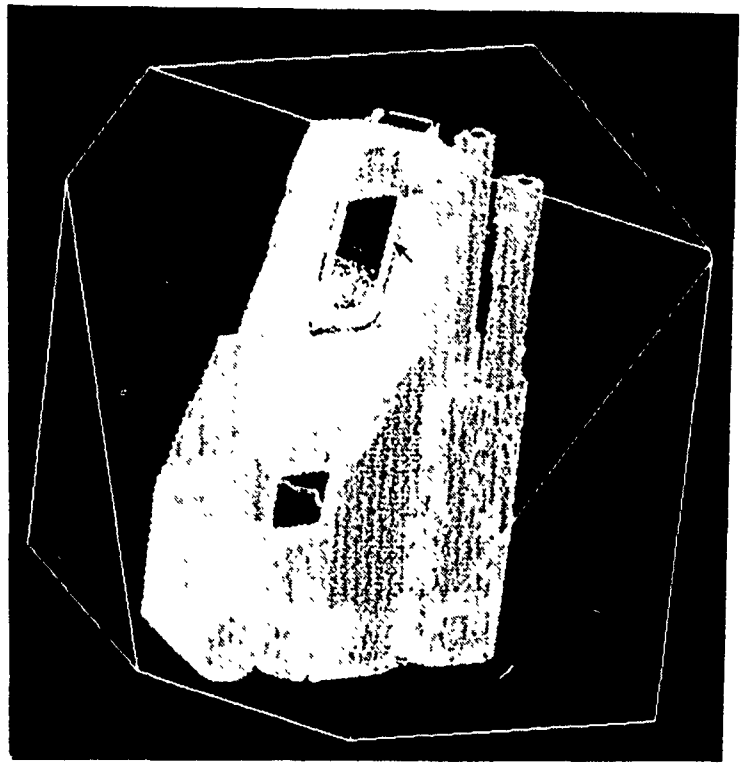

Figure 5.1-3 Diagonal cut through 3-D model of steel lamination core transformer

routines can be generated for more dedicated applications (e.g,. as currently exist for turbine blades) and will simplify the inspection task.

5.3.1 Cone Beam CT

The long data acquisition times of conventional CT systems limits the use of 3-D models for routine inspections and analysis. Acquiring and interpreting huge data sets also poses a significant challenge to 3-D modeling.

An alternate method of acquiring 3-D CT images rapidly is "cone" beam computed tomography (Appendix A). The system uses an uncollimated source to emit a cone of X-rays and a planar 2-D detector to receive the attenuated radiation. The object is rotated to obtain the viewing angles while the data is acquired into a computer memory. Backprojection of the vast data sets creates an entire set of CT cross sections of an object suitable to assemble the 3-D model for display. The technique can be performed on conventional radioscopy systems. When used in conjunction with a micro-focus source, very high resolution CT images are possible [17,18].

5.3.2 Stereolithography Modeling from CT Data

The 3-D CT data can also be used to generate a solid plastic model using a technique called stereolithography with enlarged, partial or otherwise modified data sets. Stereolithography is a process by which individual "slices" are etched using a UV laser in a photopolymer bath. As each cross section is cured, the table lowers and another layer is built upon it, requiring about 2 - 5 minutes for each layer. When the entire model is built, the photopolymer is cured in an oven for about 30 minutes. The resulting translucent plastic model is accurate to about 0.25 mm (0.010 inch).

The use of 3-D modeling for reverse engineering has economic potential for component and packaging design. Computer integrated manufacturing (CIM) requires the use computer aided design (CAD) to efficiently produce components through a complex manufacturing process. Labor intensive CAD design requires highly skilled design engineers to input specific component parameters to form a digital model which eventually becomes the finished part. The use of 3-D models would decrease the time required for CAD design.

6.0 COST BENEFIT ANALYSIS

A primary objective of the CTAD program is to assess what economic benefits may be obtained from CT and/or laminography scanning of a component. Economic benefits of inspection technology can be realized by not only a less expensive inspection but also by increased confidence in the product reliability resulting from the inspection information. CT has been shown to apply predominately to electrical components while laminography is predominantly applicable to PWAs. Radioscopy has also been shown to be applicable to PWAs and many electrical components. The economic benefits of the techniques depends not only on the relative cost of the inspection but also on the technical goal that is to be satisfied. Relative inspection cost is easy to calculate for economic payback and is considered in the following sections. Issues such as increased product reliability and associated technical benefits of inspection technologies are much more difficult to assess quantitiatively for economic payback, particularly in a generic sense, and, therefore, are only discussed in a general sense.

6.1 Cost Benefit of Printed Wiring Assembly Inspections

The inspection of PWA's for solder defects using radioscopy or laminography is viable for detecting most macroscopic solder joint defects such as solder balls, bridging, solder volume, and voiding. Due to the nature of the PWA inspection issue, inspection choices depend on the package styles used on the assembly and single or double-sided board construction. While radioscopy systems may allow imaging of obscure solder bonds on complicated package geometries (e.g., multipole relays with underlying pins), the addition of packages mounted on the opposite side of the board will almost certainly raise the degree of complication and uncertainty. Therefore, the inspection system choice, and thus economics regarding it, will undoubtedly rest upon the primary board construction being either single or double-sided. The level of difficulty increases as double-sided boards become more customized (i.e., metal cores, metal matrix composite cores, many layers, etc.) requiring special consideration.

Cost benefits discussion will be limited to scanned beam laminography and radioscopy systems which have been developed for high throughput solder bond evaluation. Computing the economic payback for an inspection system requires a thorough understanding of many variables including the product (component size and cost, production rate, number of inspection regions, etc.), specific inspection goals, quality level, inspection criteria, and desired throughput. Estimated inspection system payback will be computed using assumptions for primary factors such as system cost, board throughput, annual operating and maintenance costs. An automated system (where a computer algorithm assesses acceptability) has advantages over a semiautomated inspection system (where an operator interprets an image for acceptability) due to the ability to increase throughput, regulate inspection consistency and reduce labor costs.

As discussed earlier, laminography inspection can be accomplished using CTLAM or SBLAM. At this time only SBLAM is optimized for automated laminography inspection of circuit boards. As seen in Sections 3.3 and 3.4, CTLAM currently lacks the resolution capabilities for detecting small (<0.2 mm (< 0.008 inch)) internal solder features and is better suited for performing reverse engineering analysis on innerlayer traces which will be discussed in Section 6.1.3.

6.1.1 Single-Sided SMT PWA's

Radioscopy solder bond inspections are performed typically in two ways: semiautomated and automated decision modes. A semiautomated radioscopy system uses a multiaxis (vertical, horizontal, zoom, rotate, and optional tilt) parts manipulator which recalls a series of preset positions, and the operator views the image display in realtime to render a decision concerning solder joint quality. This is an operational improvement over completely manual positioning

systems because it automates the repetitive controller motions to precisely predetermined regions for inspection, thus saving time and leaving the operator responsible only for performing a quality check. The operator can override the semiautomated mode for manual positioning if desired. Most radioscopy systems used in electronics inspections are equipped with microfocal X-ray sources which provide very high resolution (better than 20 lp/mm) images and greater optical source positioning flexibility for discerning information. Because the final decision is being made by the operator, fatigue and inspector effectiveness contributes to lower accuracy and repeatability rates of this method over long periods of time compared to automated systems. Automated systems replace the human inspector by determining overall quality decisions for individual solder joints and leave the system operator responsible only for maintaining the system and loading and unloading PWA's.

Automated image analysis can be performed for digitized radioscopic or laminographic images. The digitized image is processed through mathematical algorithms which are specifically designed to represent the particular type and size of joint under inspection (e.g., "J" leaded, gull wing, LCC). Inspection algorithms evaluate the grey-scale image and render a decision based upon established thresholds. The creation of the algorithms is very complicated and requires extensive analysis before installation. PWA's containing nonstandard joint configurations may require customized algorithms to be developed, adding to the overall system cost and delivery schedule. Automated inspection algorithm thresholds will most likely be based upon MIL standards (e.g., DOD 2000), that are currently under industry-wide review [13]. Current automated radioscopy systems are claimed to achieve defect identification accuracies of from 95 to 99+ percent [19, 20].

This report does not include experimental testing or an analysis of automated inspection performance capability or algorithms used by those systems, particularly for circuit boards. The use of automated inspection examples are for overview purposes only and may or may not completely identify the full potential of known X-ray automated inspection systems.

The economic payback calculations for single-sided circuit board solder bond evaluation have been estimated for semiautomated radioscopy, automated radioscopy, and SBLAM. Figure 6.1-1 lists the basic assumptions as a function of the system type. The calculations assume a 5-year system depreciation according to the ACRS schedule (20, 32, 19, 12, 11, 6 percent per year respectively) and is taxed at an assumed 34-percent corporate tax rate. The capital cost of the system includes estimated tax, shipping and miscellaneous closing costs. Each system is weighted to account for a 20-percent-of-system cost increase in working capital to purchase, prepare a site and install the system, which is assumed to be returned after 5 years. All cost calculation totals are brought back to year 1 and assumes the cost of money is 10 percent. Annual operation and maintenance (O&M) costs are conservatively estimated at 5 percent of the system cost, and the salvage value is assumed to be 25 percent of the system cost after 5 years and is taxed as a gain at 34 percent. The system inspection times include time for loading the boards. The cost savings result from a labor time savings for using the inspection system and is based on replacing a 1-hour visual inspection on 100 percent of the PWA's and a 3.5-hour film X-ray examination on a 5-percent lot sampling. Appendix C discusses the fundamental calculations used to generate the economic payback estimate curves for semiautomated radioscopy, automated radioscopy and scanned beam laminography.

	Semiauto Radioscopy	Automated Radioscopy	SBLAM
Capital Cost	$200,000	$400,000	$450,000
Working Cap.(20%)	$ 40,000	$ 80,000	$ 90,000
Annual O&M (5%)	$ 10,000	$ 20,000	$ 22,500
Salvage Value (25%)	$ 50,000	$100,000	$112,500

Inspect. Time/PWA	Semiauto Radioscopy	Automated Radioscopy	SBLAM	Labor Comparison Base Visual/X-ray Inspection
Single-Sided	10 min.	1.0 min.	1.5 min.	1 hour/ 3.5 hours
Double-Sided	20 min.	system not used	3.0 min.	2 hours/ 7 hours

Max PWAs/8hr Day	Semiauto Radioscopy	Automated Radioscopy	SBLAM
Single-Sided	48	320	192
Double-Sided	24	System Not Used	107

Savings per PWA	Semiauto Radioscopy	Automated Radioscopy	SBLAM
Single-Sided	$75.63	$86.88	$86.25
Double-Sided	$151.25	System Not Used	$172.51

Figure 6.1-1 Inspection system payback calculation criteria

The semiautomated radioscopic inspection time is assumed to be 10 minutes per PWA with a savings estimated to be $75.63 per PWA over visual inspection. This is based on a burdened labor rate of $75 per hour. The automated radioscopic inspection time is assumed to be 1.5 minutes with a savings estimated to be $86.88 per PWA. The SBLAM inspection time is assumed to be 1.5 minutes with a savings of $86.25. The automated radioscopic inspection technique and SBLAM provide a 95-percent confidence level examination on assemblies containing 500 joints each and assumes an even distribution of SMT package styles. For the semiautomated radioscopy inspection, a confidence level of 80 percent is assumed to take into account operator interpretation variations. Thus, to achieve 95-percent confidence level using semiautomated analysis the assemblies must be inspected twice for a total of 20 minutes, assuming random factors in interpretation. Two pass inspection with human interpretation is of course subject to human bias and therefore may not infact provide true 95-percent confidence due to systematic effects in visual judgement of features, particularly if the same inspector is used on both passes. The estimated economic payback as a function of throughput is shown in Figure 6.1-2 for inspecting a single-sided SMT PWA.

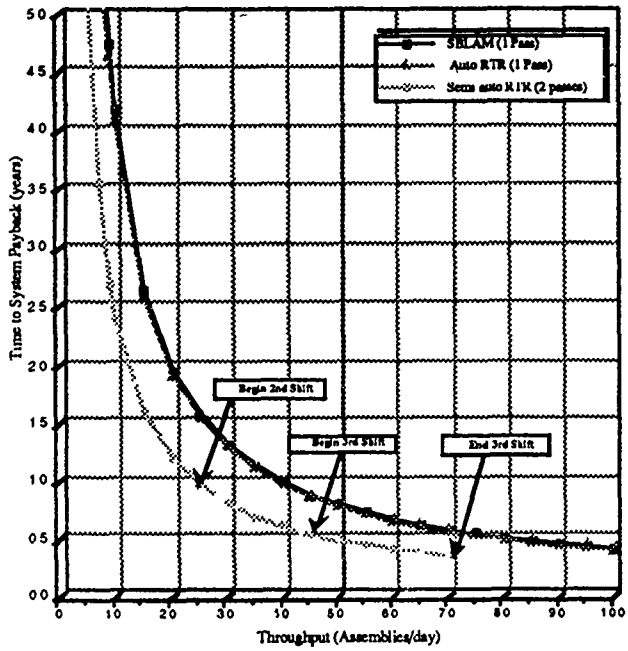

Figure 6.1-2 Estimated inspection system payback for single-sided PWA's at 95-percent confidence level

The graph in Figure 6.1-2 indicates that moving from visual inspections to X-ray based inspections will have a rapid economic payback which increases significantly with throughput. As desired throughput increases for semiautomated radioscopy, the start of a second shift after a throughput of 24 boards/day is required. The addition of a second shift will lead to the X-ray source requiring replacement sooner, but this cost is offset by the depreciation allowance for the second year (32 percent) and does not significantly affect the number of years to payoff. Similarly, the addition of a third shift is also offset by the accumulation of depreciation allowances and does not appreciably affect the number of years to payoff. The maximum throughput for a semiautomated system for a three shift day is 72 units. To increase the throughput beyond 72 units requires that another system be purchased.

Automated radioscopic and SBLAM show very similar economic payback curves for up to 100 PWA's/day and higher. Both of these techniques offer the capability of automated inspection. The initial costs are higher than the semiautomated radioscopy but the automated analysis provides a constant inspection quality that can be readily applied to statistical process control (SPC). A big advantage of the automated inspection systems is a rapid process control feedback with a consistent interpretation of the solder bond conditions. For high throughput (100 boards/day) the payback over visual inspection is within six months.

Manufacturers of single-sided boards having low throughput and limited budget would do well investing in semiautomated radioscopy systems equipped with an optional programmable parts manipulator. During testing, one particular feature, variable magnification, was found to be desirable when identifying locations on unknown boards.

Manufacturers of single-sided boards having a high throughput who can afford to purchase, develop and maintain an automated inspection system should see a rapid payback. As discussed for some SMT packaging, ambiguity in the image is still an inherent aspect of radioscopy based systems. Multi-axis features serve to displace some of the ambiguity. The automated inspection algorithms are undergoing continuous development and their suitability and accuracy for particular solder joint types must be assessed for each application. Thresholds for determining accept/reject criteria are determined between the manufacturer and system vendor and may require time to come into agreement with actual defects. Automated inspection systems usually identify the positions of

image features with respect to the board on the system terminal (via CAD programming) and is a function not available in semiautomated mode. The system also outputs defect information for SPC.

While the system may act as a stand-alone, turn key "human inspector replacement," the procedure for developing improved algorithms and thresholds for some systems is an ongoing process requiring as much effort as the manufacturer is willing to devote. In-house experts help to determine thresholds and use the information to help evoke maximum process efficiency. One major advantage to this type of system is with a well maintained and developed system, high board throughputs (in the order of 45 sec/board) can be obtained and can offer a payback within a matter of months [17].

6.1.2 Double-Sided SMT PWA's

The estimated system cost, for a worst case double-sided PWA containing 500 joints each side, assumes an even distribution of closely packed SMT components which overlap identically. Given the added complexity of the board, it is assumed that the analysis for the comparison base of a visual inspection will double to 2 hours as will the X-ray inspection on a 5-percent lot sampling. The inspection time on a semiautomated radioscopy system will double as the operator would take twice as long to interpret the image for 100-percent coverage. The semiautomated inspection time therefore becomes 20 minutes per assembly, with the labor cost savings estimated to be $151.25 per board over visual inspection and X-ray lot sampling. A confidence level of 60 percent for semiautomated radioscopy of double-sided assemblies takes into account the significant operator variability expected in a single pass inspection. To achieve a 95-percent confidence level three passes would be required.

SBLAM, providing 100 percent automated inspection of each side, is estimated to take a total of 3 minutes. A 95-percent confidence level in the inspection algorithms is assumed. Compared to the base of visual and X-ray lot sampling the labor cost savings per board is estimated at $172.51.

The estimated system payback for SBLAM and semiautomated radioscopy is shown in Figure 6.1-3. The rough data indicates that at 25 assemblies/day throughput payback will occur in 6 to 9 months. Although the curves of Figure 6.1-3 indicate a slightly faster payback with the semiautomated versus the automated inspection capability, the consistency of the inspection results favors the use of an automated X-ray inspection system for solder bond evaluation. It is generally agreed that automated analysis can provide much greater consistency and statistical data for product control which translates into a higher quality product. The value of 95-percent confidence in a one pass inspection with the automated system is considered conservative by most industry experts who expect that the confidence may in fact be closer to 98 percent or higher. The manual interpretation by comparison is considered by industry experts to be roughly only 60 percent effective on double-sided assemblies with considerable variability in this estimate. Assuming 60 percent confidence in one pass, approximately three passes are required to achieve 95-percent confidence in the inspection. The economic payback curve for semiautomated inspection is very sensitive to the number of passes. At four passes or greater for the manual interpretation, the automated systems will have a more rapid payback. The variability in the confidence of the manual interpretation represents a higher potential quality "loss" which goes as the square of the variability according to Taguchi principles [21]. These factors should be considered carefully in evaluating any inspection technology.

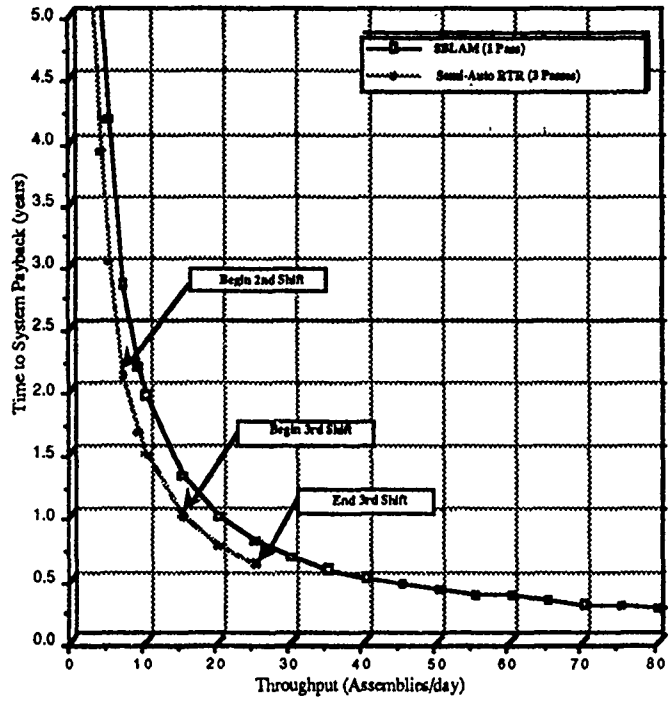

Figure 6.1-3 Estimated inspection system payback for double-sided PWA's at 95-percent confidence level

Finally, the semiautomated radioscopy inspection time limits the number of boards that can be inspected when three passes are used to achieve the 95-percent confidence level. The SBLAM system is assumed to be capable of handling up to 480 PWA's/day and offers a payoff in less than a year for throughputs as low as less than 20 PWA's/day. Assuming that the SBLAM automated algorithms achieve the desired confidence level, it is the preferred choice for double-sided board applications.

The cost analysis for an automated radioscopy system is not compared for the double-sided assembly case due the nature and difficulty of the inspection. It is assumed that the automated inspection algorithms required to interpret the confusing superimposed image of a high-density board with identically overlapping components are not available. High speed inspection using automated radioscopy systems on double-sided boards can be accomplished by designing the board and production techniques around the planned inspection method. One way is to design the board such that it minimizes radiographic superpositioning between both sides. If superpositioning is unavoidable, critical components can be mounted on the same side of the board and inspected first, then complete production on the other side of the board and inspect it afterwards. This technique is used by Delco Electronics in the production of engine controls. In cases where significant superpositioning of components adds unavoidable ambiguity, semiautomated radioscopy inspection might be recommended to allow for human interaction in the decision process and help minimize defect error rates.

6.1.3 Custom PWA's

Printed wiring assemblies with custom features or inspection goals may require alternatives from radioscopy and SBLAM technology. One area of interest is the study of the printed copper traces in multilayer boards after assembly. This "reverse trace analysis" requires sensitivity to the thin (0.070 mm (0.0028 inch)) copper traces.

In the case of reverse trace analysis SBLAM was able to identify the inner traces only very faintly and over a small field of view (~ 25.4 mm (1 inch)). On the other hand CTLAM, as seen in the figures of Section 3.4, was capable of imaging the innerlayer traces clearly and over relatively larger regions. Because the CTLAM system is designed as a research tool, it is more flexible in adjusting system parameters to achieve maximum resolution of the copper traces. Full size (within the system's field of view) tomosynthesis or computed laminography reconstructions can be instructed to correct for board warpage and achieve separations between laminograms around 0.10 mm (0.004 inch) [22].

Data acquisition on a CTLAM system used in this study can be a time consuming process. However, it yields information about the entire 3-D object. With optimized reconstruction processing, analysis is only a matter of panning through the acquired laminograms and manipulating the image controls. The system is best suited for failure analysis and special applications requiring laminograms or CT images of dense or otherwise difficult to handle PWA's for process control and research applications. The development of an economic payback model would depend upon the value gained from the special applications and would have to be analyzed case by case. CTLAM systems cost between $800K - $1500K and could realize a payback depending on the combined savings offered in laminography as well as CT applications.

While scan times can be lengthy, the CT/CTLAM systems excel beyond conventional radiography and radioscopy systems in their ability to deliver quantitative information for special PWA applications. Since throughput is slow, it is expected that the technology would be used on more expensive or mission critical components. CT/CTLAM vendors offer inspection services at competitive prices for those who require only occasional scanning.

6.2 Cost Benefit of Component Inspections

The economic value of CT inspection for electronic component studies depends, of course, on the value of the inspection results and the costs required to obtain them. Cost estimates for inspection are based on rough figures from our actual inspection charges or are projected charges if a system was to be configured for electronic component testing. Costs can vary significantly depending on batch sizes. Considerable economic savings can result as component throughput increases.

6.2.1 Connectors

The connectors studied in Section 4.1 were inspected on industrial CT systems with costs of inspection ranging from $100 to $300 depending on scan time and overhead costs. An individual CT slice itself may cost as little as $20 to $100, but unless the overhead of setup, reviewing and archiving is amortized across many units the actual cost is higher. But even $300 to settle a quality dispute with a vendor may be cost effective. Discussions over product issues run in the hundreds of dollars per hour when several individuals are present. If hard data is available, discussion time is greatly reduced.

An example of using radioscopy to image a connector detail is shown in Section 4.1.2. This is less expensive than CT scanning, perhaps costing as little as $20 to $50 including setup expenses. The radioscopic image requires that the operator have some proficiency at interpreting the display.

6.2.2 Failure Analysis of a Relay

The approximate costs for a typical destructive failure analysis of a relay was estimated in the Task 1 report [1] and is illustrated in Figure 6.2-1. The relay which underwent failure analysis is shown in Figure 6.2-2. In this example approximately $1800 was spent on evaluating a $50 component.

Component:	Miniature Circuit Board Can Relay	
Component Cost:	$50	
Case Dimensions:	5/16" dia. x 3/8"	
Suspected Failure:	Welded Contacts	

	Tests and Processes	Time	Approx. Cost	
1.	Electrical Testing	1 hour	$ 95	*
2.	Package Gas Analysis	3 days	$100	**
3.	Hermetic Seal Test	4 hours	$ 380	*
4.	Open Package	3 hours	$ 285	
5.	Full Analysis	8 hours	$ 760	*
6.	Document Results	2 hours	$ 190	*

Total Analysis Time: 18 hours company time
3 days outside vendor analysis

Total Duration: Approximately 1 Week

Approximate Total Cost: $1800

Determined Failure: Welded Contacts

* Costs distributed as 40 percent shop time and 60 percent engineering time.
** Performed by an outside vendor.

Figure 6.2-1 Typical failure analysis costs for a relay

The relay example of Figure 6.2-1 was CT scanned as part of Task 1 to identify the welded contact, and while the resolution failed to clearly distinguish the welded contacts (the contacts are approximately 0.4 mm (0.016 inch) thick), analysis of the scans inferred that there was a weld. With advanced CT capability, not available at the time of this study, it is estimated that the analysis of this relay could have been conducted in about 2 hours for a cost of approximately $500, yielding the same results as destructive analysis but at a $1300 cost saving.

The relay was also investigated in this study using radioscopy. The images shown in Figures 6.2-3 and 6.2-4 clearly identify the welded contact. The investigation required about 5 minutes, at a cost of about $15 or savings of 12,000 percent over destructive analysis. The radioscopic method represents the greatest savings in this case.

The nondestructive methods of CT or radioscopy show a cost saving over the present destructive methods with an added benefit of preserving the evidence. The method of choice may depend on how the data is to be presented and the ability of the interested parties to interpret the information.

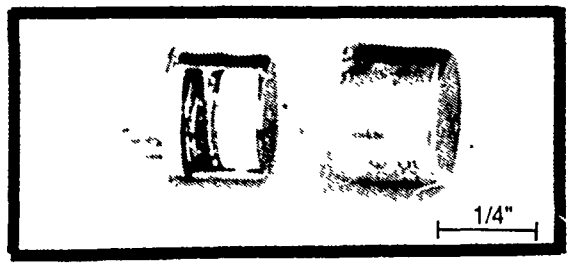

Figure 6.2-2 Photograph of can relay

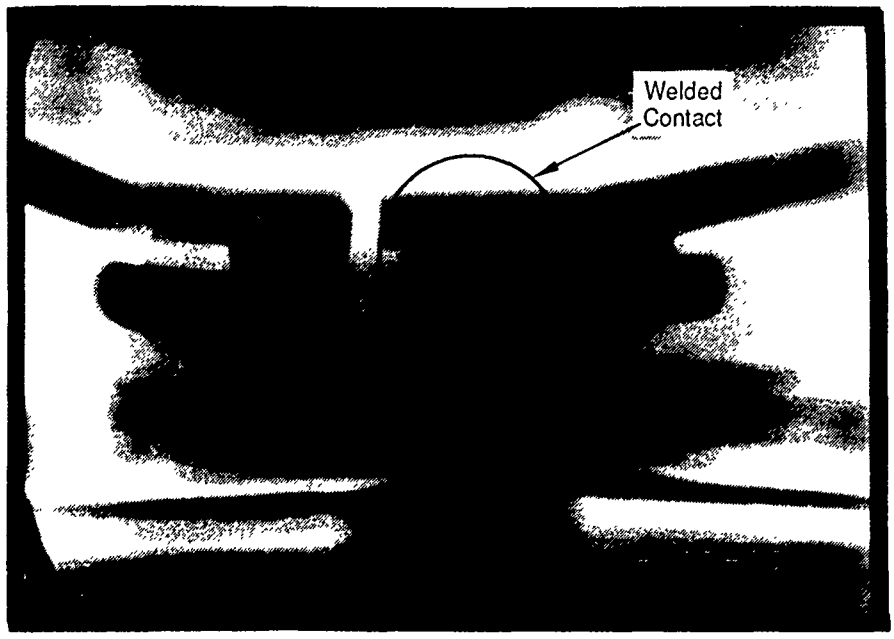

Figure 6.2-3 Radiographic image of welded contact (front view)

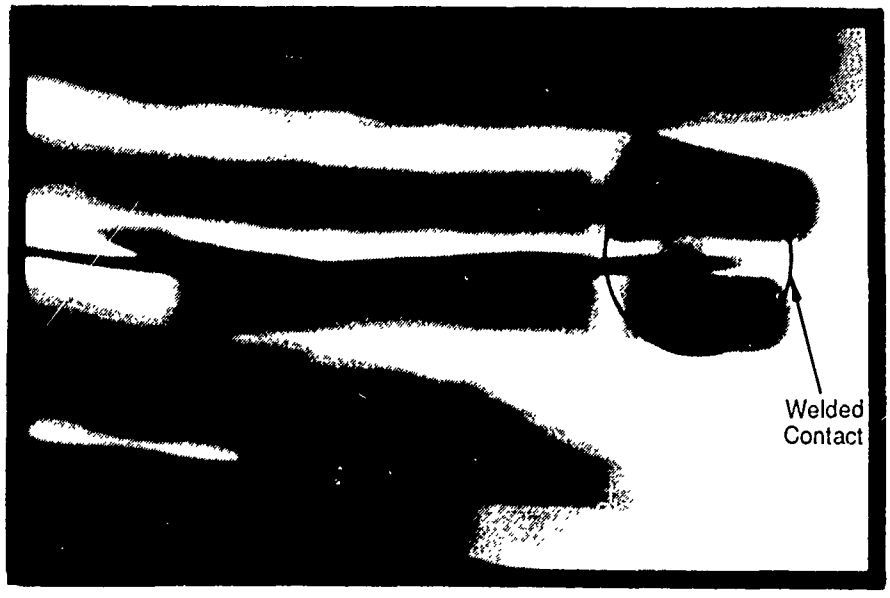

Figure 6.2-4 Radiographic image of welded contact (relay rotated 90°)

7.0 CONCLUSIONS AND RECOMMENDATIONS

This final testing Task Assignment has investigated X-ray tomographic imaging for solder bond evaluation and reverse trace analysis of printed wiring assemblies and several other electronic component categories.

7.1 Printed Wiring Assemblies

Automated inspection systems for printed wiring assembly solder bonds have short term (0.5 to 1 year) payback over visual inspection. The automated inspection algorithms were not evaluated but it is believed that they will provide greater confidence in evaluation consistency than is provided by human observation and will produce objective data. For single-sided PWA's radioscopic systems can be used. For double sided PWA's where components are mounted such that a radioscopic image shows overlapping solder bonds from each side, laminography is more appropriate. Scanned beam laminography offers a method for rapid solder bond inspection of double-sided assemblies. It is possible to utilize the laminographic imaging to build a 3D model of the solder joint. Volume and shape of the bond is one of the most important features for predicting solder joint performance.

The data from automated inspection systems can be input to statistical process control (SPC) systems. SPC is critical to modern, high throughput manufacturing, and is an important element in MIL STD 2000 for electronic manufacturing.

Laminography using an industrial CT system is also shown to provide useful data for reverse trace analysis. Individual copper trace planes in multilayer boards could be resolved for boards with 0.40 mm (0.016 inch) spacing between layers. This capability could be improved in both speed and resolution and be very useful for studying unknown or suspected flawed board designs in already constructed assemblies.

7.2 Other Electrical Components

Connectors, transformers, relays and other electrical components that have volumetric features were found to benefit from tomographic inspection for failure analysis as an alternative for destructive sampling sectioning or for product development. CT images were useful for determining internal geometric features of a complex assembly. CT has a significant benefit over conventional failure analysis tests which often destroy the evidence of failure. In the case of an alternative to destructive sampling sectioning, CT can save the part, which results in considerable cost savings for high cost electrical components.

It was also found that radioscopy could be used to determine specific features of interest in electrical components, using the human observer to evaluate the depth of the features by manipulation of the radioscopic display. The selection of radioscopy or CT for analysis depends on the component design and the nature of the desired results from the examination. Quantitative dimensional and material composition measurements can be readily obtained from the CT data, whereas radioscopy is qualitative.

7.3 Recommendations

This study recommends that automated X-ray techniques be implemented for PWA solder bond evaluation at the manufacturing line. The selection of a tomographic based inspection will depend on the specifics of the assembly design, manufacturing throughput and the SPC goals of the manufacturer.

Higher resolution CT and CTLAM equipment is becoming available. Several systems planned to be used in this study did not meet their availability schedule in order to suitably evaluate their capability. It is recommended that a study of higher resolution CT be performed to determine its economic benefit for electrical component evaluation and reverse trace analysis. In particular, micro-CT should be tested on a small portion of a PWA to evaluate the solder bond by cross-sectional tomography for comparison with laminography.

Failure analysis using CT is of considerable value and interest. Likewise, microfocus radioscopy has been shown to provide useful information. The combination of radioscopy and CT in a single system may offer engineers the tool that has been needed for cost effective nondestructive analysis of test samples and failures for small components. A demonstration to government and industry on the advantages of CT and associated X-ray inspection capability for failure analysis studies with emphasis on the electrical component area would be worthwhile.

REFERENCES

1. R. H. Bossi, R. J. Kruse, B. W. Knutson, *Computed Tomography of Electronics*, WRDC-TR-89-4112, 1989.

2. R. H. Bossi, J. L. Cline, B. W. Knutson, *Computed Tomography of Thermal Batteries and Other Closed Systems*, WRDC-TR-89-4113, 1989.

3. R. H. Bossi, J. L. Cline, E. G. Costello, B. W. Knutson, *X-Ray Computed Tomography of Castings*, WRDC-TR-89-4138, 1989.

4. R. H. Bossi, K. K. Cooprider, G. E. Georgeson, *X-Ray Computed Tomography of Composites*, WRDC-TR-90-4014, 1990.

5. A. Bindra, "Fine-Pitch Bursts onto the Market," *Electronic Engineering Times*, February 26, 1990, p 81, 84.

6. S. Stach "SMT Rework and Repair for the 1990's," Proceedings of the Sixth Annual International Electronics Packaging Conference, San Diego, CA, November 1986, pp. 686-695.

7 "Printed Wiring Boards: A Trillion-Yen Business," *Journal of EE*, January 1990, p 58 - 60.

8. J. McCreadie, "Contract Manufacturing Thrives on Fast SMT Growth," *Electronic Business*, February 19, 1990, p 17.

9. R. Iscoff, "Surface Mount Packages will Dominate the Market by 1994," *Semiconductor International*, April 1990, p 48.

10. G. Lucey, "Avoiding Obsolescence in DOD-STD-2000," Proceedings of NEPCON West, National Electronics Packaging and Production Conference, Spring 1989, pp. 641, 642.

11. J. Bell, "DOD-STD-2000: Adjusting to Reality," Proceedings NEPCON West, National Electronics Packaging and Production Conference, Anaheim, CA, March 1989, pp. 635-640.

12. M. Gill, "Stalking Six Sigma," Business Month, January 1990, pp. 42-46.

13. R. Alexander, "Future Acceptance of NAVY 'DOD' Solder Connections," Proceedings of NEPCON West, National Electronics Packaging and Production Conference, March 1990, pp. 1055-1063.

14. M. Gauthier, "Radiation-Effects Testing for Space and Military Applications," *Test and Measurement World*, February 1988.

15. "Ionizing Radiation and Its Effects Upon Electronic Components," Application Note, NICOLET Corporation.

16. P. Crepeau, TRW private communication.

17. L. A. Feldkamp, G. Jesion, and D. J. Kubinski, "Microtomography Using a Real-Time Imaging System," Industrial Computed Tomography, ASNT Topical Proceedings, July 25-27, 1989.

18. D. Vickers, W. Cox, W. McCroskey, B. Kohrs, R. Zahn, and R. Carlson, "A Revolutionary Approach to Industrial CT Using Cone-Beam Reconstruction," Industrial Computed Tomography, ASNT Topical Proceedings, July 25-27, 1989.

19. M. Juha, "The Economics of Automated X-Ray Inspection for Solder Quality," Proceedings of NEPCON West, National Electronics Packaging and Production Conference, Anaheim, CA, February 1986, pp. 949-960.

20. C. Goodwin, "Real-Time X-ray Process Control for Solder Joint Integrity," Proceedings of NEPCON West, National Electronics Packaging and Production Conference, February 1987, pp. 533-542.

21. D. Byrne, "Taguchi Methods," Chapter 2, *Taguchi and QFD: Hows and Whys for Management*, N. Ryan, ed., ASI Press, Dearborn, MI, 1988.

22. S. Buchele, H. Ellinger, F. Hopkins, "Forming Laminograms on Object-Dependent Surfaces," *Materials Evaluation,* May 1990, pp. 618-620.

This page left intentionally blank

APPENDIX A

RADIOSCOPY, COMPUTED TOMOGRAPHY, AND LAMINOGRAPHY

A1 Radioscopy

Radioscopy is defined by the American Society for Testing and Materials as the electronic production of a radiologic image that follows very closely with time the changes of the object. Radioscopy includes real-time radiographic systems that are commonly used in electronic inspections. The image is normally observed on a video monitor.

The radioscopic image is displaced as grayscale data and may be digitized for further processing if desired. The attenuation of the X-rays is related to the material path length in the objects under investigation. Defects, such as porosity, reduce the local solder thickness, increasing the transmissitivity of the X-rays. The result is viewed as a region within the solder joint which is brighter in appearance and is used to infer knowledge about the integrity of the joint.

Radioscopic imaging systems consist of an X-ray source, part manipulator, detector and image display. A very common detector is an image intensifier tube. The X-ray photons strike a phosphor/photocathode target that emits electrons which are accelerated and minified in a vacuum tube. The intensified image is observed on an output phosphor screen by a video camera. The system in Figure A1-1 is a five-axis radioscopy system which uses a microfocal X-ray source and an image intensifier. The configuration shown is universal to accepting a wide variety of components from planar PWA's to electrical components.

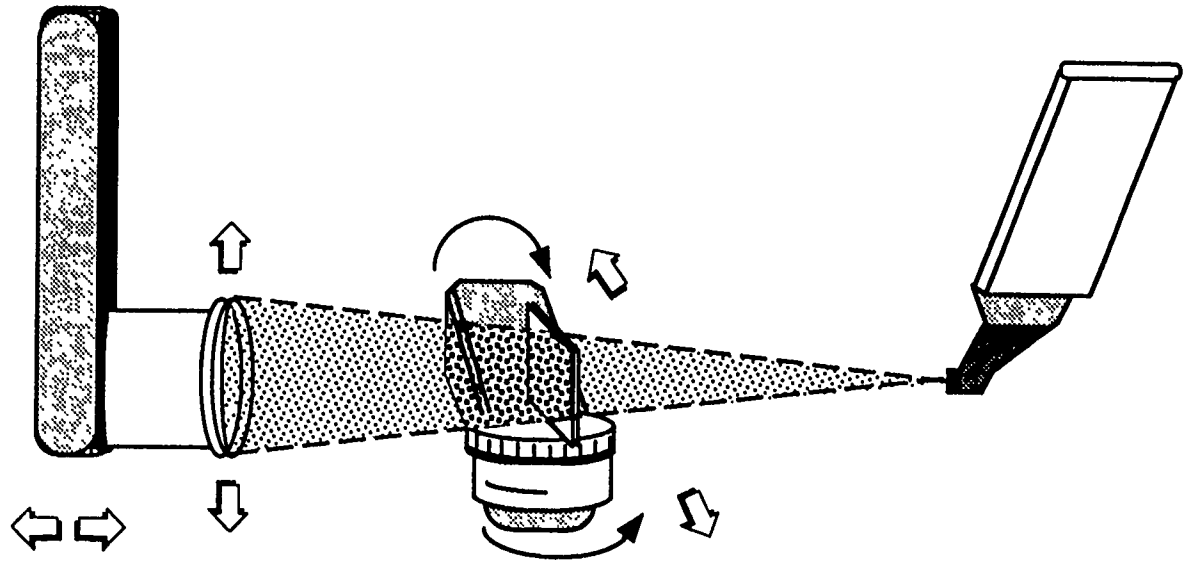

Figure A1-1 Universal 5-axis manual radioscopy inspection system

Another common detection approach involves the use of a florescent screen to convert the X-ray radiation into visible light and optical coupling to a CCD or video-type camera to record the image. For small area detection, the target of vidicon camera can be made sensitive to X-rays for direct imaging of the transmitted X-rays. Figure A1-2 is an example of this inspection approach using an X-ray sensitive vidicon to image the PWA.

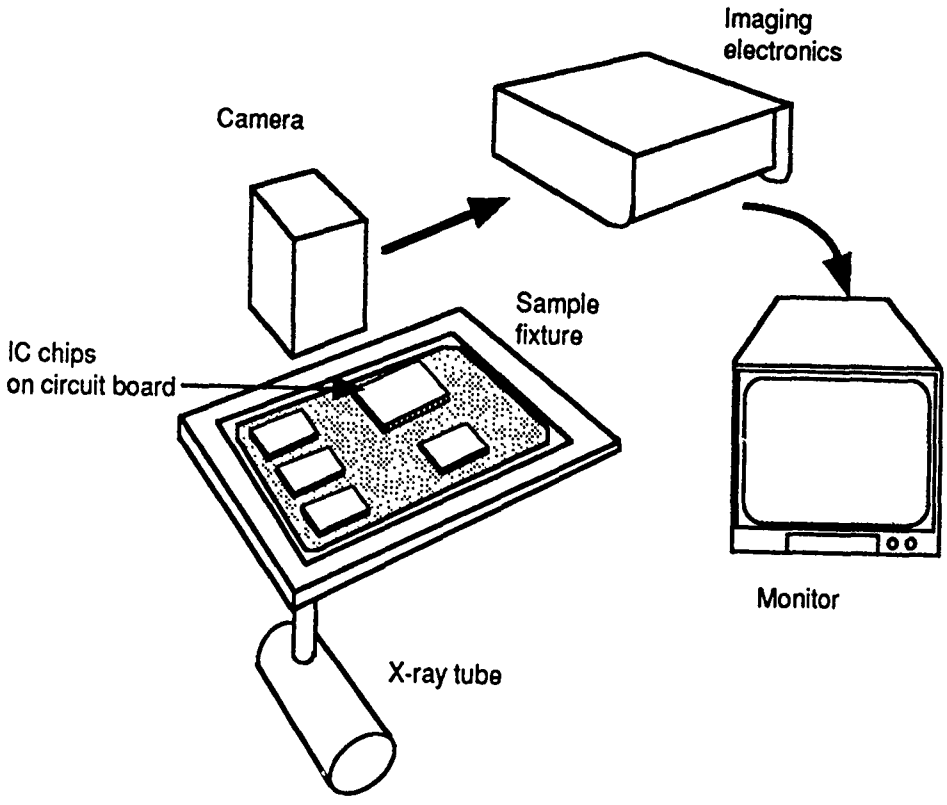

Figure A1-2 Diagram of PWA inspection system

A2 CT Systems

A2.1 Conventional CT

Computed tomography (CT) uses X-ray transmission information from numerous angles about an object to computer reconstruct cross-sectional images (i.e., slices) of the interior structure. To generate a CT image, X-ray transmission is measured by an array of detectors as shown in Figure A2-1. Data is obtained by translating and rotating the object so that many viewing angles about the object are used. A computer mathematically reconstructs the cross-sectional image from the multiple view data collected. The image data points are small volumetric measurements directly related to the X-ray attenuation coefficient of the material present in the volume elements defined by the slice thickness and the horizontal resolution capability of the CT system. A primary benefit of CT is that features are not superimposed in the image, thus making it easier to interpret than radiographic projection images and providing quantitative data for dimensional and material density/constituent measurements.

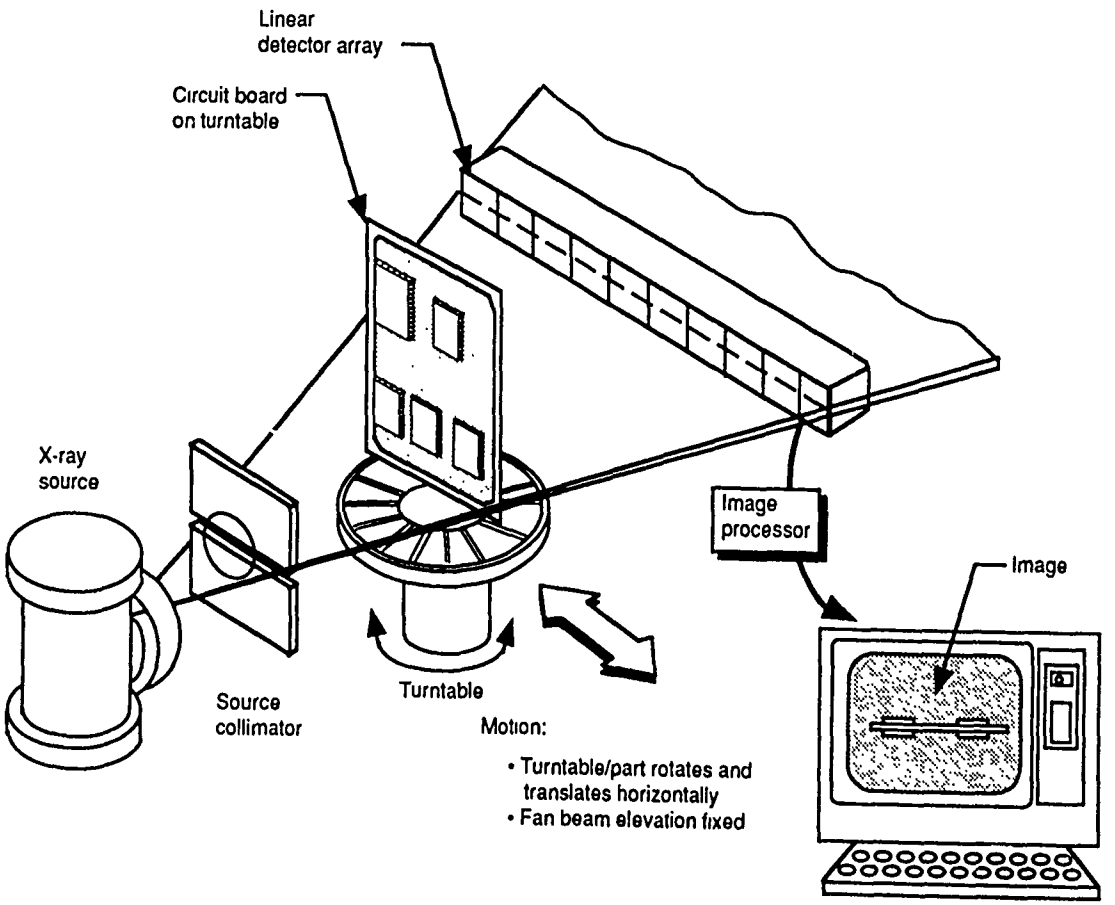

Figure A2-1 Computed tomography

A2.2 Cone Beam CT

Cone beam CT is fundamentally the same as conventional CT; however, instead of collimating to a thin slice of radiation and using a linear detector array, an entire cone of radiation is used with an area array detector, as shown in Figure A2-2. The data acquisition in each angular view includes information for multiple CT slices along the object axis. The object will be rotated for data acquisition of multiple views. The data handling and reconstruction for cone beam CT is substantially more complicated than conventional CT and a suitable display mechanism for viewing multiple plane images from the volumetric data set is needed. The advantage of the technique is that an entire volume can be scanned much more rapidly than is possible using conventional CT and taking scans at multiple axial positions. This offers a substantial cost savings for CT examinations of entire volumes.

A concern of cone beam CT is that collimation is not used and therefore X-ray scatter is detected, reducing overall image detail sensitivity. The use of large magnification (>10) in the cone beam projections can reduce the scatter influence. Cone beam CT with microfocus sources and high magnifications (>20) can be used for high-resolution CT of small (<15 mm (0.6 inch) diameter) objects.

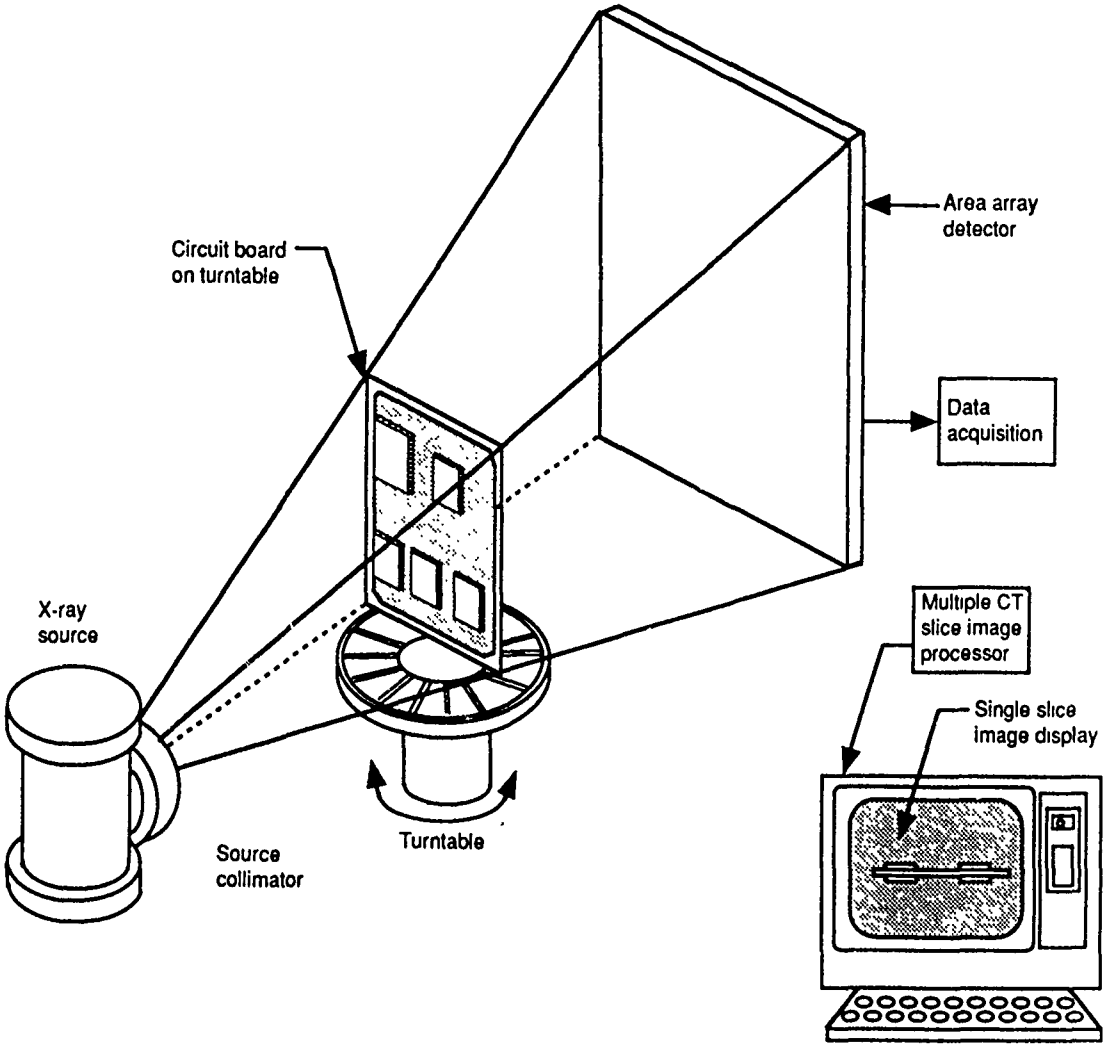

Figure A2-2 Cone beam CT

A3 Laminography

Laminography (body-section tomography, focal plane tomography, etc.) is a term given to techniques which generate a focussed plane of information in an object while defocussing surrounding planes. This is particularly effective for objects which contain structures that overlap from different planes. By defocussing planes above and below a plane of interest, the structures that are not of interest will be blurred, thus reducing their overall contrast effect in the image. The structure at the plane of interest will remain in focus and in the final image will be observed with improved sensitivity to detail. Objects that are homogeneous (i.e., do not contain structure) generally will not benefit from laminographic examination.

Laminographic imaging using X-rays dates back to the early days of radiography where physicians recorded body-section tomograms using a synchronously moving source and detection medium (i.e., film). By forming an X-ray focal plane in a patient, features within planes of interest could be brought into focus while regions not of interest could be "defocused." Various motions of synchronism were explored including linear and more complicated polytomographic (circular, figure eight, clover leaf, etc.) techniques to achieve maximum resolution capabilities.

A3.1 Scanned Beam Laminography

A modernized version of laminographic imaging replaces a mechanically moving source with a electronically scanned source, and film with a scintillating phosphor screen/CCD camera to transfer the images to a video terminal in real time. The scanned source shown in Figure A3-1 creates a focal plane (A). The object of interest (i.e., PWA) is raised or lowered through the focal plane to image the side of interest. Features on the opposite side of the assembly are "defocussed" by not being in the focal plane and are instead "averaged" across the entire field of view, thus lowering the contrast contribution in the resulting image. The X-ray beam may be hardened for optimal penetration of solder by the use of a filter material such as titanium. The addition of filtering devices will optimize the system for certain applications (i.e., solder bond inspection) and will limit its use for others (i.e., composities).

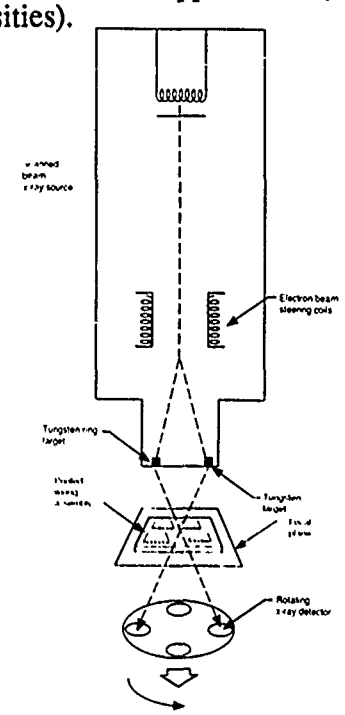

Figure A3-1 Scanned beam laminography

A3.2 Computed Laminography

Laminographic imaging may be performed from digitized radiographic images by computer reconstruction. Computed laminography is typically performed on industrial CT systems. A series of digital radiographs (DR's) are taken at various angles about the normal to an object, a process which may take approximately an hour on some industrial CT systems. The data acquisition time may vary depending on the resolution required and can range from a few DR's to 12 or more. A laminographic plane is selected, backprojected onto each DR and summed to form the final image. Computed laminography is time consuming if only a single image plane is desired, but can be highly advantageous (i.e., time and cost saving) where several inspections of a single object are required. Since DR's are taken at various angles from around the object, each DR contains superimposed information of features within the object. After backprojection, the laminographic image "focuses" on the desired image plane and "defocusses" other object features. Similarily the technique can be used on nonplaner objects to "focus" on arbitrary curved or object dependent surfaces [22]. This technique could be used to correct for the warped PWA trace planes for example. Figure A3-2 illustrates the computed laminography technique.

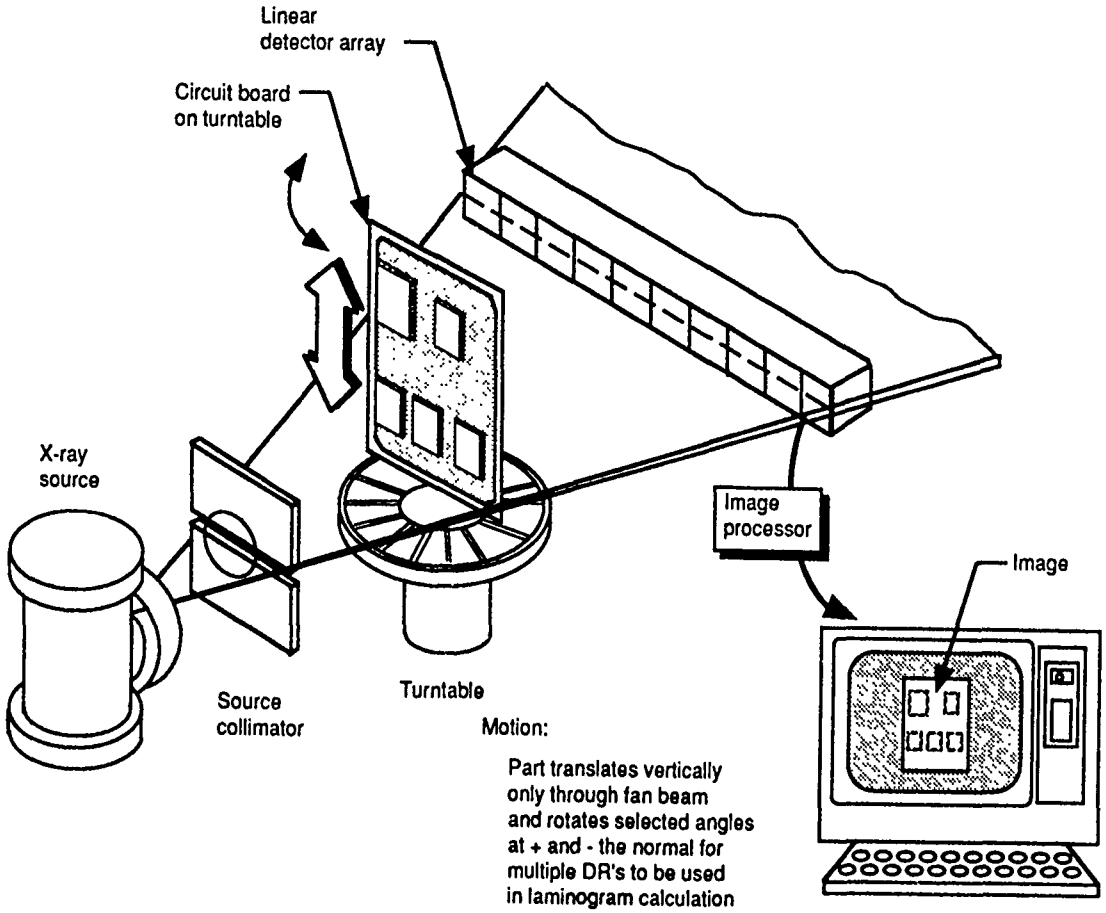

Figure A3-2 Computed laminography

APPENDIX B

CT PHANTOMS

A set of CT phantoms was developed for the Advanced Development of X-ray Computed Tomography Applications program in order to provide consistent evaluation of results from various CT systems. The phantoms serve several purposes. First, they provide a quantitative measure of the CT system capability that can be used repetitively to assure consistent performance. Second, the quantitative measurements can be used in conjunction with part images to assess a quality level necessary to achieve desired detection or measurement levels in the inspected parts. Third, the phantoms can be used to select CT systems based on the desired sensitivity level for the CT application.

The use of phantoms for CT is complicated due to the wide range of parameters in any CT inspection. Therefore, caution must be used in extrapolating phantom data to suggest a "best" overall CT system. In fact, CT systems have varying designs that result in a range of performance characteristics. The phantoms allow the user a quantitative measure of quality level that, combined with other operating parameters, may suggest an optimum system. While the phantoms used in this program measure line pair resolution and contrast sensitivity, there are several other important parameters a user must be concerned with in selecting a CT system for scanning: scan time, field of view, object penetration, data manipulation, system availability and cost.

B1 Resolution Phantom

Figure B1-1 shows the line pair resolution phantom. The phantom consists of sets of metallic and acrylic plates of specified thicknesses. Line pairs of 0.5, 1, 2 and 4 lp/mm are formed by the phantom.

The entire assembly is bolted together, and the line pair plates can be changed if additional or a different range of line pairs is desired. Following CT scanning the reconstructed image is analyzed by measuring the modulation of the CT numbers resulting from a trace across the line pairs. The modulation at each line pair set is measured as a percentage, where the modulation measured between the 3 mm (0.12 inch) thick metal and 3 mm (0.12 inch) thick acrylic steps is 100 percent. Operating parameters such as field of view, slice thickness, integration time and detector collimation will affect the results. It is desirable to obtain data at CT system parameters that are the same as that used for part scanning. The resolution phantom has been fabricated in two forms, steel/acrylic and aluminum/acrylic. The steel/acrylic phantom is for systems of 300 kVp and up, the aluminum/acrylic phantom is for systems under 300 kVp.

Figure B1-2 shows a CT image of the steel resolution phantom obtained from a high-resolution CT system. The CT image density contour line across the gauge indicates modulation for the respective line pair measurements at approximately 82 percent at 0.5 lp/mm, 46 percent at 1 lp/mm, 4 percent at 2 lp/mm, and 0 percent at 4 lp/mm.

Figure B1-3 shows a CT image of a similar resolution phantom for higher resolution tests having set of three steel shims in thicknesses of 0.13 mm (0.005 inch), 0.10 mm (0.004 inch), 0.076 mm (0.003 inch), 0.051 mm (0.002 inch), and 0.025 mm (0.001 inch) The CT system tested is unique in that it incorporates scintillating fiber optic detectors to provide spatial resolution in the 15 - 20 μm range. The image was taken using a standard 320 kV 1.25 mA X-ray source with a 3-mm focal spot. The CT image density contour line across the gauge indicates modulation down to approximately 10 lp/mm.

Figure B1-1 Photo of the resolution phantom

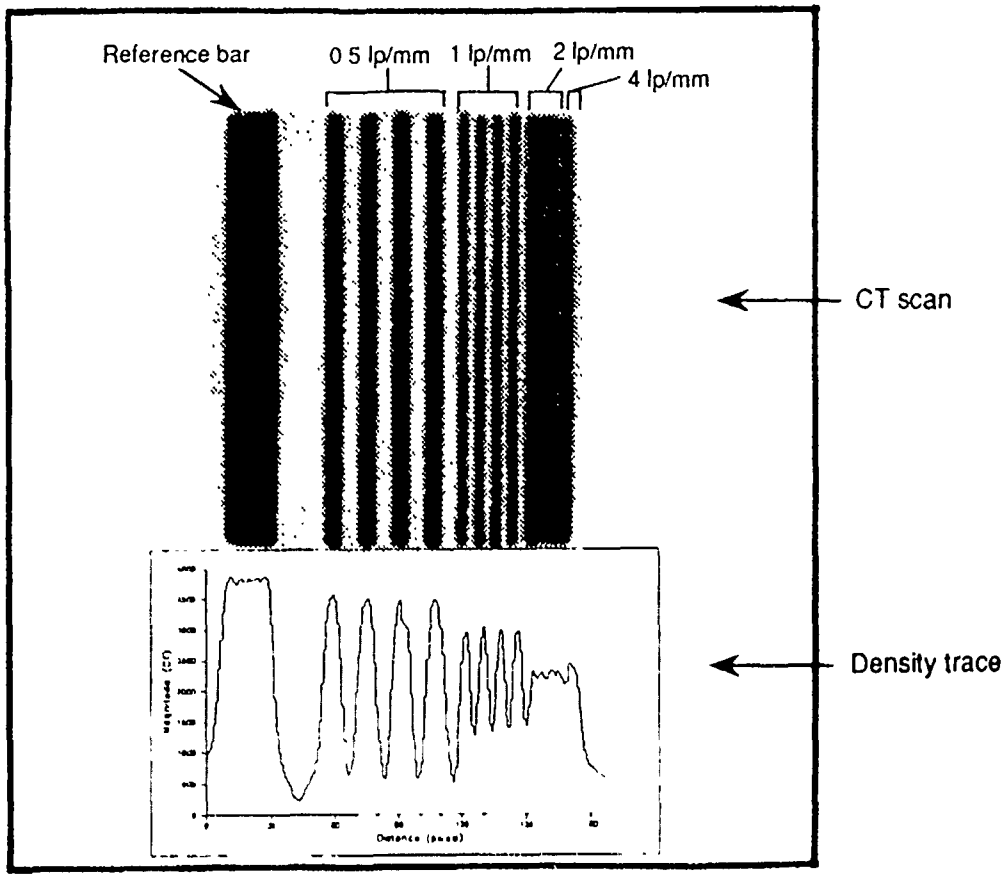

Figure B1-2 CT slice taken on the resolution phantom

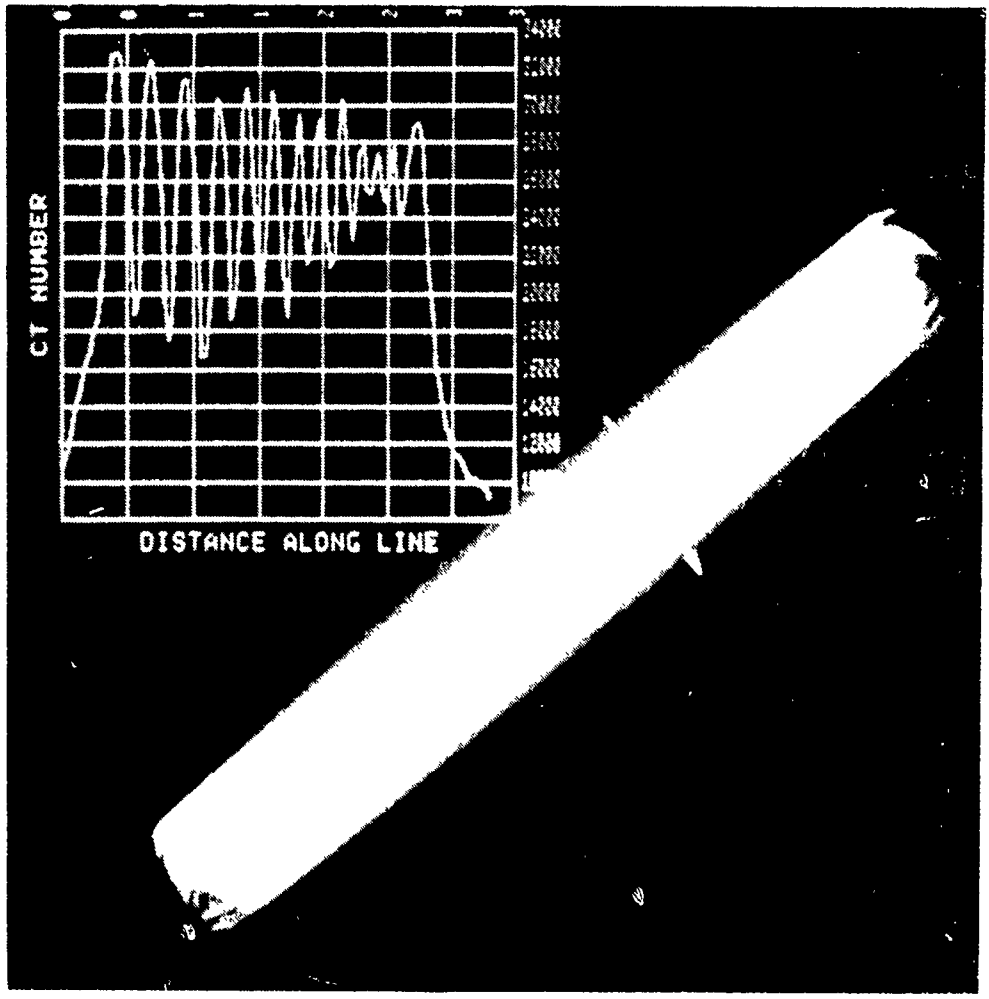

Figure B1-3 CT slice of a high-resolution line pair phantom

B2 Contrast Sensitivity Phantom

The contrast sensitivity phantom is a uniform disc of aluminum, 25 mm (1 inch) thick. Two sizes were made: one is 140 mm (5.5 inch) in diameter and the other is 70 mm (2.76 inch) in diameter. The smaller diameter size is used on systems with small fields of view or low kVp. Figure B2-1 shows an example CT slice of the large aluminum contrast sensitivity phantom with the corresponding density trace.

The measurement of contrast sensitivity is obtained by taking a region in the reconstructed image and determining the average and standard deviation for all CT numbers in the region. A typical region size of 1 cm (0.39 inch) diameter is used. Readings are usually taken at the center of the disk. The ratio of the average to the standard deviation is used as a signal-to-noise measurement. The inverse is a measure of contrast sensitivity. The signal-to-noise measurement for the image shown in Figure B2-1 is approximately 6.

The signal-to-noise ratio measurements are an important measure of system performance. The values improve with higher signal strengths. They also improve with smoothing algorithms in the reconstruction; however, this will decrease the resolution. Thus, the signal to noise and resolution must be considered together in assessing a quality level for performance.

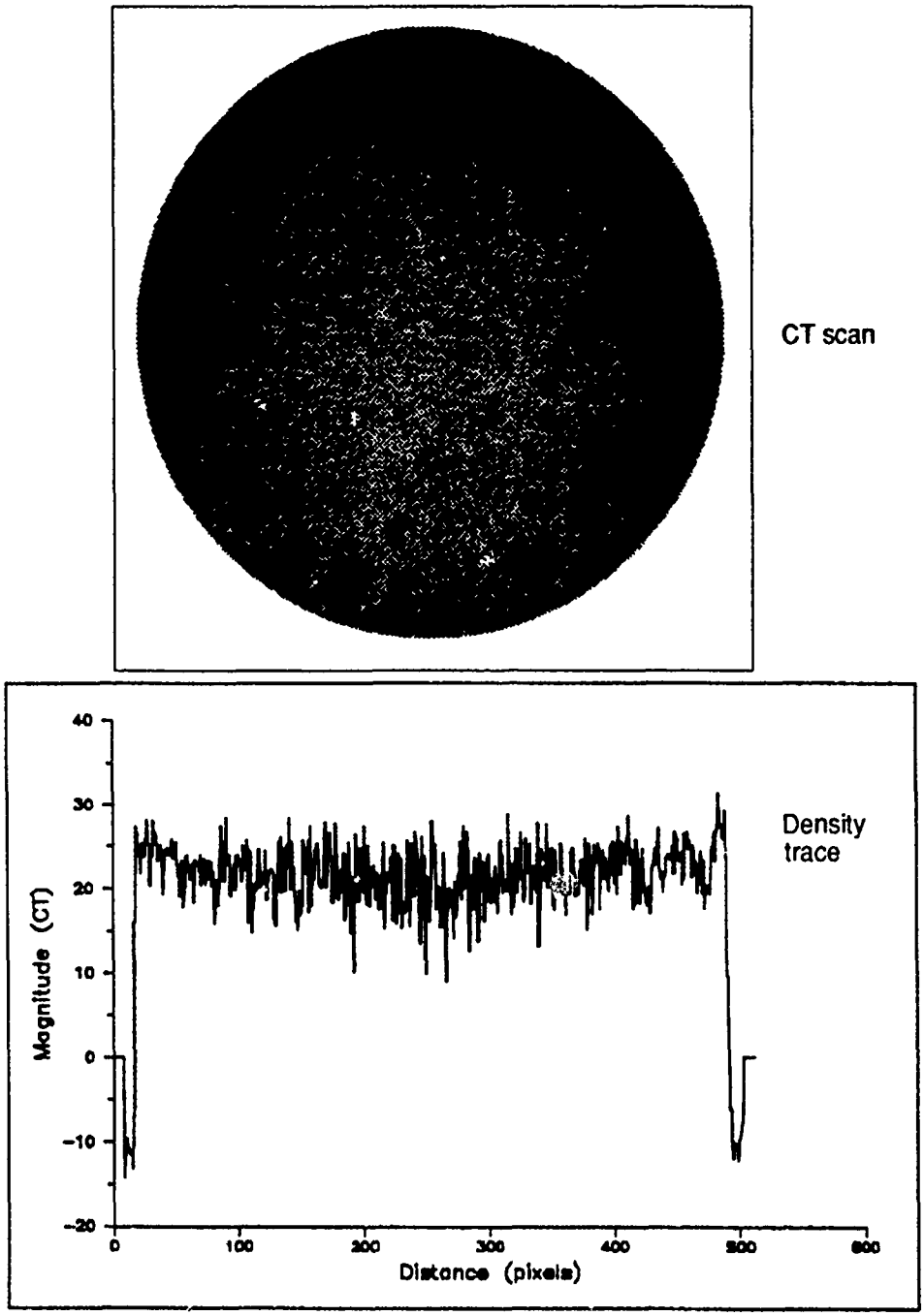

Figure B2-1 CT slice of contrast sensitivity standard

APPENDIX C

ECONOMIC PAYBACK CALCULATIONS

This appendix discusses the fundamental calculations used to generate the economic payback estimate curves for semiautomated radioscopy, automated radioscopy and scanned beam laminography. Figure C-1 is a summary of the cost analysis payback results. Figure C-2 is an example spreadsheet that has been divided into sections for explanation.

	Semiautomated Radioscopy	Automated Radioscopy	SBLAM
Single-Sided Assemblies			
Inspection Time/assembly	20 min.	1 min.	1.5 min.
Throughput/8 hour shift	24 assemblies	480 assemblies	320 assemblies
Time to Payback at Throughput for 8 hour shift	12 months	1 month	1.5 months
Time to Payback at 24 assemblies/day	12 months	19 months	20 months
Double-Sided Assemblies			
Inspection Time/assembly	1 hr (3 passes)	System Not Used	3 min.
Throughput/8 hour shift	8 assemblies	System Not Used	160 assemblies
Time to Payback at Throughput for 8 hour shift	24 months	System Not Used	1.5 months
Time to Payback at 24 assemblies/day	7 months (3 shifts/day)	System Not Used	9 months
Approximate First Year Total System Expenses	$240,000	$480,000	$540,000

Figure C-1 Summary of cost analysis payback results

C1 Labor Savings Comparison Base - Section A

The economic payback calculations first requires that the labor savings comparison base be determined. The base is assumed to be the cost of performing a visual inspection on 100 percent of the assemblies plus the cost of performing a full radiographic inspection on a lot sampling of 5 percent of the assemblies. The labor comparison base is computed in section A of Figure C-1 on a per assembly basis as follows:

Assume 1 hr for visual inspection @ \$75/hr = \$75
Assume 3.5 hrs for 5 percent lot sampling @ \$75/hr = (3.5 * 0.05)(\$75) = \$13.13
Total comparison base = \$88.125/assembly.

C2 Assembly Throughput/Cost Savings Parameters - Section B

The inspection time is used to determine the approximate cost savings per assembly inspection and this is combined with the throughput of assemblies to determine the cost savings (or payback) per year. Assuming a single-sided assembly requires twenty minutes for inspection in a semiautomated radioscopy system, the labor cost is computed as follows:

(20 min.)(1hr/60 min.)(\$75/hr) = \$25 per inspection.

The inspection cost is subtracted from the labor base of \$88.13 to get a labor cost savings for the inspection. The labor cost savings per assembly becomes:

\$88.125 - \$25 = \$63.125 labor cost savings per assembly.

Using the labor cost savings per assembly, the desired throughput per day is entered to determine the cost savings per year. The assumed throughput value for the example in Section B of Figure C-1, is 48 assemblies per day:

(48 assemblies/day)*(\$63.125 savings/assembly) = \$3,030 savings/day

(\$3,030 savings/day)*(260 days/yr) = \$787,800 savings/year.

C3 System Cost/Payback Assumptions - Section C

Section C of Figure C-1 calculates the values for expenses as a percentage of system cost and lists other relevant assummed values for the calculations. The expenses are computed as follows:

Assumptions	Percent of System Cost	Values
Increase in working capital	20%	\$40,000
Annual expenses (O&M)	5%	\$10,000
Salvage value	25%	\$50,000
Other Assumptions:		
Corporate tax rate	34%	
Cost of capital	10%	

C4 Depreciation Schedule - Section D

The standard values for determining ACRS (Accelerated Cost Recovery System) depreciation are computed in Section D of Figure C-1 based on standard IRS allowed depreciation rates for 5-year amortization of manufacturing equipment. Each year is computed using rates of 0.2, 0.32, 0.19, 0.12, 0.11 and 0.06 for years 1 through 6 respectively. For example, in the first year the after tax depreciation return is:

(Depreciation) (Tax Rate) = ($40,000) (0.34) = $13,600

where Depreciation = (System Cost) (ACRS Rate for year 1) = ($200,000) (0.20).

C5 Annual System Cost Schedule - Section E

With the system purchased in year 0 we assume the payback and all expenses are realized in year 1. Expenses are subtracted from the expected annual payback and taxed at 34 percent to give the net payback per year after taxes. Depreciation is then added to the net payback to give a final annual total payback (expense). The calculations are repeated for each year using the corresponding after tax depreciation from section D. Salvage value is considered a gain: it is taxed and subtracted from the net in year 5. Calculations for years 1 and 2 are shown below:

Year 1: ($787,800 - $10,000) (1 - 0.34)+ $13,600 = $526,948
Year 2: ($787,800 - $10,000) (1 - 0.34) + $21,760 = $535,108

where Annual System Cost = Net Payback After Taxes/Yr + Depreciation After Taxes
and Net Payback After Taxes/Yr = (Payback/Yr - Expenses/Yr) (1 - Tax Rate).

C6 Present Vaue of Payback Totals - Section F

Each total is brought back to year 0 using the formula for present value of cash flows and is listed under the column "PV of Totals":

$PV = FV/(1 + k)n$
where PV = Present Value in year 0
FV = Future Value of year n
k = discount rate (cost of capital)
n = number of years discounted.

The values of the total savings value in years 1 and 2 brought back to year 0 (given a 10 percent cost of capital) is shown below:

	Future Value	Present Value (Year 0)
Year 1:	$526,948	$479,044
Year 2:	$535,108	$442,238

The present value is accumulated until the year in which the value of the accumulation is greater than the year 0 expense. Fractions of a year are computed as a remainder by dividing the expense by that year's present value. For the example spreadsheet in Figure C-2 this occurs in the first year. Since only 0.50 dollars of year 1 present value were required to meet expenses, then the payback is in 0.50 years or 6 months.

A payback curve is developed by varying the throughput desired per day while holding all other variables constant in Section B of the spreadsheet. The payback values are listed as in section G of Figure C-2 and plotted as graphs in Section 6.1.

Payback Schedule for Manual RTR System, SS Case

Section A

Labor Comparison Base	
Rate $/hr	$75 00
100% visual (#hrs)	1
5% of lot X-ray (hrs)	3 5
Cost/total insp (Base)	$88 125

Section B

Board Throughput/Cost Savings Parameters			
Manual RTR Ins. Time (min)	20	Max Bds/8hrdy	24
Manual Cost/total insp	$25 00	Max Bds/16hrdy	48
Cost Savings/bd over Visual Insp.	$63.125		
Hours/25 boards	8 33		
Hours/100 boards	33.33		
Throughput Brds/day	48		
Cost Savings per year	$787,800		

Section C

System Cost/Payback Assumptions		
	Cap Expense	$200,000
20% sys. cost	Inc WC	$40,000
	Payback/yr	$787,800
5% sys. cost	Expenses/yr	$10,000
25% sys. cost	Salvage Val	$50,000
	Tax Rate (Tc)	0.34
	Cost of Capital	10%

Section D

Depreciation Schedule				
Year	Cost	ACRS Rate	Depreciation	Dep * Tc
1	$200,000	0 2	$40,000	$13,600
2	$200,000	0.32	$64,000	$21,760
3	$200,000	0 19	$38,000	$12,920
4	$200,000	0 12	$24,000	$8,160
5	$200,000	0 11	$22,000	$7,480
6	$200,000	0.06	$12,000	$4,080

Section E

Annual Payback Schedule Including expenses and depreciation

Year	Cap Expense	Inc. Wrk Cap.	Payback/yr	Expenses/yr	Net payback/yr	Dep * Tc	Salvage Value	Tax on SV Gain	Totals
0	($200,000)	($40,000)							($240,000)
1			$787,800	$10,000	$513,348	$13,600			$526,948
2			$787,800	$10,000	$513,348	$21,760			$535,108
3			$787,800	$10,000	$513,348	$12,920			$526,268
4			$787,800	$10,000	$513,348	$8,160			$521,508
5			$787,800	$10,000	$513,348	$7,480			$520,828
6		$40,000	$787,800	$10,000	$513,348	$4,080	$50,000	($17,000)	$590,428

Section F

Present Value of Payback Totals (brought to yr 1)

PV of Totals	Total PV @ yr 1	Years to Sys Pybk	Remainder
$479,044	$239,044	0	0.50

Section G

Annual System Payback

Thruput Brds/day	Cost Savings/yr
5	5.13
10	2 38
15	1.59
20	1 19
25	0.95
30	0.80
35	0 68
40	0.60
45	0 53
50	0 48
55	0 44
60	0 40
65	0 37
70	0 34
75	0 32
80	0 30
85	0.28
90	0 27
95	0.25
100	0 24

Figure C-2 Example spreadsheet used to generate economic payback estimates

U.S. Government Printing Office 548-076